Chapter 3

Single Effect Evaporation – Vapor Compression

Objectives

This chapter focuses on evaluation of the single effect evaporation system combined with various types o f heat pumps. The evaluation in the following:
- Process description.
- Model development.
- Performance evaluation.

The systems considered in this chapter include thermal, mechanical, absorption, and adsorption vapor compression.

3.1 Single Effect Thermal Vapor Compression

The single-effect thermal vapor-compression desalination process is of very limited use on industrial scale. However, thermal vapor compression is used with the MEE system, which is known as MEE–TVC. The thermal vapor compression method is attractive due to its simple operation, inexpensive maintenance, simple geometry, and absence of moving parts. Modeling, simulation, and analysis of the single-effect evaporation unit forms the basis for studying of the MEE system and the MEE combined with vapor compression. The following sections include description of the process elements, the steady-state mathematical model for the TVC system, solution method, examples, and system performance as a function of the design and operating parameters. The mathematical model for the process is previously developed by El-Dessouky, 1997.

3.1.1 Process Description

Single effect thermal vapor compression (TVC) seawater desalination process in its simple form is illustrated schematically in Fig. 1. The main components of the unit are the evaporator, the steam jet ejector, and the feed heater or the condenser. The evaporator consists of an evaporator/condenser heat exchanger, a vapor space, a water distribution system, and a mist eliminator. On the other hand, the steam jet ejector is composed of a steam nozzle, a suction chamber, a mixing nozzle, and a diffuser. The feed heater or the heat sink unit is usually a counter-current surface condenser in which the non-condensable gases leave at a temperature approaching the temperature of the feed water. This permit the cooling of the non-condensable gases to the minimum possible temperature, thereby, minimizing the amount of vapor that may escape with the gases and decreases the volume of pumped gases. In addition, it is possible to operate the counter-current condenser so that the exit water is within 3 to 5 ^{o}C of the condensation temperature of the saturated vapor. This improves the thermal performance of the unit and minimizes the mass flow rate of cooling water.

The intake seawater at a flow rate of (M_{cw}+M_f) at temperature T_{cw} and salt concentration X_f is introduced into the tube side of the condenser where its temperature increases to T_f. The cooling water M_{cw} is dumped back to the sea. The function of circulating the cooling water in the condenser is the removal of the excess heat added to the system in the form of motive steam necessary to drive the steam jet ejector. It is important to emphasize that the evaporator does not consume the supplied heat, instead, it simply degrades its quality. The heating of the feed seawater M_f in the condenser from T_{cw} to T_f is essential to increase the thermal performance of the process. The heat needed to warm the seawater inside the condenser is supplied by condensing a controlled portion of vapor formed by boiling in the evaporator M_c. The vapor condensation temperature and consequently the pressure in the vapor space for both the evaporator and the condenser is controlled by

- The cooling water flow rate, M_{cw}.
- Feed water temperature, T_{cw}.
- The available heat transfer area in the condenser, A_c.
- The overall heat transfer coefficient between the condensing vapor and the circulating seawater, U_c.

Accordingly, the condenser has three functions: (1) remove excess heat from the system, (2) improve the process performance ratio, PR, and (3) adjust the boiling temperature inside the evaporator.

The feed seawater M_f is chemically treated and deaerated before being pumped to the evaporator. The chemical treatment is needed to prevent the foaming and the tendency for scale formation in the evaporator. Both factors may seriously impair unit operation. Within, the evaporator, the feed water at T_f is sprayed at the top where it falls in the form of thin film down the succeeding rows of tubes arranged horizontally. The feed water temperature is raised from T_f to the boiling temperature T_b. The magnitude of T_b is dictated by the nature of chemicals used to control the scale formation and the state of the heating steam. This temperature is mastered through settling the pressure in the vapor space of the evaporator. The vapor formed by boiling with a rate of M_d is free of salts. The temperature of the generated vapor T_v is less than the boiling temperature T_b by the boiling point elevation (BPE). The vapor generated therein flows through a knitted wire mist separator known as wire mesh demister to remove the entrained brine droplets. The vapor should be completely freed from brine droplets to prevent the contamination of both the product water and the heat transfer surfaces on which it condenses. Also, the presence of entrained water droplets with the vapor flowing into the steam jet ejector will erode the ejector nozzle and diffuser. The saturation temperature of the vapor

departing the demister is lower than T_v due to the temperature depression because of the frictional pressure loss in the demister. The vapor flows from the demister flows to the condenser where it splits into two portions, the first part M_c condenses outside the tubes of the condenser while the rest M_{ev} is entrained by the steam jet ejector. Although the two streams are drawn separately in the flow diagram, to show the process, they flow from the evaporator to the condenser in the same pipeline. The non-condensable gases accumulated in the vapor space of the condenser must be vented to avoid the downgrading of the heat transfer capacity of the condenser. The blanket of non-condensable gases masks some of the heat transfer area from condensing operation. If the condenser operates at a pressure less than the atmospheric pressure, a pumping device such as an ejector or a vacuum pump is needed to draw off the vent gases from the system. It is worth mentioning that parts of the process description are similar to those given in the Chapter 2. However and as discussed in the preface, the repetition provides the reader with a complete picture for each pocess.

The schematic diagram for the steam jet thermo-compressor or steam booster with its corresponding state points and the variation in both the velocity and the pressure for the motive and entrained vapor through the ejector are shown in Fig. 2. The ejector is used to increase the pressure of the entrained vapor M_{ev} from pressure P_{ev} to a higher pressure P_s. This process takes place through converting the pressure energy of motive steam M_m to generate vacuum and compress the entrained vapor to the required pressure. As the motive steam at flow rate of M_m expands in the nozzle from state 1 to state 2, its static pressure energy is converted to kinetic energy. The nozzle is a converging/diverging shape to expand the steam to velocities greater than the speed of sound (supersonic). The suction chamber is used to keep the nozzle properly positioned with respect to the diffuser and to direct the entrained vapor. The entrained vapor M_{ev} enters the suction chamber at pressure P_{ev} where it mixes with the motive steam. The mixing process is violent and rapid. The two streams mix together as they pass through the converging section of the venturi diffuser. The mixture enters the throat section of the diffuser, completely mixed, at the sonic velocity of the mixture. The mixed stream is self compressed through the diverging section of the venturi diffuser, where the cross sectional area increases and the velocity decreases, converting the kinetic energy of the mixture to static pressure energy. The mixture leaves the ejector at a pressure P_s that is intermediate to the motive (P_m) and suction (P_{ev}) pressures.

The steam jet ejector must be designed and operated at critical conditions to allow normal and stable operation. This condition is associated with absence of violent fluctuations in the suction pressure. If the ejector is designed to operate with a full stable range, it will have a constant mass flow rate of the entrained vapor for different discharge pressures when the upstream conditions remain

constant. The ejector is critical when the compression ratio is greater than or equal to the critical pressure ratio of the suction vapor. For water vapor this ratio is 1.81. That is, the suction pressure must be less than 0.55 times the discharge pressure to obtain critical or stable conditions in the steam jet ejector.

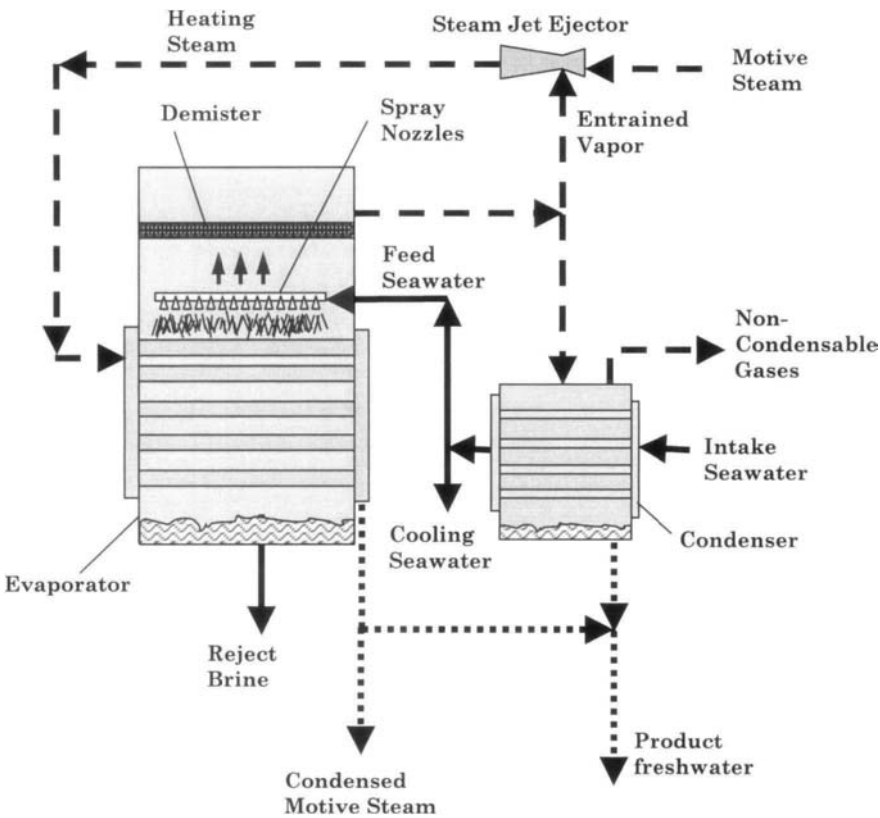

Fig. 1. Single effect thermal vapor compression evaporator-desalination process

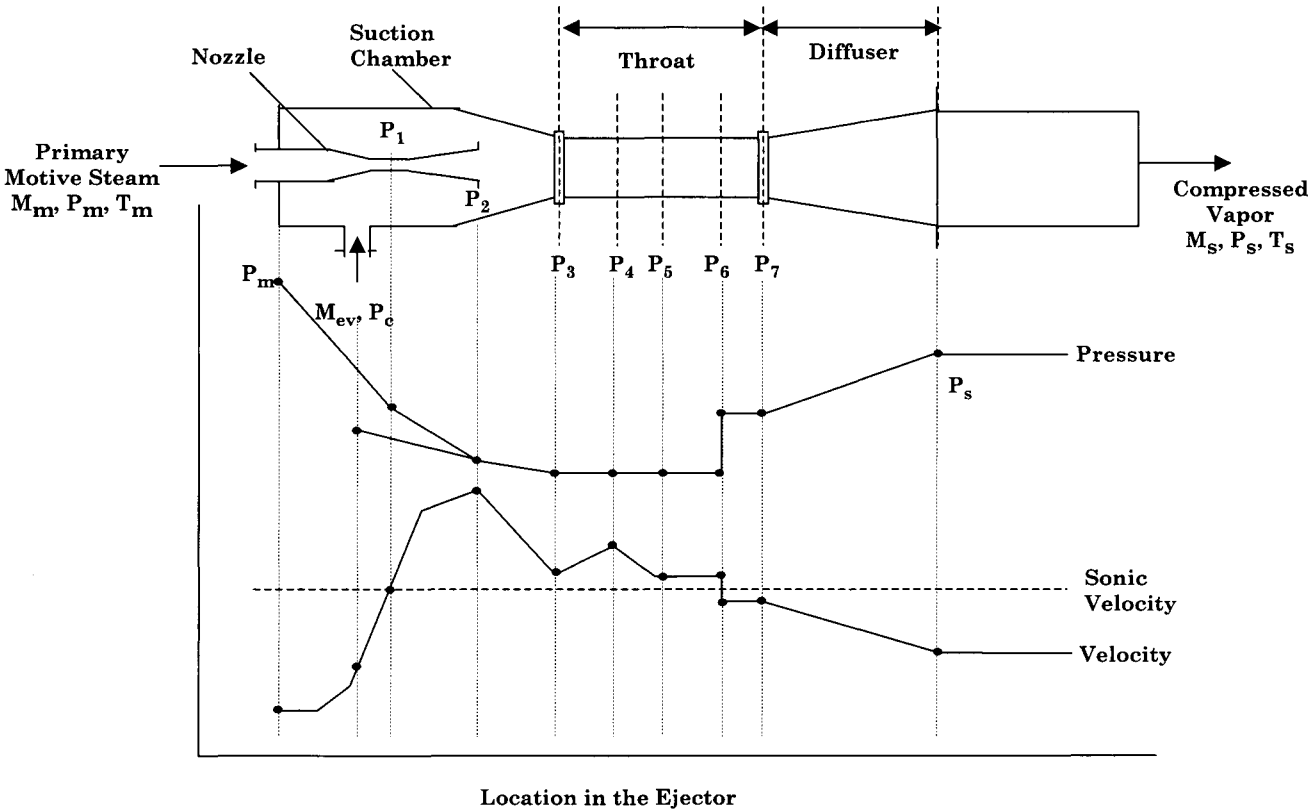

Fig. 2. Variation in stream pressure and velocity as function of location along the ejector.

3.1.2 Process Modeling

Development of the TVC model is divided into seven sections:
- Performance parameters.
- Material balance.
- Evaporator and condenser energy balances.
- Boiling point elevation and thermodynamic losses.
- Evaporator and condenser heat transfer areas.
- Steam jet ejector design equations.

Performance Parameters

Performance of the TVC is determined in terms of the following variables:
- The amount of product fresh water per unit mass of motive steam, or the performance ratio, PR.
- The specific heat transfer surface area, sA.
- The specific cooling water flow rate, sM_{cw}.

The above system parameters are defined by the following relations:

$$PR = \frac{M_d}{M_m} \tag{1}$$

$$sA = \frac{A_e + A_c}{M_d} \tag{2}$$

$$sM_{cw} = \frac{M_{cw}}{M_d} \tag{3}$$

where M is the mass flow rate and the subscript c, cw, d, e, and m denotes the condenser, cooling water, distillate product, evaporator, and motive steam, respectively. The variables A_e and A_c are the heat transfer area in the evaporator and condenser, respectively.

Material Balance

The distillate and rejected brine flow rates are obtained by solution of the overall mass and salt balances. The two balance equations assume that the distillate water is salt free. The two balance equations are given by

$$M_f = M_d + M_b \tag{4}$$

$$\frac{M_d}{M_f} = \frac{X_b - X_f}{X_b} \tag{5}$$

where M is the mass flow rate, X is the salinity, and the subscripts b, d, and f denote the rejected brine, distillate, and feed seawater.

Evaporator and Condenser Energy Balances

In the evaporator, the dry saturated steam flowing from the steam jet ejector and admitted into the evaporator ($M_m + M_{ev}$) is used in to raise the temperature of the feed seawater M_f from the inlet temperature T_f to the boiling temperature T_b. In addition, it supplies the latent heat required to evaporate the specified mass of vapor, M_d, or:

$$Q_e = M_f C_p (T_b - T_f) + M_d \lambda_v = (M_m + M_{ev}) \lambda_s \tag{6}$$

where Q_e is the thermal load of the evaporator, C_p is the specific heat at constant pressure of the brine, and λ is the latent heat of evaporation. Correlations for C_p and λ are given in Appendix A.

The condenser operates on the remaining fraction of vapor formed in the evaporator, M_c, which is not entrained by the steam jet ejector. The condensation latent heat is transferred to the feed seawater with a mass flow rate of $M_f + M_{cw}$. The fraction M_f of the seawater feed is introduced into the evaporator, while the remaining part, M_{cw}, which is known as the cooling water, is rejected back to the sea. The feed seawater temperature is assumed equal to 25 °C. As for the feed vapor it is assumed saturated at a temperature equal to T_c, which is lower than the boiling temperature, T_b, by the boiling point elevation and thermodynamic losses.

The heat load of the condenser is given by

$$Q_c = (M_f + M_{cw}) C_p (T_f - T_{cw}) = M_c \lambda_c \tag{7}$$

where Q_c is the thermal load of the condenser. The subscript c, cw, and f denote the condenser, cooling seawater, and un-entrained vapor.

Boiling Point Elevation and Thermodynamic Losses

The generated vapor is at the saturation temperature, T_v, which corresponds to the pressure in the evaporator vapor space. This temperature is less than the boiling temperature T_b by the boiling point elevation BPE, where,

$$T_b = T_v + BPE \tag{8}$$

The boiling point elevation (BPE), at a given pressure, is the increase in the boiling temperature due to the salts dissolved in the water. Correlation for the boiling point elevation of seawater is given Appendix B.

The condensation temperature of vapor outside the tube bundle of the condenser T_c is less than the boiling temperature in the evaporator T_b by the boiling point elevation (BPE) and the saturation temperature depression associated with pressure losses in the demister (ΔT_p) and inside the condenser horizontal tubes (ΔT_c). Thus:

$$T_c = T_b - (BPE + \Delta T_p + \Delta T_c) \tag{9}$$

The correlation for the pressure drop in the demister is given in Appendix B. As for the pressure drop of the vapor flowing over the condenser tubes it is assumed has a negligible value. This is the pressure recovery due to flow deceleration compensates the pressure drop caused by friction. Therefore, the net pressure fall and consequently the saturation temperature depression in the condensation process can be neglected, Marto (1991), Muller (1991), Sinnott (1996).

Evaporator and Condenser Heat Transfer Area

The dimensions of the required heat transfer surface area in the evaporator A_e are obtained from:

- The amount of the heat to be transferred Q_e.
- The overall heat transfer coefficient U_e.
- The difference between the condensation temperature of the steam, T_s, and the boiling temperature of the seawater T_b.

This relation is given by

$$A_e = \frac{Q_e}{U_e(T_s - T_b)} \tag{10}$$

The heating surface area of the evaporators A_e is usually, but not always, taken as that in contact with the boiling liquid, whether on the inside or outside of the tubes.

The heat transfer between the condensing vapor and the feed water in the condenser can be written in terms of an overall heat transfer coefficient (U_c), condenser heat transfer area (A_c), and the logarithmic mean temperature difference $(LMTD)_c$, thus:

$$A_c = \frac{Q_c}{U_c (LMTD)_c} \tag{11}$$

The $(LMTD)_c$ is defined as:

$$(LMTD)_c = \frac{T_f - T_{cw}}{\ln \dfrac{T_c - T_{cw}}{T_c - T_f}} \tag{12}$$

In Eqs. 11 and 12 the overall heat transfer coefficient is based on the outside surface area and is related to the individual thermal resistance by the following well-known expression:

$$\frac{1}{U_e} = \frac{1}{h_i}\frac{r_o}{r_i} + R_{f_i}\frac{r_o}{r_i} + \frac{r_o \ln(r_o / r_i)}{k_w} + R_{f_o} + \frac{1}{h_o} \tag{13}$$

where h is the heat transfer coefficient, R_f is the fouling resistance, k_w is the thermal conductivity of tube material and r is the radius. The subscripts i and o refer to the inner and outer tube surfaces, respectively. Correlations for the evaporator and condenser heat transfer coefficients are given in the Appendix C.

Steam Jet Ejector

The most important and critical step in modeling the TVC desalination system is the evaluation of the performance of the steam jet ejector. The main data required from analyzing the steam jet ejector is the determination of the mass of motive steam required per unit mass of the entrained vapor (Ra), given the pressure of the motive steam (P_m), discharge pressure (P_s) and the suction pressure (P_{ev}). There are a limited number of methods available in the literature to analysis the steam jet ejector. However, these methods require tedious and lengthy calculation procedures. Additionally, most of these methods are based on using many correction factors that depend heavily on the detail design of the ejector. The technique developed here is established on the data and method presented by Power, 1994. Power found that none of procurable ways were

superior to his simple method. The method is most accurate for motive steam pressures above 5.1 bar and low compression ratios associated with (Ra) values less than 4. The curves used in the calculations represent smoothed data from several sources and agree with manufacturer's data within the about 10% over the best-fit range. El-Dessouky, 1997, developed the following relationships to evaluate the performance of the steam jet ejector. The entertainment ratio is defined by:

$$Ra = 0.296 \frac{(P_s)^{1.19}}{(P_{ev})^{1.04}} \left(\frac{P_m}{P_{ev}}\right)^{0.015} \left(\frac{PCF}{TCF}\right) \tag{14}$$

where Ra is the entrainment ratio and defined as the mass of motive steam per unit mass of entrained vapor, P_m, P_s and P_{ev} are the pressures of the motive steam, discharge mixture and entrained vapor respectively, PCF is motive steam pressure correction factor and TCF is the entrained vapor temperature correction factor. The following two equations are developed to calculate both PCF and TCF.

$$PCF = 3x10^{-7} (P_m)^2 - 0.0009 (P_m) + 1.6101 \tag{15}$$

$$TCF = 2x10^{-8} (T_{ev})^2 - 0.0006 (T_{ev}) + 1.0047 \tag{16}$$

where P_m is in kPa and T_{ev} is in °C. The previous equations are valid only for ejector operating with steam as the motive fluid and the entrained gas is water vapor. These equations are valid in the following ranges: $Ra \leq 4$, $500 \geq T_{ev} \geq 10$ °C, $3500 \geq P_m \geq 100$ kPa, and $\frac{P_s}{P_{ev}} \geq 1.81$.

It is interesting to realize that the consideration of the thermodynamic losses such as BPE, and temperature depression corresponding to the pressure drops in the demister increases in the energy demand for the jet ejector. This is because the vapor must be compressed, not simply through the working temperature drop ($T_s - T_b$), but through the working temperature drop plus the thermodynamic losses, i.e., $\{T_s - [T_b - (BPE + \Delta T_p)]\}$, or $(T_s - T_{ev})$.

Solution Procedure

The following set of specifications are used in solution of the TVC system:

- The seawater temperature.
- The feed water temperature.
- The seawater salinity.
- The salinity of the rejected brine.
- The thickness of the demister pad.

- The vapor velocity in the demister.
- The density of the demister pad.
- Boiling temperature.
- Ejector compression ratio.
- Motive steam pressure.

The solution procedure is shown in Fig. 3 and proceeds as given below:

- The mass flow rates of the reject brine and feed seawater, M_b and M_f, for a specified distillate water flow rate, M_d, of 1 kg/s, are calculated from Eqs. 4 and 5.
- The boiling point elevation, BPE, is calculated from the correlation in Appendix B.
- The saturation temperature T_v is calculated from Eq. 8 and the corresponding saturation pressure, P_v, is obtained from the steam tables or calculated from the correlation given in Appendix (A).
- The pressure drop in the demister (ΔP_p) is calculated from the correlation given in Appendix (B). This value is used to calculate the vapor pressure past the demister, P_{ev}, which is equal to $P_v - \Delta P_p$.
- The saturation vapor temperature, T_{ev}, is calculated at the saturation vapor pressure, P_{ev}, from the steam tables or the saturation temperature correlation given in Appendix A.
- The compressed vapor pressure, P_s, is obtained from the specification of the compression ratio, Cr, and the entrained vapor pressure, P_{ev}. This is followed by calculation of the saturation temperature, T_s, at the corresponding vapor pressure, P_s, from the steam tables or the correlation given in Appendix A.
- The evaporator thermal load, Q_e, is calculated from Eqs. 6.
- The overall heat transfer coefficient in the evaporator, U_e, is calculated from the correlation given in Appendix C.
- The overall heat transfer coefficient in the condenser, U_c, is calculated from the correlation given in Appendix C.
- The entrainment ratio, Ra, is calculated from Eqs. 14-16.
- The mass flow rates of the motive steam and entrained vapor, M_s and M_{ev}, are obtained by substituting the values of the entrainment ratio, Ra, and the evaporator load, Q_e, in Eq. 6.
- The condenser load, Q_c, and the cooling water flow rate, M_{cw}, are obtained from the condenser energy balance, Eq. 7.
- The evaporator and condenser areas, A_e and A_c, are obtained from Eqs. 10 and 11.
- The system performance parameters, PR, sA, and sM_{cw}, are calculated from Eqs. 1-3.

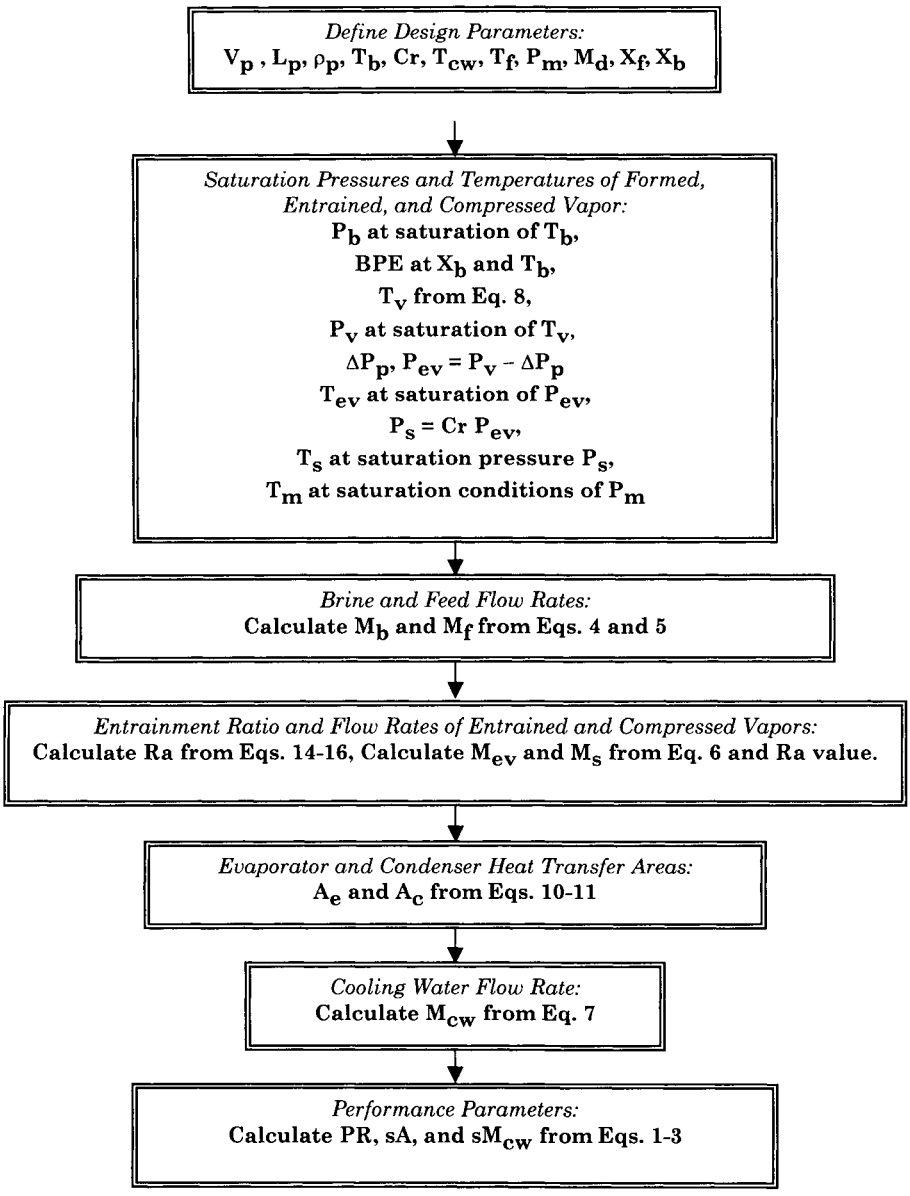

Fig. 3. Solution procedure of the TVC mathematical model

3.1.3 System Performance

Evaluation of the TVC system is illustrated in the following examples. The first includes a design problem to determine the specific heat transfer area, the flow rate of the cooling water, and the performance ratio. The second example rates the performance of an existing system, where the heat transfer area of the evaporator and the condenser are known.

Example 1:

A single-effect thermal vapor-compression system is designed at the following operating conditions:

- Boiling temperature, T_b, of 75 °C.
- Compression ratio, Cr, of 2.5.
- Motive steam pressure, P_m, of 750 kPa.
- Brine reject concentration, X_b = 70000 ppm
- Intake seawater salinity, X_f = 42000 ppm
- Intake seawater temperature, T_{cw} = 25 °C
- System capacity, M_d = 1 kg/s
- Boiling temperature, T_b = 75 °C
- Feed seawater temperature, $T_f = (T_b - 5) = 70$ °C
- Condenser efficiency, η = 0.9.

Solution

Substituting for X_f = 42000 ppm, X_b = 70000 ppm, and M_d = 1 kg/s in Eq. 4 results in

$$M_f = X_b/(X_b - X_f) = 70000/(70000 - 42000) = 2.5 \text{ kg/s}$$

Equation 4 is then used to calculate M_b,

$$M_b = M_f - M_d = 2.5 - 1 = 1.5 \text{ kg/s}$$

The boiling point elevation, BPE, is calculated from the correlation given in Appendix B. The values of B and C are evaluated from

$$BPE = (0.0825431 + 0.0001883\,(75) + 0.00000402\,(75)^2)\,(7) + (-0.0007625 + 0.0000902\,(75) - 0.00000052\,(75)^2)\,(7)^2$$

$$+(0.0001522-0.000003\ (75) - 0.00000003\ (75)^2)\ (7)^3$$
$$= 0.903\ ^oC$$

The resulting value of T_V is calculated from Eq. 8,

$$T_V = T_b - BPE = 75 - 0.903 = 74.097\ ^oC$$

The corresponding saturation vapor pressure, P_v, is obtained from the correlation given in Appendix A,

$$P_V = EXP((-7.419242+ (0.29721)$$
$$((0.01)(74.097+273.15-338.15))$$
$$-0.1155286\ ((0.01)\ (74.097+273.15-338.15))^2$$
$$+0.008685635\ ((0.01)\ (74.097+273.15-338.15))^3$$
$$+ 0.001094098\ ((0.01)\ (74.097+273.15-338.15))^4$$
$$-0.00439993\ ((0.01)\ (74.097+273.15-338.15))^5$$
$$+0.002520658\ ((0.01)\ (73.01+273.15-338.15))^6$$
$$-0.0005218684\ ((0.01)\ (74.097+273.15-338.15))^7)$$
$$((647.286/(74.097+273.15))-1))(22089000/1000)$$
$$= 37.1\ kPa$$

The pressure drop in the demister is evaluated from the correlation given in Appendix B. In this equation ρ_p, V, L, and δ_w are set equal to 300 kg/m^3, 1.8 m/s, 0.1 m, and 0.28 mm. This results in

$$\Delta P_p = 3.88178\ (\rho_p)^{0.375798}\ (V)^{0.81317}\ (\delta_w)^{-1.56114147}$$
$$= 390\ Pa/m$$

Which gives a total pressure drop of 0.039 kPa through the demister. The vapor pressure past the demister is then calculated

$$P_{ev} = P_v - \Delta P_p = 37.1 - 0.039 = 37.061\ kPa$$

Therefore, the vapor saturation temperature past the demister, T_{ev}, is assumed equal to the saturation temperature, T_v. Another assumption applied here is the equality of the vapor condensation temperature, T_c, in the condenser and the vapor temperature in the evaporator, T_v.

The specified value for the compression ratio, Cr, and the entrained pressure value, P_{ev}, are used to calculated pressure of the compressed vapor, P_s, which is

$P_s = (Cr)\ (P_{ev}) = (2.5)\ (37.1) = 92.75$ kPa

The corresponding saturation temperature, T_s, is calculated from the correlation for the saturation temperature given Appendix A,

$$T_s = \left(42.6776 - \frac{3892.7}{(\ln(P_s/1000) - 9.48654)}\right) - 273.15$$

$$= \left(42.6776 - \frac{3892.7}{(\ln(92.75/1000) - 9.48654)}\right) - 273.15$$

$$= 97.6\ ^{o}C$$

The overall heat transfer coefficients in the evaporator and condenser are calculated from the correlations given in Appendix C

$$U_e = \begin{pmatrix} 1969.5 + 12.057\,(T_b) - 0.85989 \times 10^{-1}\,(T_b)^2 \\ + 0.25651 \times 10^{-3}\,(T_b)^3 \end{pmatrix} \times 10^{-3}$$

$$= \begin{pmatrix} 1969.5 + 12.057\,(75) - 0.85989 \times 10^{-1}\,(75)^2 \\ + 0.25651 \times 10^{-3}\,(75)^3 \end{pmatrix} \times 10^{-3}$$

$$= 2.62\ kW/m^2\ ^{o}C$$

$$U_c = \begin{pmatrix} 1719.4 + 3.2063\,(T_c) + 1.5971 \times 10^{-2}\,(T_c)^2 \\ - 1.9918 \times 10^{-4}\,(T_c)^3 \end{pmatrix} \times 10^{-3}$$

$$= \begin{pmatrix} 1719.4 + 3.2063\,(74.097) + 1.5971 \times 10^{-2}\,(74.097)^2 \\ - 1.9918 \times 10^{-4}\,(74.097)^3 \end{pmatrix} \times 10^{-3}$$

$$= 1.96\ kW/m^2\ ^{o}C$$

The entrainment ratio, Ra, is obtained from Eq. 14. This requires calculations of the correction factors, PCF and TCF, from Eqs. 15 and 16. These results are

$$PCF = 3 \times 10^{-7}\ (P_m)^2 - 0.0009\ (P_m) + 1.6101$$

$$= 3 \times 10^{-7}\ (750)^2 - 0.0009\ (750) + 1.6101$$

$$= 1.104$$

$$TCF = 2 \times 10^{-8}\ (T_c)^2 - 0.0006\ (T_c) + 1.0047$$

$$= 2 \times 10^{-8}\ (74.097)^2 - 0.0006\ (74.097) + 1.0047$$

$= 0.96$

$$Ra = 0.296 \frac{(P_s)^{1.19}}{(P_{ev})^{1.04}} \left(\frac{P_m}{P_{ev}}\right)^{0.015} \left(\frac{PCF}{TCF}\right)$$

$$= 0.296 \frac{(92.75)^{1.19}}{(37.1)^{1.04}} \left(\frac{750}{37.1}\right)^{0.015} \left(\frac{1.104}{0.96}\right) = 1.82$$

The amount of motive steam is obtained by solution of the evaporator balance, Eq. 6. This gives

$$M_f Cp\ (T_b - T_f) + M_d\ \lambda_v = (M_s + M_{ev})\ \lambda_s$$

In the above equation, λ_v and λ_s, are calculated from the correlation given in Appendix A. T_s (96.46)

$$\lambda_v = 2501.897149 - 2.407064037\ T_v + 1.192217 \times 10^{-3}\ T_v^{\,2} - 1.5863 \times 10^{-5}\ T_v^{\,3}$$

$$= 2501.897149 - 2.407064037(74.097) + 1.192217 \times 10^{-3}\ (74.097)^2 - 1.5863 \times 10^{-5}\ (74.097)^3$$

$$= 2323.6 \text{ kJ/kg}$$

$$\lambda_s = 2501.897149 - 2.407064037\ T_s + 1.192217 \times 10^{-3}\ T_s^{\,2} - 1.5863 \times 10^{-5}\ T_s^{\,3}$$

$$= 2501.897149 - 2.407064037(97.6) + 1.192217 \times 10^{-3}\ (97.6)^2 - 1.5863 \times 10^{-5}\ (97.6)^3$$

$$= 2263.6 \text{ kJ/kg}$$

The heat capacity is calculated at T_b and X_f from the correlation given Appendix A and its value is equal to 3.86 kJ/kg °C. Substitution of the values for T_b, T_f, M_d, M_f, Cp, λ_v and λ_s in Eq. 6 gives

$$(2.5)(3.86)\ (75-70) + (1)(2326.37) = (M_m + M_{ev})(2266.76)$$

M_m/Ra replaces the amount of entrained vapor, M_{ev}, which results in

$$(2.5)(3.99)(75-70) + (1)(2323.6) = (M_m + M_m/1.82)\ (2263.6)$$

Solving the above equation gives $M_m = 0.67$ kg/s. The amount of entrained vapor, M_{ev}, is then calculated from the entrainment ratio value,

$M_{ev} = M_m/Ra = 0.67/1.82 = 0.37$ kg/s

The cooling water flow rate is obtained from the condenser balance, Eq. 7.

$(M_f + M_{cw})\ (Cp)\ (T_f - T_{cw}) = (\eta)\ (M_d - M_{ev})\ (\lambda_c)$
$(2.5 + M_{cw})\ (3.97)\ (70-25) = (0.9)\ (1-0.37)\ (2323.6)$
Solution of the above equation gives $M_{cw} = 4.83$ kg/s. The evaporator and condenser loads are obtained from Eqs. 6 and 7, respectively. The resulting values are:

$Q_e = (M_m + M_{ev})(\lambda_s) = (0.67 + 0.37)(2263.6) = 2354.1$ kW

$Q_c = \eta\ (M_c)(\lambda_c) = (0.9)(0.63)(2323.6) = 1317.5$ kW

In the condenser load the value of λ_c is identical to λ_v. This is because of neglecting various forms of thermodynamic losses caused by pressure drop and during condensation. The evaporator and condenser areas are then calculated from Eqs. 10 and 11.

$$A_e = \frac{Q_e}{U_e(T_s - T_b)} = \frac{2354.1}{(2.62)(97.6-75)} = 39.8\ m^2$$

$$A_c = \frac{Q_c}{(U_c)(LMTD)_c} = \frac{1317.5}{(1.96)(16.25)} = 41.18\ m^2$$

The $(LMTD)_c$ value in the condenser is calculated from Eq. 12

$$(LMTD)_c = \frac{(T_f - T_{cw})}{\ln\dfrac{T_c - T_{cw}}{T_c - T_f}} = \frac{70-25}{\ln\dfrac{73.01-25}{73.01-70}} = 16.25\ ^{\circ}C$$

Since the distillate flow rate is set at 1 kg/s, the above values for M_{cw}, A_c, and A_e are the specific values. The performance ratio is calculated from Eq. 1, which gives

$PR = M_d/M_m = 1/0.675 = 1.48$

and the resulting specific cooling water flow rate, M_{cw}, and the specific heat transfer area, sA, given by Eqs. 2 and 3, $sM_{cw} = M_{cw}/M_d = 4.83$, and $sA = (A_e+A_c)/M_d = 44.47 + 41.18 = 85.65\ m^2/(kg/s)$.

Example 2:

The heat transfer areas for the evaporator and condenser of in a single-effect thermal vapor-compression system are 37.1 m^2 and 54.8 m^2, respectively. The boiling temperature in the evaporator is 65 °C. The steam jet ejector operates at a compression ratio of 3.2 and a motive steam pressure of 550 kPa. Other data includes a salinity of 70,000 ppm for the brine reject, a feed seawater salinity of 42,000 ppm, and a seawater temperature of 25 °C. The feed seawater temperature to the evaporator is less than the boiling temperature by 5 °C. Assume that thermodynamic losses in the demister, transmission lines, and during condensation have negligible effects on the system. Also, assume that the condenser efficiency is equal to 90%. Evaluate the performance ratio of the system, the specific flow rate of cooling water, and the production capacity.

Solution:

The boiling point elevation is evaluated at T_b = 65 °C and X_b = 70,000 ppm, where

$$\begin{aligned}BPE &= (0.0825431+0.0001883\ (65) +0.00000402\ (65)^2)\ (7)\\ &\quad +(-\ 0.0007625+0.0000902\ (65) - 0.00000052\ (65)^2)\ (7)^2\\ &\quad +(0.0001522-0.000003\ (65) - 0.00000003\ (65)^2)\ (7)^3\\ &= 0.87\ ^oC\end{aligned}$$

This gives a vapor temperature of

$$T_v = T_b - BPE = 65 - 0.87 = 64.13\ ^oC$$

Invoking the negligible effect of thermodynamic losses gives the following equality

$$T_v = T_{ev} = T_c = 63.074\ ^oC$$

The correlations in Appendix A are used to calculate the corresponding saturation pressure and the latent heat, with values of 22.95 kPa and 2350.86 kJ/kg, respectively. The pressure of the compressed vapor is obtained from

$$Cr = P_s/P_{ev}$$
$$3.2 = P_s/22.95$$

$$P_s = 73.45 \text{ kPa}$$

which gives a saturation temperature of 91.29 °C. Accordingly, the expansion ratio for the ejector is obtained from

$$Er = P_m/P_{ev}$$
$$Er = 550/22.95 = 23.9$$

The overall heat transfer coefficients in the evaporator and condenser are calculated from the correlations given in Appendix C

$$U_e = \left(\begin{matrix}1969.5 + 12.057\,(T_b) - 0.85989\text{x}10^{-1}\,(T_b)^2 \\ + 0.25651\text{x}10^{-3}\,(T_b)^3\end{matrix}\right)\text{x}10^{-3}$$

$$= \left(\begin{matrix}1969.5 + 12.057\,(65) - 0.85989\text{x}10^{-1}\,(65)^2 \\ + 0.25651\text{x}10^{-3}\,(65)^3\end{matrix}\right)\text{x}10^{-3}$$

$$= 2.46 \text{ kJ/s m}^2\ ^\circ\text{C}$$

$$U_c = \left(\begin{matrix}1719.4 + 3.2063\,(T_c) + 1.5971\text{x}10^{-2}\,(T_c)^2 \\ - 1.9918\text{x}10^{-4}\,(T_c)^3\end{matrix}\right)\text{x}10^{-3}$$

$$= \left(\begin{matrix}1719.4 + 3.2063\,(63.074) + 1.5971\text{x}10^{-2}\,(63.074)^2 \\ - 1.9918\text{x}10^{-4}\,(63.074)^3\end{matrix}\right)\text{x}10^{-3}$$

$$= 1.935 \text{ kJ/s m}^2\ ^\circ\text{C}$$

The entrainment ratio, Ra, is then calculated, where

$$PCF = 3\text{x}10^{-7}\ (P_m)^2 - 0.0009\ (P_m) + 1.6101$$
$$= 3\text{x}10^{-7}\ (550)^2 - 0.0009\ (550) + 1.6101$$
$$= 1.2058$$

$$TCF = 2x10^{-8}\ (T_c)^2 - 0.0006\ (T_c) + 1.0047$$
$$= 2x10^{-8}\ (63.074)^2 - 0.0006\ (63.074) + 1.0047 = 0.966$$

$$Ra = 0.296 \frac{(P_s)^{1.19}}{(P_{ev})^{1.04}} \left(\frac{P_m}{P_{ev}}\right)^{0.015} \left(\frac{PCF}{TCF}\right)$$
$$= 0.296 \frac{(73.45)^{1.19}}{(22.95)^{1.04}} \left(\frac{550}{22.95}\right)^{0.015} \left(\frac{1.20585}{0.966}\right) = 2.47$$

The condenser rating gives the following thermal load

$$A_c = \frac{Q_c}{(U_c)(LMTD)_c}$$
$$54.8 = \frac{Q_c}{(1.935)(13.9)}$$
$$Q_c = 1474.24\ kW$$

In the above equation $(LMTD)_C$ value is obtained from

$$(LMTD)_c = \frac{(T_f - T_{cw})}{\ln \frac{T_c - T_{cw}}{T_c - T_f}} = \frac{60 - 25}{\ln \frac{63.074 - 25}{63.074 - 60}} = 13.9\ ^\circ C$$

The thermal load of the condenser is then used to calculate the flow rate of the condensed vapor, or,

$Q_c = \eta\ (M_c)(\lambda_c)$
$1474.24 = (0.9)(M_c)(2350.86)$

This gives M_c = 0.69 kg/s. Similarly, the thermal load of the evaporator is calculated from the rate equation, where,

$$A_e = \frac{Q_e}{U_e(T_s - T_b)}$$
$$37.1 = \frac{Q_e}{(2.46)(91.29 - 65)}$$
$$Q_e = 2400\ kW$$

The evaporator thermal load together with the latent heat for condensation of the compressed are used to calculate the flow rate of the compressed vapor flow rate:

$Q_e = (M_s)(\lambda_s)$
$2400 = (M_s)\ (2280)$
$M_s = 1.05$ kg/s

Recalling that the entrainment ratio (Ra) is defined as

$Ra = M_m/M_{ev}$

where $M_m = M_s - M_{ev}$. Substitution for the M_m expression in the above equation together with the value of Ra gives the value M_m, or,

$2.47 = (M_s - M_{ev})/M_{ev} = (1.05 - M_{ev})/M_{ev}$

This gives $M_{ev} = 0.303$ kg/s. Therefore

$M_m = 1.05 - 0.303 = 0.747$ kg/s

Therefore, the total system capacity is equal to the sum of M_c and M_{ev}, or, 0.99 kg/s for M_d. Substituting for $X_f = 42000$ ppm, $X_b = 70000$ ppm, and $M_d = 0.99$ kg/s in the balance equations gives

$$M_f = \frac{M_d X_b}{X_b - X_f} = \frac{(0.99)(70000)}{(70000 - 42000)} = 2.475 \text{ kg/s}$$

$$M_b = M_f - M_d = 2.475 - 0.99 = 1.485 \text{ kg/s}$$

The cooling water flow rate is obtained from the condenser balance, Eq. 7.

$(M_f + M_{cw})\ (Cp)\ (T_f - T_{cw}) = (\eta)\ (M_d - M_{ev})\ (\lambda_c)$
$(2.475 + M_{cw})\ (3.97)\ (60 - 25) = (0.9)\ (0.99 - 0.303)\ (2350.86)$

Solution of the above equation gives $M_{cw} = 7.98$ kg/s.

Performance Charts

System performance is presented in terms of variations in the system design parameters as a function of the boiling temperature, T_b, the compression ratio, Cr, and the pressure of the motive steam, P_m. The system parameters include variations in the overall heat transfer coefficient in the evaporator (U_e)

and the condenser (U_c), the performance ratio, PR, the specific heat transfer area, sA, and the specific cooling water flow rate, sM_{cw}.

Variations in the system performance ratio as a function of the boiling temperature, motive steam pressure, and compression ratio are shown in Figs. 4-6. As is shown the system performance ratio varies over a range of 1-2. The higher performance ratio values are obtained at low boiling temperatures, low compression ratios, and high motive steam pressures. At low boiling temperatures, the amount of motive steam consumed to compress the entrained vapor is low. This is because of the small increase in the vapor pressure at low temperatures. For example, the vapor pressure between 55 and 60 °C increases from 15.8 to 19.9 kPa is 26.5%. On the other hand, the vapor pressure increases from 70.14 to 84.55 kPa as the temperature increases from 90 to 95 °C.

At low compression ratios, the amount of motive steam consumed to compress the entrained vapor is small. Therefore, the system performance ratio is higher. The same result also applies at high motive steam pressures. Irrespective of this, the sensitivity of the performance ratio to variations in the motive steam pressure is less pronounced than those found as a function of the boiling temperature and the compression. This result is shown in Fig. 6 with limited variations in the system performance ratio as the motive steam pressure is increased over a range of 250-1750 kPa. For each set of data in Fig. 6, the boiling temperature and the compression ratio are kept constant. At such conditions, the amount of latent heat consumed by the boiling brine is constant, which implies a constant temperature for the compressed vapor. As the pressure of the motive steam is increased its latent is lower. Therefore, to maintain constant latent heat in the compressed vapor, it is necessary to entrain larger amounts of the vapor leaving the evaporator. This reduces the consumed amount of motive steam.

Variations in the specific heat transfer area are shown in Figs. 7-9. The results are shown as function of the boiling temperature, the motive steam pressure, and the compression ratio. As is shown in Fig. 7, the specific heat-transfer area decreases drastically as the boiling temperature is increased. This result is caused by the increase in the overall heat transfer coefficient in the evaporator and the condenser at high boiling temperatures. As the overall heat transfer coefficient increases, because of the decrease in the resistance to heat transfer, the area for heat transfer is decreased. The specific heat transfer area is also decreased at higher boiling temperatures. This is because the amount of distillate formed only depends on the salinity of the feed seawater and the rejected brine.

Similar results are shown in Fig. 8 for variations in the specific heat transfer area as a function of the compression ratio. At constant boiling

temperatures and higher compression ratios, the pressure of the compressed vapor is larger. This is because the pressure of the entrained vapor does not change at constant boiling temperatures. Simultaneously, the temperature of the compressed vapor is also increased as the compression ratio is elevated. The increase in the temperature of the compressed vapor enhances the rates of heat transfer. This is caused by the increase of the driving force for heat transfer across the evaporator, which is measured by the difference of T_s-T_b. As a result, the evaporator heat transfer area is reduced at higher compression ratios. Irrespective of this, the heat-transfer area increases in the condenser. This is because of the increase in the condenser load, which is caused by the reduction in the amount of entrained vapor at higher compression ratios. However, the decrease in the evaporator area is more pronounced than the increase in the condenser area. The net result of the above is the decrease in the specific heat transfer area upon the increase of the compression ratio.

Effect of the motive steam pressure on the specific heat transfer area is shown in Fig. 9. The results are obtained at a compression ratio of 1.895 and boiling temperature range of 55-82 °C. These results are similar to those obtained for the variations in the system performance ratio, Fig. 4. As is shown in Fig. 9, the specific heat transfer area is insensitive to variations in the motive steam pressure. This is because of limited variations in the overall heat transfer coefficient in the evaporator and condenser as well as the amount of entrained vapor.

Variations in the specific cooling water flow rate are shown in Figs. 10-12. The results are obtained over the same parameter range as discussed before. As is shown, the specific cooling water flow rate is highly sensitive to variations in the boiling temperature and the compression ratio, Figs. 10 and 11. However, it is insensitive to variations in the motive steam pressure, Fig. 12. This result is consistent with the discussion given for variations in other design parameters, i.e., and performance ratio and specific heat transfer area. Sensitivity of the specific cooling water flow rate with respect to the boiling temperature and the compression ratio is caused by large increase in the overall heat transfer coefficient in the evaporator and condenser. An opposite behavior is observed upon the increase in the motive steam pressure. In this regard, limited sensitivity in the specific cooling water flow rate is found upon the increase in the motive steam pressure.

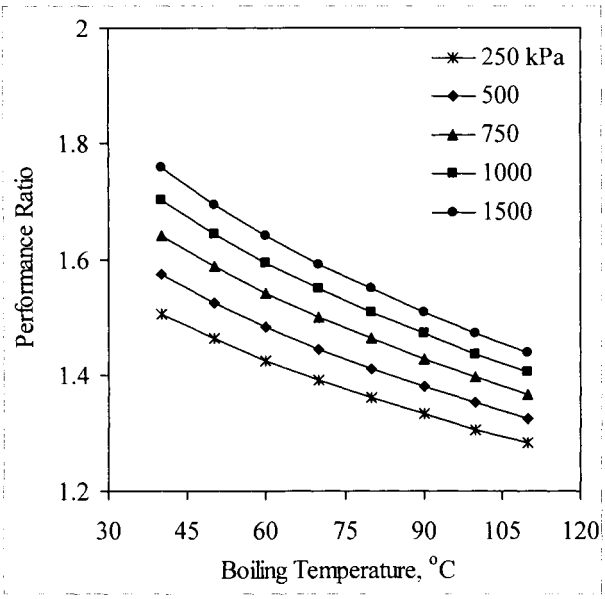

Fig. 4. Variations in the performance ratio as a function of the boiling temperature and the motive steam pressure.

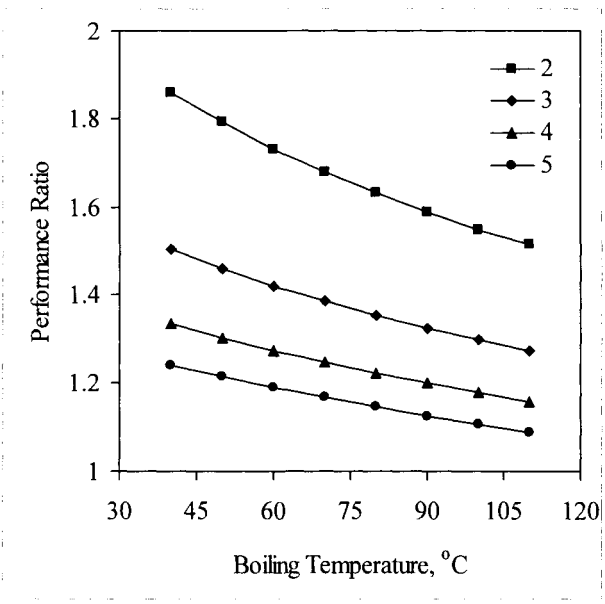

Fig. 5. Variations in the performance ratio as a function of the boiling temperature and the compression ratio.

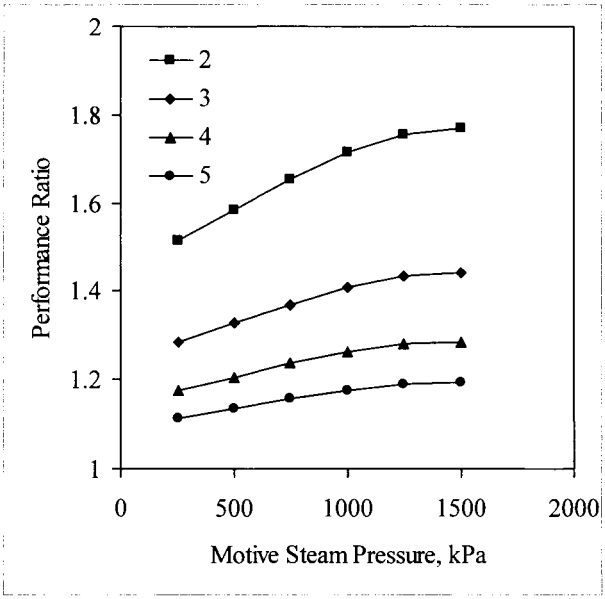

Fig. 6. Variations in the performance ratio as a function of the motive steam pressure and the compression ratio.

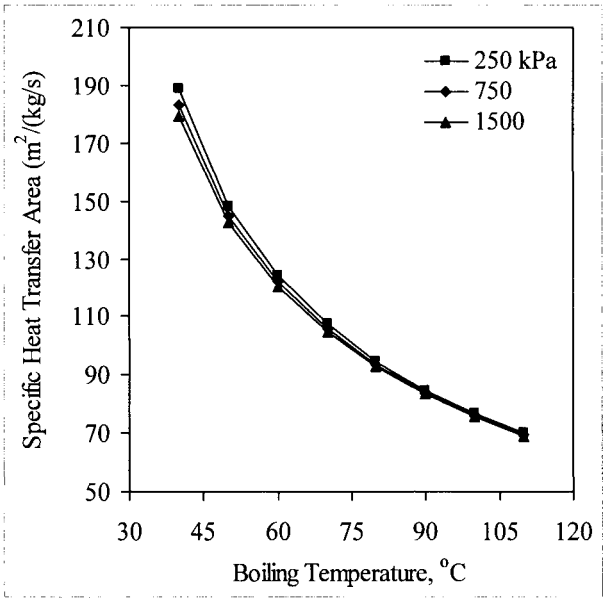

Fig. 7. Variations in the specific heat transfer area as a function of the boiling temperature and the motive steam pressure.

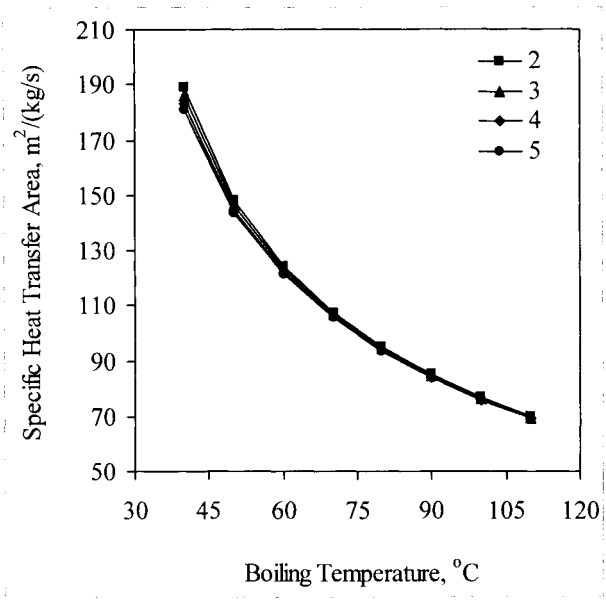

Fig. 8. Variations in the specific heat transfer area as a function of the boiling temperature and the compression ratio.

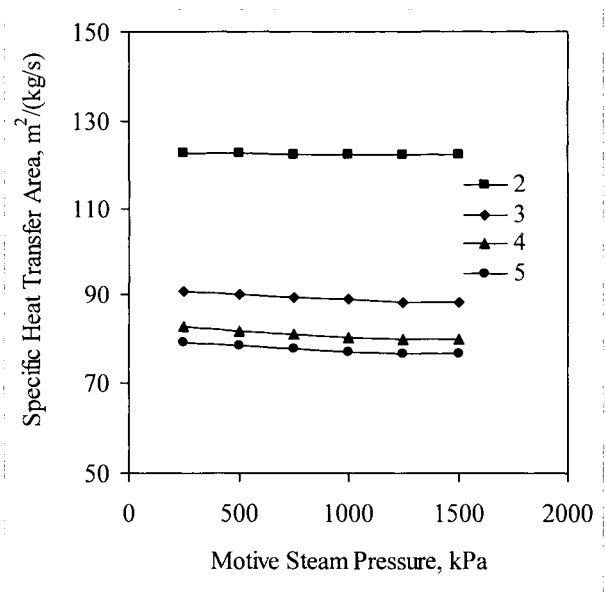

Fig. 9. Variations in the specific heat transfer area as a function of the motive steam pressure and the compression ratio.

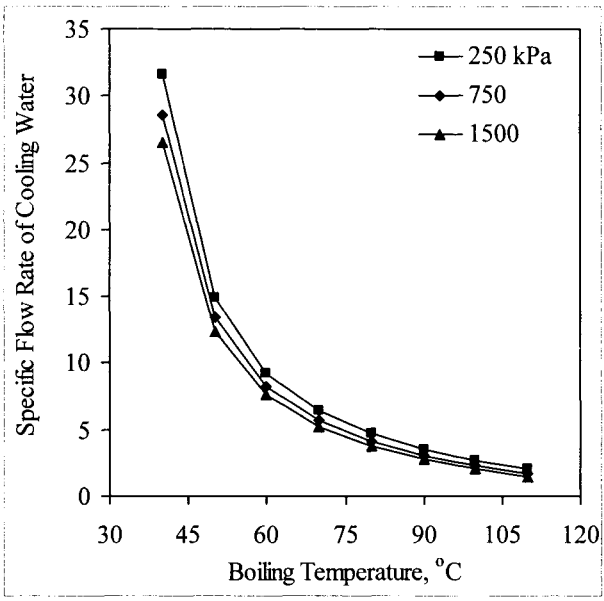

Fig. 10. Variations in the specific flow rate of cooling water as a function of the boiling temperature and the motive steam pressure.

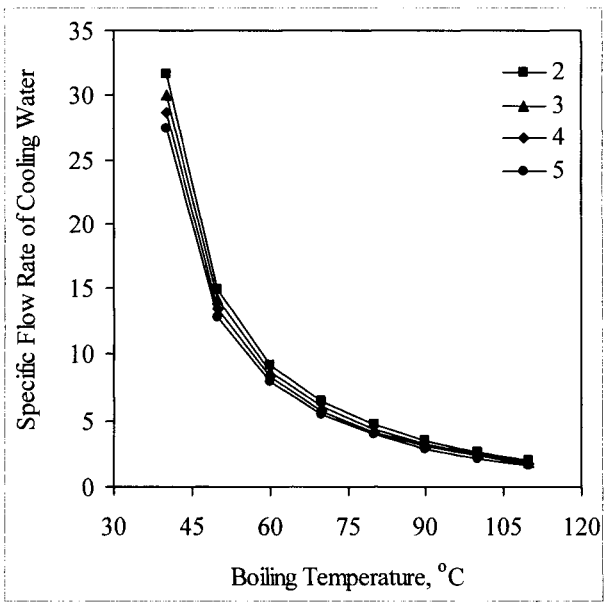

Fig. 11. Variations in the specific flow rate of cooling water as a function of boiling temperature and the compression ratio.

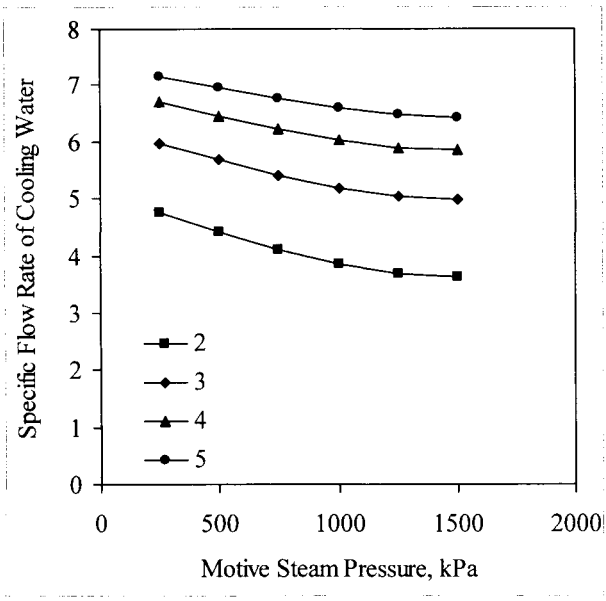

Fig. 12. Variations in the specific flow rate of cooling water as a function of the motive steam pressure and the compression ratio.

3.1.4 Summary

The TVC system is not found on industrial scale, however, its modeling, design, and analysis is considered because it provides the basis for the more complex system of multiple effect evaporation with thermal vapor compression. The mathematical for the TVC system includes material and energy balance equations for the condenser and evaporator. Also, the model includes the heat transfer equations for the condenser and evaporator as well as an empirical equation for the steam jet ejector. The analysis of the system is made as a function of variations in the thermal performance ratio, the specific heat transfer area, and the specific flow rate of cooling water. The analysis is performed over a range of the boiling temperature, the motive steam pressure, and the compression ratio. The following conclusions are made in the light of the results and discussion given in the previous section:

- The performance ratio decreases with the increase of the boiling temperature and the compression ratio. This is because of the increase in the motive steam consumption. This increase is necessary in order to achieve the required level of vapor compression.

- The performance ratio increases, but with limited sensitivity, upon the increase in the motive steam pressure. This result is caused by small increase in the amount of entrained vapor at higher motive steam pressures. In turn, this reduces the amount of consumed motive steam.
- The specific heat transfer area and the specific cooling water flow rate are sensitive to variations in the boiling temperature and the compression ratio. Both design parameters decrease with the increase of the boiling temperature and the compression ratio. This is because of the increase in the overall heat transfer coefficient in the evaporator and condenser, which causes large enhancement in the heat transfer rate.
- The specific heat transfer area and the specific cooling water flow rate have limited sensitivity with variations in the motive steam pressure.

In summary, it is recommended to operate of the single-effect vapor-compression desalination unit at intermediate values for the boiling temperature, i.e., 70-80 °C, and low compression ratios, i.e., values close to 2. This is necessary to have performance ratios close to or higher than 1.5. In addition, at such conditions high reduction is observed in the specific heat transfer area and the specific cooling water flow rate. This reduction will lower the first cost, i.e., construction cost of the evaporator, condenser, and seawater pump. In addition, the operating cost will be lower as a result of reduction in the energy required to operate the seawater-pumping unit.

References

El-Dessouky, H., Modeling and simulation of thermal vapor compression desalination plant, Symposium on Desalination of Seawater with Nuclear Energy, Taejon, Republic of Korea, 26-30 May, 1997.

Marto, P.J. Heat transfer in condensers, in Boilers, Evaporators and Condensers, Kakac, S., Editor, John Wiley, N.Y., 1991.

Muller, A.C., Condensers, in Hemisphere Handbook of Heat Exchanger Design, Hewitt, G.F., Editor, Hemisphere, N.Y., 1991.

Power, B.R., Steam jet ejectors for process industries, McGraw-Hill, Inc., N.Y., 1994.

Sinnott, R.K., Coulson & Richardson's Chemical Engineering, Vol. 6, 2nd Ed., Butterworth Heinemann, Oxford, 1996.

Problems

1. Use the ejector model (Eqs. 14-16) to develop a performance diagram for the steam jet ejector as a function of the entrainment ratio (Ra = M_m/M_{ev}), compression ratio (Cr = P_s/P_{ev}), and expansion ratio (Er = P_m/P_{ev}). The chart will cover the following ranges ($0.2 \leq w \leq 10$), ($0.2 \leq Cr \leq 5$), and ($1 \leq Er \leq 1000$). Discuss variations in the entrainment ratio as a function of the expansion and compression ratios.
2. A TVC system is used to desalinate seawater at 35 °C with 42000 ppm salinity. The maximum allowable brine temperature is 100 °C. The heat transfer coefficient for the evaporator and the two preheaters is constant and equal to 5.016 kW/m^2 °C. The specific heat transfer area is 109.46 m^2 per (kg/s) of fresh water and the heat transfer area of the distillate preheater is 200 m^2. The flow rates of the hot and cold stream in the preheaters are equal. The temperatures of the distillate and rejected brine flowing from the preheaters are 45 °C and 40 °C, respectively. Calculate the thermal performance ratio.
3. Calculate the thermal performance ratio and the specific heat transfer area for a TVC system operating the following conditions:
   - Motive steam pressure = 845.4 kPa
   - Distillate product temperature = 100 °C
   - Boiling temperature = 95 °C
   - Feed salinity = 42000 ppm
   - Feed temperature = 30.44 °C
4. A TVC system generates a distillate product at a flow rate of 1 kg/s. The system operating temperatures are as follows:
   - The boiling temperature, T_b, is 90 °C.
   - The feed temperature, T_f, is 85 °C.
   - The compressed vapor temperature, T_s, is 102 °C.
   - The motive steam pressure, P_m, is 15 bar.

   Determine the heat transfer areas in the evaporator and the condenser, the thermal performance ratio, the flow rates of feed seawater and reject brine, and the flow rate of cooling seawater. Assume the following:
   - The specific heat of seawater and brine streams is constant and equal to 4.2 kJ/kg °C.
   - Use the correlations for the overall heat transfer coefficient given in Appendix C.
   - Neglect thermodynamic losses in the demister and during condensation.
5. A single effect evaporator with a thermal load, Q_e, of 26500 kJ/s and the heating steam temperature is 105 °C is converted into a TVC system. The seawater temperature, T_{cw}, is 15 °C and the feed seawater temperature, T_f, is less than the boiling temperature, T_b, by 5 °C. The motive steam pressure

is 10 bars. Calculate the performance ratio before and after turning the system into the TVC configuration. Also, calculate the heat transfer area of the evaporator and condenser. Note that turning the system from the single effect configuration to the TVC mode has no effect on effect on the heat transfer area.

6. The heat transfer area in the evaporator and condenser for a TVC system is 90 and 30 m^2, respectively. The system is designed to operate at temperature of 85 °C for the boiling brine and an intake seawater temperature of 15 °C. Calculate the feed seawater temperature, the heating steam temperature, the steam flow rate, the cooling seawater flow rate, and the system performance ratio. Use a motive steam pressure of 5 bars.
7. A thermal vapor compression system operates at the following conditions:
   - Product flow rate = 10 kg/s
   - Feed water salinity = 42000 ppm
   - Feed water temperature = 14.4 °C
   - Pressure of motive steam = 4.6 kWm2 °C

   Calculate the following:
   - The evaporator heat transfer area.
   - The thermal performance ratio.
   - The change in the thermal performance ratio for the following conditions:
     - The feed water temperature increases to 30 °C.
     - The evaporation increases to 100 °C.
     - The motive steam pressure decreases to 500 kPa.
8. If the seawater temperature drops to 5 °C in problem 4, determine this effect on the system thermal performance ratio. Note that the heat transfer area remains constant as well as the heating steam temperature and the brine boiling temperature. What would be your recommendation to restore the system performance ratio to its original value.

3.2 Single Effect Mechanical Vapor Compression

The single-effect mechanical vapor-compression desalination process (MVC) is the most attractive among various single stage desalination processes. The MVC system is compact, confined, and does not require external heating source, which is opposite to thermal, absorption, or adsorption vapor compression. The system is driven by electric power; therefore, it is suitable for remote population areas with access to power grid lines. Another advantage of the MVC system is the absence of the down condenser and the cooling water requirements. This is because the compressor operates on the entire vapor formed within the system. Other advantages of the system include:

- Moderate investment cost.
- Proven industrial reliability to long lifetime operation.
- Simple seawater intake and pretreatment.
- The system adopts the horizontal falling film tube configuration, which allows for high heat transfer coefficient.
- The low temperature operation, 60 °C, allows for reduced scaling and heat losses and minimum requirement of thermal insulation.
- The system is modular type and it is simple to enlarge production volume by adopting additional modules.
- High product purity.
- Simple system adjustment to load variations, through temperature manipulation.

The major part of literature studies of the MVC system is focused on description of system characteristics and performance. Literature studies concerning modeling and analysis are limited to a small number, which includes:

- In 1981, Matz and Fisher compared the economics of the MVC system to the reverse osmosis (RO) desalination processes. The analysis was motivated by the need for integrated and compact desalination systems for remote resort areas. The MVC and RO systems are operated by electric current and do not require energy from external steam boilers. Comparison, based on power consumption, show that the specific power consumption for the RO system is 10-8 kWh/m^3 and for the MVC is 18.5–10 kWh/m^3. Further, the study predicted that future development of either system is expected to reduce the power consumption down to 5 kWh/m^3 for the RO system and to 8 kWh/m^3 for the MVC system. The main conclusion made by Matz and Fisher, 1981, is that neither system has a definitive edge, regarding the total production cost. This is because other cost elements in the RO system, which include membrane replacement and intensive chemical treatment, result in comparable total product cost for both systems.
- Lucas and Tabourier, 1985, reported performance data for single, two, four, and six effect MVC systems. The capacities for these systems vary from 300-

2500 m^3/d for the single and the six effect systems, respectively. They reported a specific power consumption of 11 kWh/m^3, which lay within the range reported by Matz and Fisher, 1981. In the single-effect configuration, the compressor increases the vapor temperature from 58 °C to 63 °C, which gives a compression ratio of 1.3. This ratio is 1.85 in the four-effect system, because the vapor temperature is increased from 49.5 °C to 62.5 °C. A range of 2-4 °C is reported for the temperature difference between the hot and cold streams in the feed preheaters.

- Matz and Zimerman (1985) reported similar performance and economic data for single and two effect vapor compression systems. The system operate at capacities between 50-1000 m^3/d, low top brine temperature between 50-70 °C, and specific power consumption slightly below 10 kWh/m^3.
- A decade later, Zimerman (1994) reported expansion of the MVC industry to more than 200 units operating in single or multi-effect modes. Although, the number is much larger than the few units found in 1985, it represents a small fraction in the global desalination industry, more than 12,000 operating units dominated by MSF and RO.
- Veza, 1995, reported on reliability of two MVC units installed in Canary Islands in 1987 and 1989. Over this period, the plant factor for both units vary between 87 and 90% with specific power consumption of 10.4-11.2 kWh/m^3 and a production capacity of 500 m^3/d/unit. The high plant factor is caused by low temperature operation, 60 °C, which reduces the scale formation rate.
- Comparison of the MVC versus other single effect desalination processes is studied by Al-Juwayhel et al., 1997. The study includes mathematical models for MVC system as well as other systems. Analysis of the MVC system focused on determination of the specific power consumption as a function of the top brine temperature. Model results are found consistent with literature data, where the specific power consumption varied over a range of 8-16 kWh/m^3.

In summary, it can be concluded that the MVC system remains to be used on a limited scale, however, it has high operation reliability, its specific power consumption is comparable to the RO system, and its production capacity suits either small or large consumption rates. Simulation studies are focused on economic comparison of MVC, RO, and other desalination systems. Other simulation analysis includes simplified mathematical models for the system or models for analyzing the plant energy consumption.

3.2.1 Process Description

The MVC system contains five major elements, which include mechanical vapor compressor, evaporator, preheaters for the intake seawater, brine and product pumps, and venting system. Figure 13 shows a schematic diagram for

the system. As is shown, the compressor and evaporator form one single unit. The evaporator contains falling film horizontal tubes, spray nozzles, suction vapor tube, and wire-mesh mist eliminator. The feed preheaters are plate type heat exchanger, which operates on the intake seawater and the hot liquid streams leaving the evaporator.

The feed seawater enters the evaporator at a flow rate of M_f and a temperature of T_f. The feed seawater is sprayed over the horizontal tubes. The spray forms a falling film over succeeding tube rows. Formation of the thin film enhances the heat transfer rate and makes the evaporation process more efficient. The seawater temperature increases from T_f to T_b before evaporation commences. The formed vapors, M_d, are at a temperature of T_b. The vapors transfer from the evaporator section to the compressor through the vapor suction tube, which is guarded by a wire-mesh mist eliminator. This is necessary to avoid entrainment of brine droplets in the vapor stream, which would result in damage of the compressor blades. Limited temperature depression occurs as the vapors flow through the demister. The vapors flow tangentially through the compressor, where it is superheated from T_b to T_s. Upon compression, the vapors are forced inside the horizontal tubes, where it loses the superheat energy and its temperature drops from T_s to the saturation temperature T_d. Condensation takes place at T_d and the released latent heat is transferred to the brine film. The temperature difference T_s-T_b affects the compressor power consumption and is dictated by the temperature of the feed seawater.

The balance of energy within the system is maintained by recovery of the thermal load in the rejected brine and product streams. This is achieved in the feed preheater, which a plate type heat exchanger. In this unit, the intake seawater is at a low temperature, t_{cw}, and a flow rate M_f. The rejected brine and product streams leaving the evaporator are at higher temperatures of T_b and T_d, respectively. As heat is exchanged between the three streams the temperature of the seawater is increased to T_f and the temperature of the rejected brine and product streams is reduced to T_o.

Temperature profiles of the system are shown in Fig. 14. As is shown, the temperature of the feed seawater increases from T_{cw} to T_f in the preheater unit. Simultaneously, the temperatures of the rejected brine and the product stream decrease from T_b and T_d, respectively, to the same temperature T_o. Inside the evaporator, the temperature of the feed seawater increases from T_f to the boiling temperature T_b. The formed vapor is at the same boiling temperature, which is higher than the saturation temperature, T_v, by the boiling point elevation, T_b-T_v.

The formed vapor is compressed and superheated to a temperature T_s. Condensation of the compressed vapor takes place at a temperature of T_d.

Ranges of the temperature difference of various streams are:
- The difference (T_s-T_d) varies from 4 to 10 °C,
- The difference (T_b-T_f) varies from 1-5 °C,
- The difference (T_d-T_b) varies from 1-5 °C, and
- The difference (T_o-T_{cw}) varies from 1-5 °C.

Maintaining the temperature differences within these ranges is essential to achieve the following:
- Keep the compressor power consumption within practical limits.
- Avoid excessive increase in the evaporator heat transfer area.
- Operate the preheater units at reasonable LMTD values to minimize the heat transfer area.

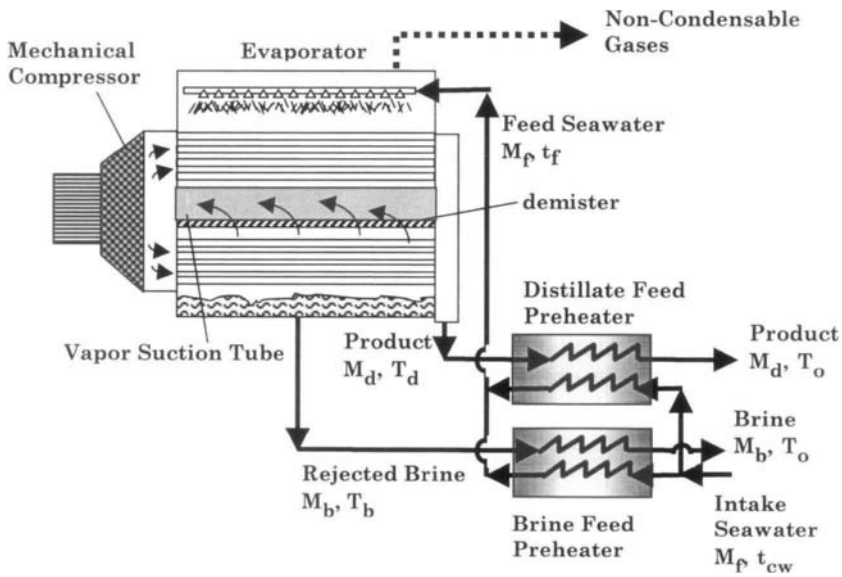

Fig. 13. Single effect mechanical vapor compression (MVC).

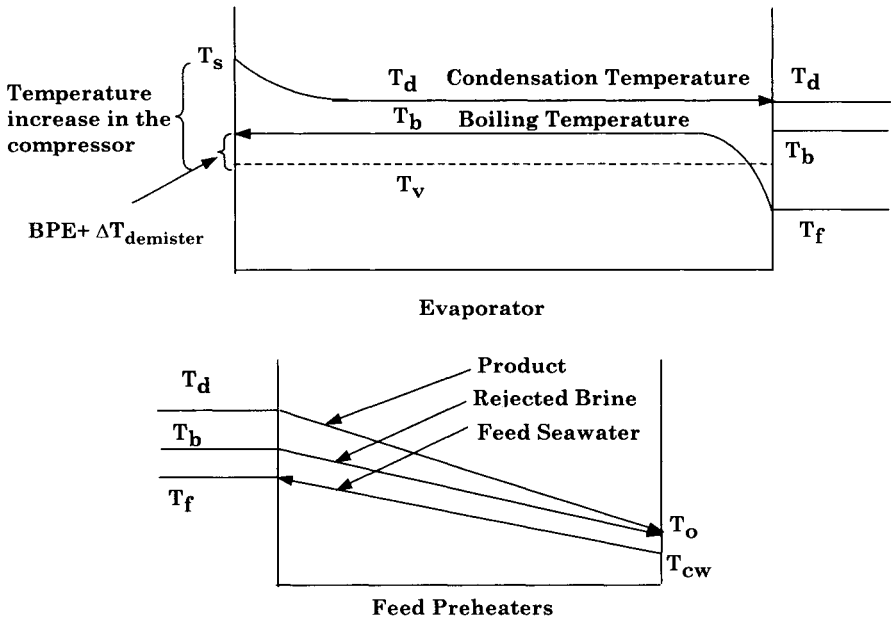

Fig. 14. Temperature profiles in MVC.

3.2.2 Process Modeling

Two models are developed for the MVC system; the first model includes several simplifying assumptions. This results in closed form solution that does not require iterative solution method. Such model is simple to use and generates useful results, which can be used for quick assessment of design and operating data. The second model negates the simplifying assumptions adopted in the first model. This makes the equations non-linear; therefore iterative solution is needed to determine the system characteristics.

Simplified MVC Model

The assumptions invoked in development of this model include the following:

- Different heat transfer areas for the preheaters,
- Constant, but not equal, overall heat transfer coefficients in the evaporator and preheaters.
- Equal temperature for the effluent heating streams in the preheaters.
- The heat capacity for all streams is constant and equal to 4.2 kJ/kg °C.

- The latent heat of formed vapor and condensing steam are temperature dependent.
- Effect of the boiling point elevation is neglected.
- The distillate is salt free.
- The driving force for heat transfer in the evaporator is assumed constant and equal to the difference between the condensation and evaporation temperatures.

The model is into four parts, which include the following:
- Material balances.
- Evaporator and preheaters energy balances.
- Evaporator and preheaters heat transfer area.
- Performance parameters.

Material Balances

The overall mass and salt balances are given by

$$M_f = M_d + M_b \tag{17}$$

$$M_f X_f = M_b X_b \tag{18}$$

where M is the mass flow rate, X is the salinity, and the subscripts b, d, and f denotes the rejected brine, distillate, and feed seawater. Equation 1 can be used to eliminate M_f from Eq. 18 and to generate a relation between M_b and M_d. This result is given by

$$M_b = M_d (X_f/(X_b - X_f)) \tag{19}$$

Similarly, M_b can be eliminated from Eq. 18 to generate a relation between M_f and M_d. This result is given by

$$M_f = M_d (X_b/(X_b - X_f)) \tag{20}$$

Evaporator and Feed Preheaters Energy Balances

Two preheaters are used to increase the feed temperature from the intake seawater temperature T_{cw} to T_f. The intake seawater is divided into two portions, αM_f and $(1-\alpha)M_f$. In the first preheater, heat is exchanged between αM_f and the condensed vapors, and in the second preheater, heat is exchanged between $(1-\alpha)M_f$ and the rejected brine. The thermal load of the two heat exchangers is given in terms of the intake seawater

$$Q_h = M_f C_p (T_f - T_{cw}) \quad (21)$$

The seawater feed flow rate given by Eq. (20) is substitute in Eq. (21). This gives

$$Q_h = M_d C_p (X_b/(X_b - X_f)) (T_f - T_{cw}) \quad (22)$$

Equation (21) can be also written in terms of the heat load of the condensed vapor and the rejected brine, which gives

$$Q_h = M_d C_p (T_d - T_o) + M_b C_p (T_b - T_o) \quad (23)$$

The brine flow rate, M_b, given by Eq. (19) is substituted in Eq. (23). This reduces Eq. (23) into

$$Q_h = M_d C_p (T_d - T_o) + M_d (X_f/(X_b - X_f)) C_p (T_b - T_o) \quad (24)$$

Equating Eqs. (22) and (24) gives

$$(M_d C_p (T_d - T_o) + M_d (X_f/(X_b - X_f)) C_p (T_b - T_o)) = M_d C_p (X_b/(X_b - X_f)) (T_f - T_{cw}) \quad (25)$$

Equation (25) is simplified to determine the outlet temperature of the heating streams, T_o, which gives

$$T_o = (T_{cw} - T_f) + (X_f / X_b) T_b + ((X_b - X_f)/X_b) T_d \quad (26)$$

In the evaporator, heat is supplied to the feed seawater, where its temperature increases from T_f to T_b. Also, latent heat is consumed by the formed vapor at a temperature of T_b. This energy is supplied by the latent heat of condensation for the compressed vapors at T_d and by the superheat of the compressed vapors, T_s-T_d. The evaporator thermal load is given by

$$Q_e = M_f C_p (T_b - T_f) + M_d \lambda_b = M_d \lambda_d + M_d C_{p_v} (T_s - T_d) \quad (27)$$

In the above equation λ_b and λ_d are the latent heat of formed vapor at T_b and condensing vapor at T_d. The feed flow rate given by Eq. (20) is substituted in Eq. (27). The resulting equation is

$$M_d (X_b/(X_b - X_f)) C_p (T_b - T_f) + M_d \lambda_b = M_d \lambda_d + M_d C_{p_v} (T_s - T_d) \quad (28)$$

Equation (28) is then simplified to determine the seawater feed temperature, T_f. This is given by

$$T_f = ((X_b - X_f)/X_b)\,((\lambda_b - \lambda_d)/C_p - (C_{p_v}/C_p)\,(T_s - T_d)) + T_b \tag{29}$$

Evaporator and Condenser Heat Transfer Area

The heat transfer area for the evaporator is determined in terms of thermal load, the driving force for heat transfer, and the overall heat transfer coefficient. The thermal load for the evaporator is equal to the sum of the latent heat of formed vapor at T_b and the sensible heat added to the feed seawater to increase its temperature from T_f to T_b. The driving force for heat transfer is assumed equal to the difference between the condensation and evaporation temperatures, T_d-T_b. As for the overall heat transfer coefficient it is calculated from the correlation given in Appendix C. This evaporator heat transfer area is then given by

$$A_e = \frac{M_d\lambda_b + M_f C_p(T_b - T_f)}{U_e(T_d - T_b)} = \frac{M_d\lambda_d + M_d C_{p_v}(T_s - T_d)}{U_e(T_d - T_b)} \tag{30}$$

The heat transfer area for the two preheaters obtained in similar manner, however, the driving force for heat transfer is taken as the logarithmic mean at the preheater ends. These equations are given by

$$A_d = \frac{M_d C_p(T_d - T_o)}{U_d(LMTD)_d} = \frac{\alpha M_f C_{p_\ell}(T_f - T_{cw})}{U_d(LMTD)_d} \tag{31}$$

$$\begin{aligned} A_b &= \frac{M_b C_p(T_b - T_o)}{U_b(LMTD)_b} \\ &= \frac{M_d(X_f/(X_b - X_f))C_p(T_b - T_o)}{U_b(LMTD)_b} \\ &= \frac{(1-\alpha)M_f C_p(T_f - T_{cw})}{U_b(LMTD)_b} \end{aligned} \tag{32}$$

The $(LMTD)_d$ is defined as:

$$(LMTD)_d = \frac{(T_d - T_f) - (T_o - T_{cw})}{\ln\dfrac{T_d - T_f}{T_o - T_{cw}}} \tag{33}$$

The $(LMTD)_b$ is defined as:

$$(LMTD)_b = \frac{(T_b - T_f) - (T_o - T_{cw})}{\ln \frac{T_b - T_f}{T_o - T_{cw}}} \tag{34}$$

Performance Parameters

Performance of the MVC is determined in terms of the following variables:
- The specific power consumption, kWhr/m^3.
- The specific heat transfer surface area, sA.

The compressor mechanical energy is given

$$W = \frac{\gamma}{\eta(\gamma - 1)} P_v v_v \left(\left(\frac{P_s}{P_v} \right)^{\left(\frac{\gamma - 1}{\gamma} \right)} - 1 \right) \tag{35}$$

where W is specific power consumption, P is the pressure, v is the specific volume, η is the compressor efficiency, and γ is the isentropic efficiency. It should be noted that the inlet pressure (P_v) is equal to the vapor pressure of the formed vapor at (T_b) and the outlet pressure (P_s) is the compressed vapor pressure at (T_s).

The specific heat transfer area is obtained by summing Eqs. (30-32). The resulting summation is divided by M_d, which results in

$$\begin{aligned} sA &= \frac{A_e + A_d + A_b}{M_d} \\ &= \frac{\lambda_d + C_{p_v}(T_s - T_d)}{U_e(T_d - T_b)} + \frac{C_p(T_d - T_o)}{U_d(LMTD)_d} + \frac{(X_f/(X_b - X_f))C_p(T_b - T_o)}{U_b(LMTD)_b} \end{aligned} \tag{36}$$

Solution of MVC Simple Model

Solution of the above model is sequential and requires no iterations. Solution proceeds as follows:
- The mass flow rates of the reject brine and feed seawater, M_b and M_f, are calculated from Eqs. (20) and (21).
- The seawater feed temperature, T_f, is obtained from Eq. (29).
- The effluent temperature of heat streams, T_o, is obtained from Eq. (26).

- The areas for evaporator, brine preheater, and product preheater, are calculated from Eqs. (30-32).
- The specific power consumption, W, is obtained from Eq. (35).
- The specific heat transfer area, sA, is obtained from Eq. (36).

Example 1:

A single-effect mechanical vapor-compression system is to be designed at the following conditions:

- The distillate flow rate, M_d = 1 kg/s.
- The heat capacity of the vapor is constant, C_{p_v} = 1.884 kJ/kg °C.
- The heat capacity of all liquid streams is constant, C_p = 4.2 kJ/kg °C.
- The overall heat transfer coefficient in the evaporator, U_e = 2.4 kJ/s m^2 °C.
- The overall heat transfer coefficient in the brine preheater, U_b = 1.5 kJ/s m^2 °C.
- The overall heat transfer coefficient in the product preheater, U_d = 1.8 kJ/s m^2 °C.
- The intake seawater temperature, T_{cw} = 25°C.
- The condensed vapor temperature, T_d = 62 °C.
- The compressed vapor temperature, $T_s = T_d + 3$ = 65 °C.
- The evaporation temperature, $T_b = T_d - 2$ = 60 °C.
- The feed seawater salinity, X_f = 42000 ppm.
- The salinity of the rejected brine, X_b = 70000 ppm.
- Compressor efficiency, η = 58.9%

Calculate the specific power consumption, the heat transfer areas for the evaporator and preheaters, and the specific heat transfer area.

Solution

Substituting for X_f = 42000 ppm, X_b = 70000 ppm, and M_d = 1 kg/s in Eq. (20) results in

$$M_f = X_b/(X_b - X_f) = 70000/(70000 - 42000) = 2.5 \text{ kg/s}$$

Equation (17) is then used to calculate M_b,

$$M_b = M_f - M_d = 2.5 - 1 = 1.5 \text{ kg/s}$$

The latent heats of condensation and evaporation, λ_d and λ_b, are then calculated from the correlation given in Appendix (A).

$$\lambda_d = 2499.5698 - 2.204864\ T_d - 2.304x10^{-3} T_d^2$$
$$= 2499.5698 - 2.204864\ (62) - 2.304x10^{-3}\ (62)^2 = 2354.01\ kJ/kg$$
$$\lambda_b = 2499.5698 - 2.204864\ T_b - 2.304x10^{-3} T_b^2$$
$$= 2499.5698 - 2.204864\ (60) - 2.304x10^{-3}\ (60)^2 = 2358.98\ kJ/kg$$

Equation (29) is used to calculate T_f

$$T_f = ((X_b - X_f)/X_b)\ ((\lambda_b - \lambda_d)/Cp - (Cp_v/Cp)\ (T_s - T_d)) + T_b$$
$$= ((70000-42000)/70000)\ ((2358.98-2354.01)/4.2 - (1.884/4.2)\ (65 - 62)) + 60$$
$$= 59.39\ ^oC$$

Equation (26) is used to calculate T_o

$$T_o = (T_{cw} - T_f) + (X_f / X_b)\ T_b + ((X_b - X_f)/X_b)\ T_d$$
$$= (25 - 58.73) + (42000/70000)\ (60) + ((70000 - 42000)/70000)\ (62)$$
$$= 26.4\ ^oC$$

The evaporator area is calculated from Eq. (30)

$$A_e = \frac{M_d \lambda_d + M_d C_{p_v} (T_s - T_d)}{U_e (T_d - T_b)}$$
$$= \frac{(1)(2354.01) + (1)(1.884)(65 - 62)}{(2.4)(62 - 60)}$$
$$= 492.77\ m^2$$

The value of $(LMTD)_d$ is obtained from Eq. (33)

$$(LMTD)_d = \frac{(T_d - T_f) - (T_o - T_{cw})}{\ln \frac{T_d - T_f}{T_o - T_{cw}}}$$
$$= \frac{(62 - 59.39) - (26.4 - 25)}{\ln \frac{62 - 59.39}{26.4 - 25}} = 1.94\ ^oC$$

Similarly the value of $(LMTD)_b$ is determined from Eq. (34)

$$(LMTD)_b = \frac{(T_b - T_f) - (T_o - T_{cw})}{\ln \frac{T_b - T_f}{T_o - T_{cw}}}$$

$$= \frac{(60 - 59.39) - (26.4 - 25)}{\ln \frac{60 - 59.39}{26.4 - 25}} = 0.95\ ^{o}C$$

The heat transfer area for the two preheaters are determined from Eqs. (31-32)

$$A_d = \frac{M_d C_p (T_d - T_o)}{U_d (LMTD)_d} = \frac{(1)(4.2)(62 - 26.4)}{(1.8)(1.94)} = 42.78\ m^2$$

$$A_b = \frac{M_b C_p (T_b - T_o)}{U_b (LMTD)_b} = \frac{(1.5)(4.2)(60 - 26.4)}{(1.5)(0.95)} = 148.94\ m^2$$

The specific power consumption, W, is calculated from Eq. (35). This requires determination of P_O, P_i, v_i, and γ. The compressor inlet and outlet pressures, P_i and P_O, is equal to the saturation pressure of compressed vapor at T_s and the formed vapor at T_d, respectively. These values can be obtained from the steam tables or from the correlation given in Appendix A:

$$P_o = 10.17246 - 0.6167302 (T_s) + 1.832249 x 10^{-2} (T_s)^2$$
$$- 1.77376 x 10^{-4} (T_s)^3 + 1.47068 x 10^{-6} (T_s)^4$$
$$= 10.17246 - 0.6167302 (65) + 1.832249 x 10^{-2} (65)^2$$
$$- 1.77376 x 10^{-4} (65)^3 + 1.47068 x 10^{-6} (65)^4 = 25.03\ kPa$$

$$P_i = 10.17246 - 0.6167302 (T_b) + 1.832249 x 10^{-2} (T_b)^2$$
$$- 1.77376 x 10^{-4} (T_b)^3 + 1.47068 x 10^{-6} (T_b)^4$$
$$= 10.17246 - 0.6167302 (60) + 1.832249 x 10^{-2} (60)^2$$
$$- 1.77376 x 10^{-4} (60)^3 + 1.47068 x 10^{-6} (60)^4 = 19.88\ kPa$$

The specific volume of inlet vapor at T_b can be obtained from steam tables or the correlation given in the Appendix (A). This given by

$$v_i = 163.3453 - 8.04142(T_b) + 0.17102(T_b)^2$$
$$-1.87812x10^{-3}(T_b)^3 + 1.03842x10^{-5}(T_b)^4 - 2.28215x10^{-8}(T_b)^5$$
$$= 163.3453 - 8.04142(60) + 0.17102(60)^2$$
$$-1.87812x10^{-3}(60)^3 + 1.03842x10^{-5}(60)^4 - 2.28215x10^{-8}(60)^5$$
$$= 4.836\ m^3/kg$$

The value of the compression ratio γ is 1.32. The specific power consumption is then calculated from Eq. (35)

$$W = \frac{\gamma}{\eta(\gamma-1)} P_i v_i \left(\left(\frac{P_o}{P_i} \right)^{\left(\frac{\gamma-1}{\gamma}\right)} - 1 \right)$$

$$= \frac{1.32}{0.589(1.32-1)} (19.88)(7.69) \left(\left(\frac{25.03}{19.88} \right)^{\left(\frac{1.32-1}{1.32}\right)} - 1 \right) \left(\frac{1000}{3600} \right)$$

$$= 17.13\ kWhr/m^3$$

The specific heat transfer area is obtained directly by summing the values of A_e, A_b, and A_b. This is because the distillate flow-rate is set at 1 kg/s. The value of sA is equal to 492.78 + 42.78 + 148.94 = 684.49 m^2.

Example 2:

A single-effect mechanical vapor-compression system has the following design data:

- Evaporator heat transfer area = 400 m^2.
- Distillate feed preheater heat transfer area = 7 m^2.
- Brine feed preheater heat transfer area = 15 m^2.
- The heat capacity of the vapor is constant, C_{p_v} = 1.884 kJ/kg °C.
- The heat capacity of all liquid streams is constant, C_p = 4.2 kJ/kg °C.
- The overall heat transfer coefficient in the evaporator, U_e = 2.4 kW/m^2 °C.
- The overall heat transfer coefficient in the brine preheater, U_b = 6.3 kW/ m^2 °C.
- The overall heat transfer coefficient in the distillate preheater, U_d = 6.7 kW/m^2 °C.
- The intake seawater temperature, T_{cw} = 25°C.

- The compressed vapor temperature, $T_s = (T_d + 7)\ ^oC$.
- The feed seawater salinity, $X_f = 42000$ ppm.
- The salinity of the rejected brine, $X_b = 70000$ ppm.
- Compressor efficiency, $\eta = 58.9\%$

Calculate the following:

- Flow rate of the distillate product.
- Flow rate of the brine reject
- Flow rate of the feed seawater.
- Temperature of the feed seawater.
- Temperature of the outlet brine and product streams.
- Temperature of the brine stream leaving the evaporator.
- Temperature of the condensate product stream.

Solution of this problem is iterative, where the following equations are solved iteratively. Equation solution can be simultaneous or sequential. The equations include the following:

$$M_f = (M_d X_b)/(X_b - X_f)$$

$$M_b = M_f - M_d$$

$$T_f = ((X_b - X_f)/X_b)\ ((\lambda_b - \lambda_d)/Cp - (Cp_v/Cp)\ (T_s - T_d)) + T_b$$

$$T_o = (T_{cw} - T_f) + (X_f / X_b)\ T_b + ((X_b - X_f)/X_b)\ T_d$$

$$A_e = \frac{M_d \lambda_d + M_d C_{p_v} (T_s - T_d)}{U_e (T_d - T_b)}$$

$$A_d = \frac{M_d C_p (T_d - T_o)}{U_d (LMTD)_d}$$

$$A_b = \frac{M_b C_p (T_b - T_o)}{U_b (LMTD)_b}$$

The assumed initial guess include the following:

- $M_d = 0.8$ kg/s
- $T_d = 74\ ^oC$
- $T_b = 72\ ^oC$

Solution of the first two equations gives M_f and M_b

$$M_f = M_d X_b / (X_b - X_f) = (0.8)(70000)/(70000 - 42000) = 2 \text{ kg/s}$$

$$M_b = M_f - M_d = 2 - 0.8 = 1.2 \text{ kg/s}$$

The latent heats of condensation and evaporation, λ_d and λ_b, are calculated from correlation given in Appendix (A)

$$\lambda_d = 2499.5698 - 2.204864\, T_d - 2.304x10^{-3} T_d^2$$
$$= 2499.5698 - 2.204864\,(74) - 2.304x10^{-3}\,(74)^2 = 2323.79 \text{ kJ/kg}$$

$$\lambda_b = 2499.5698 - 2.204864\, T_b - 2.304x10^{-3} T_b^2$$
$$= 2499.5698 - 2.204864\,(72) - 2.304x10^{-3}\,(72)^2 = 2328.88 \text{ kJ/kg}$$

The third equation is used to calculate T_f

$$T_f = ((X_b - X_f)/X_b)\,((\lambda_b - \lambda_d)/Cp - (Cp_v/Cp)\,(T_s - T_d)) + T_b$$
$$= ((70000-42000)/70000)\,((2328.88-2323.79)/4.2 - (1.884/4.2)\,(7)) + 72$$
$$= 71.22\ ^oC$$

The fourth equation is used to calculate T_o

$$T_o = (T_{cw} - T_f) + (X_f / X_b)\, T_b + ((X_b - X_f)/X_b)\, T_d$$
$$= (25 - 71.22) + (42000/70000)\,(72) + ((70000 - 42000)/70000)\,(74)$$
$$= 26.58\ ^oC$$

The heat transfer equations are then used to update the initial guess, where the evaporator area is used to calculate a new value for M_d

$$A_e = \frac{M_d \lambda_d + M_d C_{p_v} (T_s - T_d)}{U_e (T_d - T_b)}$$
$$400 = \frac{(M_d)(2323.79) + (M_d)(1.884)(7)}{(2.4)(74 - 72)}$$

which gives $M_d = 0.82$ kg/s

The value of $(LMTD)_d$ for distillate product preheater is calculated

$$(LMTD)_d = \frac{(T_d - T_f) - (T_o - T_{cw})}{\ln \frac{T_d - T_f}{T_o - T_{cw}}} = \frac{(74 - 71.22) - (26.58 - 25)}{\ln \frac{74 - 71.22}{26.58 - 25}} = 2.124\ ^oC$$

Similarly the value of $(LMTD)_b$ is calculated for the brine preheater

$$(LMTD)_b = \frac{(T_b - T_f) - (T_o - T_{cw})}{\ln \frac{T_b - T_f}{T_o - T_{cw}}} = \frac{(72 - 71.22) - (26.58 - 25)}{\ln \frac{72 - 71.22}{26.58 - 25}} = 1.133 \ ^{o}C$$

The heat transfer area for the two preheaters are then used to update the condensate and brine streams leaving the evaporator

$$A_d = \frac{M_d C_p (T_d - T_o)}{U_d (LMTD)_d}$$

$$7 = \frac{(0.82)(4.2)(T_d - 26.58)}{(6.7)(2.124)}$$

which gives a new value for $T_d = 55.5$ °C

$$A_b = \frac{M_b C_p (T_b - T_o)}{U_b (LMTD)_b}$$

$$15 = \frac{(0.82)(4.2)(T_b - 26.58)}{(6.3)(1.133)}$$

which gives a new value for $T_b = 57.6$ °C. The iterations continue to give the following final solution:

- $M_d = 0.8$ kg/s
- $M_b = 1.2$ kg/s
- $M_f = 2$ kg/s
- $T_d = 74.8$ °C
- $T_b = 72.8$ °C
- $T_o = 27.8$ °C
- $T_f = 70.8$ °C

The specific power consumption (W) is calculated from Eq. (35). This requires determination of P_S, P_v, and v_v The compressor inlet and outlet pressures, P_v and P_S, is equal to the saturation pressure of compressed vapor at T_s and the formed vapor at T_d, respectively. These values can be obtained from the steam tables or from the correlation given Appendix (A):

- $P_v = 35.2$ kPa
- $P_S = 38.3$ kPa

- $v_v = 4.49\ m^3/kg$

The value of the compression ratio γ is 1.32. The specific power consumption is then calculated from Eq. (35)

$$W = \frac{\gamma}{\eta(\gamma-1)} P_v v_v \left[\left(\frac{P_s}{P_v} \right)^{\left(\frac{\gamma-1}{\gamma}\right)} - 1 \right]$$

$$= \frac{(0.8)(1.32)}{0.589\,(1.32-1)} (35.26)(4.49) \left[\left(\frac{38.311}{35.26} \right)^{\left(\frac{1.32-1}{1.32}\right)} - 1 \right] \left(\frac{1000}{3600} \right)$$

$$= 5\ kWhr/m^3$$

Detailed MVC Model

The assumptions used to develop the second model include the following:

- Different heat transfer areas for the preheaters
- Equal temperature for the effluent heating streams.
- The heat capacities for brine and product streams depend on temperature and composition.
- The Overall heat transfer coefficient in the preheaters is constant, but not equal.
- The latent heat of formed vapor and condensing steam are temperature dependent.
- The specific heat of the vapor is constant.
- The effect of the boiling point elevation, BPE, is included in the calculations.
- The distillate is salt free.
- The driving force for heat transfer in the evaporator is assumed constant and equal to the difference between the condensation and evaporation temperatures.

The basic model equations are similar to those given for the simplified model. However, mathematical manipulations of the energy balances cannot be made because of the nonlinear nature of the equations. Correlations for the boiling point elevation, saturation pressure, saturation volume, evaporator heat transfer coefficient, enthalpies of fresh water vapor and liquid, and the specific heat of the seawater and brine are given in the appendices. The following is a list of the equations used in the detailed model.

Material and salt balances

$$M_b = M_d\ (X_f /(X_b - X_f)) \tag{37}$$

$$M_f = M_d + M_b \tag{38}$$

Preheaters energy balances

$$M_f\, C_p\, (T_f - T_{cw}) = M_d\, C_p\, (T_b - T_o) + M_b\, C_p\, (T_b - T_o) \tag{39}$$

Evaporator energy balances

$$M_f\, C_p\, (T_b - T_f) + M_d\, \lambda_v = M_d\, \lambda_d + M_d\, C_{p_v}\, (T_s - T_d) \tag{40}$$

Evaporator heat transfer area

$$A_e = \frac{M_d \lambda_d + M_d C_{p_v} (T_s - T_d)}{U_e (T_d - T_b)} \tag{41}$$

Distillate/feed preheater heat transfer area

$$A_d = \frac{M_d C_p (T_d - T_o)}{U_d (\mathrm{LMTD})_d} = \frac{\alpha M_f C_p (T_f - T_{cw})}{U_d (\mathrm{LMTD})_d} \tag{42}$$

$$(\mathrm{LMTD})_d = \frac{(T_d - T_f) - (T_o - T_{cw})}{\ln \dfrac{T_d - T_f}{T_o - T_{cw}}} \tag{43}$$

Brine/feed preheater heat transfer area

$$A_b = \frac{M_b C_p (T_b - T_o)}{U_b (\mathrm{LMTD})_b} = \frac{(1-\alpha) M_f C_p (T_f - T_{cw})}{U_b (\mathrm{LMTD})_b} \tag{44}$$

$$(\mathrm{LMTD})_b = \frac{(T_b - T_f) - (T_o - T_{cw})}{\ln \dfrac{T_b - T_f}{T_o - T_{cw}}} \tag{45}$$

Performance parameters

$$W = \frac{\gamma}{\eta(\gamma-1)} P_i v_i \left(\left(\frac{P_o}{P_i} \right)^{\left(\frac{\gamma-1}{\gamma} \right)} - 1 \right) \tag{46}$$

$$sA = \frac{A_e + A_d + A_b}{M_d} = \frac{\lambda_d + C_{p_v}(T_s - T_d)}{U_e(T_d - T_b)} + \frac{(H(T_d) - H(T_o))}{U_d(LMTD)_d} + \frac{(X_f/(X_b - X_f))C_p(T_b - T_o)}{U_b(LMTD)_b} \tag{47}$$

Solution of MVC detailed Model

Specification made to solve the above equation system include:

- The distillate flow rate, M_d = 1 kg/s.
- The intake seawater temperature, T_{cw} = 25°C.
- The condensed vapor temperature, T_d = 62 °C.
- The range for compressed vapor temperature, $T_s = T_d + 3$ = 65 °C.
- The evaporation temperature, $T_b = T_d - 2$ = 60 °C.
- The heat capacity of the vapor is constant, C_{p_v} = 1.884 kJ/kg °C.
- The overall heat transfer coefficient in the brine preheater, U_b = 1.5 kJ/s m^2 °C.
- The overall heat transfer coefficient in the product preheater, U_d = 1.8 kJ/s m^2 °C.
- The feed seawater salinity, X_f = 42000 ppm.
- The salinity of the rejected brine, X_b = 70000 ppm.
- Compressor efficiency, η = 58.9%.

Solution proceeds as follows:

- The mass flow rates of the reject brine and feed seawater, M_b and M_f, are calculated from Eqs. (37-38).
- The temperatures of the seawater feed and the effluent heating stream, T_f and T_o, are obtained by iterative solution of Eqs. (39-40).
- The areas for evaporator, brine preheater, and product preheater, are calculated from Eqs. (41,42, 44).
- The specific power consumption, W, is obtained from Eq. (46).
- The specific heat transfer area, sA, is obtained from Eq. (47).

Example 3:

As presented in the simple model, substituting X_f = 42000 ppm, X_b = 70000 ppm, and M_d = 1 kg/s in Eq. 4 gives M_f = 2.5 kg/s. This value is substituted in Eq. (37) giving M_b = 1.5 kg/s. The overall heat transfer coefficients in the evaporator is then calculated from the following correlation

$$U_e = \left(1961.9 + 3.2(T_d) + 12.6\text{x}10^{-2}(T_b)^2 - 3.16\text{x}10^{-4}(T_b)^3\right)\text{x}10^{-3}$$
$$= \left(1961.9 + 3.2(60) + 12.6\text{x}10^{-2}(60)^2 - 3.16\text{x}10^{-4}(60)^3\right)\text{x}10^{-3}$$
$$= 2.438\ \text{kJ/s m}^2\ ^\circ\text{C}$$

Iterations are made to solve Eqs. (39) and (40), which proceeds as follows:

Iteration	T_f	T_o
Initial Guess	27.00000	59.00000
Iteration 1	27.00000	59.02030
Iteration 2	27.00932	59.00000
Iteration 3	26.54499	59.33199
Iteration 4	26.54495	59.33193

The evaporator area is calculated from Eq. (41)

$$A_e = \frac{M_d\lambda_d + M_d C_{p_v}(T_s - T_d)}{U_e(T_d - T_b)}$$
$$= \frac{(1)(2354.01) + (1)(1.884)(65-62)}{(2.438)(62-60)}$$
$$= 483.78\ \text{m}^2$$

The value of $(LMTD)_d$ is obtained from Eq. (43)

$$(LMTD)_d = \frac{(T_d - T_f) - (T_o - T_{cw})}{\ln\dfrac{T_d - T_f}{T_o - T_{cw}}}$$
$$= \frac{(62-59.33) - (26.54-25)}{\ln\dfrac{(62-59.33)}{(26.54-25)}} = 2.055\ ^\circ\text{C}$$

Similarly the value of $(LMTD)_b$ is determined from Eq. (45)

$$(LMTD)_b = \frac{(T_b - T_f) - (T_o - T_{cw})}{\ln \frac{T_b - T_f}{T_o - T_{cw}}}$$

$$= \frac{(60 - 59.33) - (26.54 - 25)}{\ln \frac{60 - 59.33}{26.54 - 25}} = 1.046 \ ^{o}C$$

The heat transfer area for the two preheaters are determined from Eqs. (42-44)

$$A_d = \frac{M_d(H(T_d) - H(T_o))}{U_d(LMTD)_d} = \frac{(1)\ (259.35 - 111.04)}{(1.8)(2.055)} = 40.08 \ m^2$$

$$A_b = \frac{M_b C_p (T_b - T_o)}{U_b (LMTD)_b} = \frac{(1.5)(3.845)(60 - 26.54)}{(1.5)(1.045)} = 123.01 \ m^2$$

The specific power consumption, W, and the specific heat transfer area are obtained from Eqs. (46) and (47), respectively. It should be noted that the value of W is identical to that obtained in the simplified model, because T_s and T_b have the same values. Therefore, values of P_s, P_v, and v_v, are the same and have values of 25.038 kPa, 19.78 kPa, and 7.69 m^3/kg, respectively. The resulting specific power consumption is 17.127 kWh/m^3. As for the specific heat transfer area, it is equal to the sum of A_e, A_d, and A_b; this gives a total value of 646.87 $m^2/(kg/s)$.

3.2.3 System Performance

The detailed model is used to simulate and analyze the performance of the MVC desalination process. Analysis is made as a function of the brine boiling temperature, T_b, and the temperature difference of the condensing vapor and the boiling brine, T_d -T_b. The brine boiling temperature is varied between 60 and 105 °C and temperature difference between 1 and 4 °C. All calculations are made for a distillate flow rate of 1 kg/s and a temperature difference of 3 °C between the compressed and condensing vapors, T_s-T_d. Results include the specific power consumption and the specific heat transfer areas for the evaporator and the two preheaters.

The specific power consumption for the system is shown in Fig. 15. As is shown, the specific power consumption increases at lower boiling temperatures and upon the increase of the temperature difference between the condensing vapor and the boiling brine. The decrease in the specific power consumption at

higher boiling temperatures is caused by the decrease in the vapor specific volume. Similarly, increase of the temperature difference between the condensing and formed vapors gives a larger compression ratio. Either effect increases the compressor power consumption. Levels of the specific power consumption shown in Fig. 15 vary between high values of 25 kWh/m^3 to low values below 10 kWh/m^3. In practice, the specific power consumption for the MVC system is close to 15 kWh/m^3 at a boiling temperature of 60 °C. Superposing these values on Fig. 15, indicate that the system is operated at temperature difference of 3 °C for (T_s-T_d) and between 1-2 °C for (T_d-T_b).

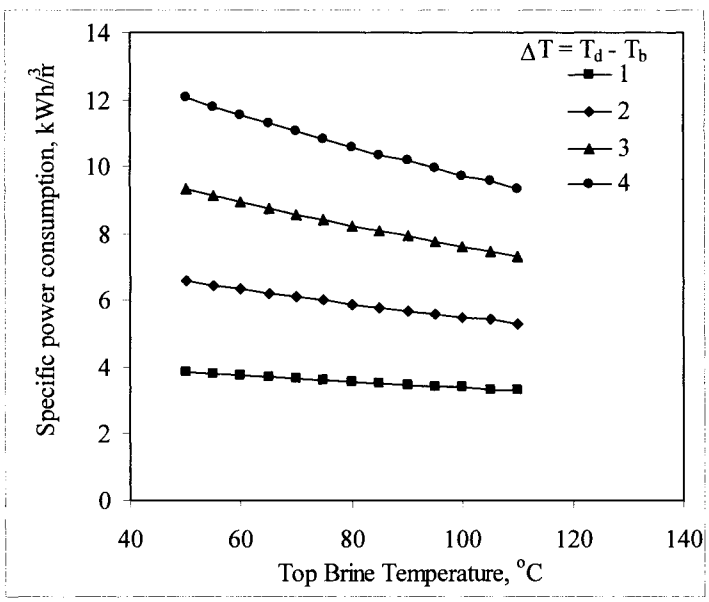

Fig. 15. Variation in specific power consumption for the evaporator as a function of top brine temperature and temperature difference of condensing steam and boiling brine.

Variations for the evaporator specific heat transfer area are shown in Fig. 16. The specific heat transfer area decreases at higher boiling temperatures and increases upon the decrease of the temperature difference between condensing vapor and boiling brine. Higher boiling temperatures enhance the heat transfer rates; this is because of the decrease in the liquid density and viscosity and the increase of the thermal conductivity of the liquid and metal walls. As a result, the overall heat transfer coefficient increases and results in reduction of the heat transfer area. The temperature difference of the condensing vapor and boiling

brine is the driving force for heat transfer across the evaporator tubes. Lowering this difference decreases the driving force for heat transfer and in turn increases the heat transfer area. As is shown in Fig. 16, the evaporator heat transfer area is more sensitive to variations in the temperature difference of the condensing vapor and boiling brine. Variations in the evaporator heat transfer area are limited to a low value of 8% as the boiling temperature is increased from 60 to 105 °C. On the other hand, a four folds increase occurs in the evaporator heat transfer area as the temperature difference of the condensing vapors and boiling brine is increased from 1 to °C. In actual practice, the evaporator specific heat transfer area varies between 400-600 $m^2/(kg/s)$ at boiling temperature of 60 °C. Applying this value to the data shown in Fig. 16 gives a 2 °C for the operating difference between the temperatures of the condensing vapor and boiling brine. This is an interesting result because it is consistent with the previous superposition result obtained for the specific power consumption data.

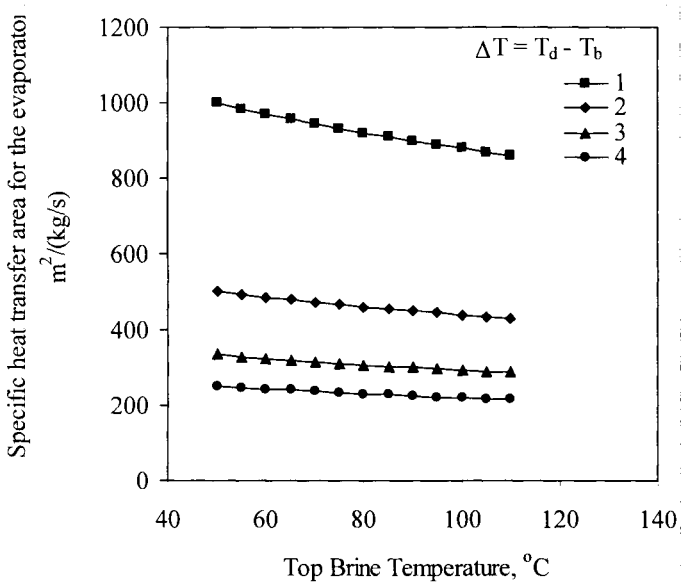

Fig. 16. Variation in specific heat transfer area for the evaporator as a function of top brine temperature and temperature difference of condensing steam and boiling brine.

Figure 17 shows the results for the specific heat transfer area for the distillate-feed preheater. The area increases at higher boiling temperatures, T_b, and lower difference for the condensing vapor and boiling brine (T_d-T_b). The heat

load of the preheater is given in terms of the temperature difference (T_d-T_o). This difference increases at higher boiling temperatures, T_b, since T_d is kept higher than T_b by 1-4 °C. Decrease of the temperature difference for the condensing vapor and the boiling brine dictates the decrease of the feed seawater temperature, T_f. This decrease is necessary to supply the evaporator with a smaller amount of energy in order to provide for the smaller enthalpy difference of the condensing and forming vapors. It is expected that the decrease in the T_f value should increase the value of $(LMTD)_d$. However, this decrease is also associated with simultaneous decrease in the T_d, which occurs at a larger rate. As a result, the $(LMTD)_d$ value decreases as the temperature difference of the condensing vapor and the boiling brine is decreased. The decrease in the value of $(LMTD)_d$ results in a larger in heat transfer area.

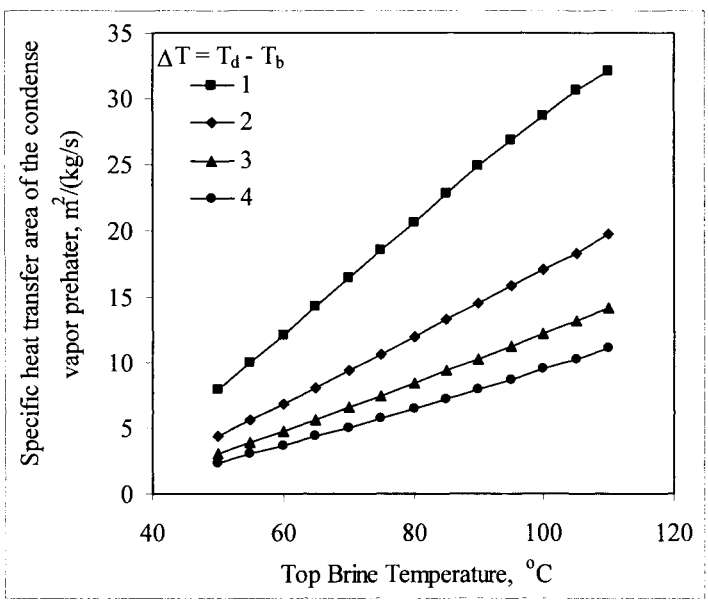

Fig. 17. Variation in specific heat transfer area of condensed vapor preheater as a function of top brine temperature and temperature difference of condensing steam and boiling brine.

The specific heat transfer area for the brine-feed preheater is shown in Fig. 18. As is shown, the heat transfer area increases upon the increase of the brine boiling temperature, T_b, and the temperature difference of the condensing vapor and boiling brine, T_d -T_b. The increase in the brine boiling temperature increases

the preheater thermal load, which is defined in terms of the difference, T_b-T_o. As for the increase in the preheater area with the increase in the temperature difference of the condensing vapor and the boiling brine, it is caused by the decrease in the $(LMTD)_b$ value. As discussed above increase in the value of (T_d - T_b) at constant T_b increases the feed seawater temperature, T_f. This increase reduces the temperature difference at the hot end of the preheater, because the brine temperature remains constant. The decrease in the temperature difference at the hot end of the preheater reduces the $(LMTD)_b$ value and in turn increases the preheater area.

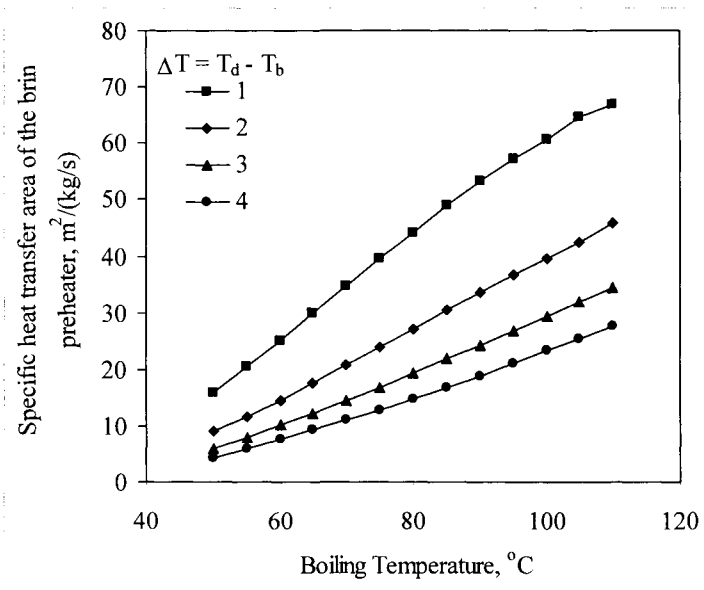

Fig. 18. Variation in specific heat transfer area of brine preheater as a function of top brine temperature and temperature difference of condensing steam and boiling brine.

Comparison of the specific heat transfer area for the two preheaters show that the brine preheater area is 3 to 5 times larger than the distillate preheater area. This is because of the higher thermal load found in the brine preheater, where the brine mass flow rate, M_b, is 1.5 kg/s, while the distillate flow rate, M_d, is only 1 kg/s. Difference dependence is found for variation in the area of the two preheaters as a function of the temperature difference of the condensing vapor and boiling brine. The area for the distillate-feed preheater is found to increase at lower differences and the opposite behavior is found for the brine-feed

preheater. This result indicate that selection of the temperature difference between the condensing vapor and the boiling brine should be optimized to minimize the heat transfer areas for the two preheaters as well as the evaporator preheater and the specific power consumption.

Results for the total specific heat transfer area is illustrated in Fig. 19. As is shown the total specific increases with the increase in the brine boiling temperature and the temperature difference of the condensing vapor and boiling brine. The evaporator specific heat transfer area dictates this behavior, since its specific area is larger than the specific areas for the two preheaters.

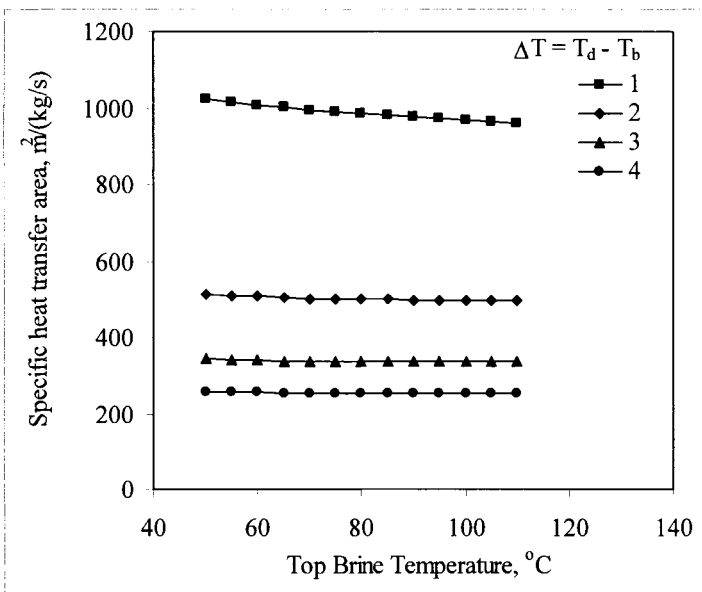

Fig. 19. Variation in the specific heat transfer area as a function of top brine temperature and temperature difference of condensing steam and boiling brine.

3.2.4 Industrial Data and Practice

Limited amount of literature data or industrial technical reports can be found on characteristics of the single-effect MVC system. The majority of available data reports specific power consumption, capacity, product purity, plant factor, material of construction, overall dimensions, and the brine boiling temperature. It is common that specific data on the heat transfer areas or temperatures of various streams are not reported. Moreover and as discussed the

introduction, the number of literature studies on the MVC system is small and the majority of the articles focus on the process main characteristics, i.e., capacity, plant factor, and specific power consumption.

Table 1 includes a summary of data extracted from literature on single-effect MVC system. The last column in the table includes predictions of the detailed model. The model predictions are made at a brine boiling temperature of 60 °C, which consistent with industrial practice. The model predicts a specific power consumption of 10.24 kWh/m^3, which is consistent literature data. This value is obtained for a temperature difference of 3 °C for (T_s-T_d). The evaporator specific heat transfer area is also consistent with value reported by Veza, 1995. This value is obtained at a temperature difference of 2 oC for (T_d-T_b), which is lower than the reported value, Lucas and Tabourier, 1985. Although, no values are reported for the specific heat transfer area of the feed preheaters, the predicted values are consistent with the thermal load of each unit.

Table 1
Comparison of industrial data and model predictions

	Matz and Fisher 1981	Matz and Zimerman 1985	Lucas and Tabourier 1985	Veza 1995	Model
Specific Power Consumption kWh/m^3	17-18	10	10	10-11	10.24
Capacity, m^3/d	50-500	250-450	25-300	500	-
Boiling Temperature, °C	40-50	50-70	-	59	60
Evaporator area m^2/(kg/s)	-	-	-	448.9	483
Brine-Feed Preheater specific area, m^2/(kg/s)	-	-	-	-	206
Distillate-Feed Preheater specific area, m^2/(kg/s)	-	-	-	-	50
T_d-T_b, °C	-	-	1	-	2
T_o-T_{cw}, °C	-	-	2-4	-	1.17
T_b-T_f and T_d-T_f, °C	-	-	2-3	-	0.3 and 2.3
T_s-T_b, °C	-	-	5	-	3

3.2.5 Summary

Analysis of the system performance by the mathematical models shows consistency of predictions and industrial practice. The specific power consumption is found to vary over a similar range, 9-17 kWh/m^3 at 60 °C. In addition, the predicted evaporator specific heat transfer area is close to the industrial practice, with values between 400-600 m^2/(kg/s) at 60 °C. The temperature values predicted by the model are also found consistent with reported industrial data.

References

Al-Juwayhel, F., El-Dessouky, H., and Ettouney, H., Analysis of single-effect evaporator desalination systems combined with vapor compression heat pumps, **114**(1997)253-275.

IDA Worldwide Desalting Plants Inventory, Wangnick, Report No. 13, December 1995, Int. Desalination Association (IDA), Gnarrenburg.

Lucas, M., and Tabourier, B., The mechanical vapour compression process applied to seawater desalination: A 1500 ton/day unit installed in the nuclear power plant of Flamanville, France, Desalination, **52**(1985)123-133.

Matz, R., and Fisher, U., A comparison of the relative economics of sea water desalination by vapor compression and reverse osmosis for small to medium capacity plants, Desalination, **36**(1981)137-151.

Matz, R., and Zimerman, Z., Low-temperature vapour compression and multi-effect distillation of seawater. Effects of design on operation and economics. Desalination, **52**(1985)201-216.

Veza, J.M., Mechanical vapour compression desalination plants – A case study, Desalination, **101**(1995)1-10.

Zimerman, Z., Development of large capacity high efficiency mechanical vapor compression (MVC) units, Desalination, **96**(1994)51-58.

Problems

1. An MVC system is to be designed to produce 5000 m^3/d of fresh water. The boiling temperature is 70 °C and the temperatures of the compressed vapor and condensate are higher by 8 °C and 3 °C, respectively. The salinity of the

feed seawater is 38000 ppm and the rejected brine salinity is 70000 ppm. For preliminary design considerations neglect thermodynamic losses, assume constant specific heat for all liquid stream (4.2 kJ/kg °C), constant specific heat for the vapor streams (1.884 kJ/kg °C), and constant overall heat transfer coefficients of 2.7, 7.2, and 7.8 for the evaporator, distillate preheater, and brine preheater, respectively. Calculate the following: M_b, M_f, T_f, T_o, A_b, A_d, A_e, and W.

2. Determine the effect of dependence of the specific heat of liquid streams, boiling point rise, latent heat, pressure, enthalpy, overall heat transfer coefficients, and specific volume on temperature and concentration on the design values obtained in problem 1. Use the correlations given in the appendices to calculate the physical properties and thermodynamic losses.
3. An MVC system is used to desalinate seawater at 35 °C with 42000 ppm salinity. The maximum allowable brine temperature is 100 °C. The heat transfer coefficient for the evaporator and the two preheaters is constant and equal to 5.016 kW/m^2 °C. The specific heat transfer area is 109.46 m^2 per (kg/s) of fresh water and the heat transfer area of the distillate preheater is 200 m^2. The flow rates of the hot and cold stream in the preheaters are equal. The temperatures of the distillate and rejected brine flowing from the preheaters are 45 °C and 40 °C, respectively. Calculate the specific power consumption.
4. An MVC system has the following design data:

   M_d = 1 kg/s, A_d = 10 m^2.

   A_b = 20 m^2, A_e = 500 m^2.

   U_e = 2.4 kW/m^2 °C, U_d = 6.7 kW/m^2 °C.

   U_b = 6.3 kW/m^2 °C, X_f = 42000 ppm.

   X_b = 70000 ppm.

   Determine T_b, T_d, T_o, T_f, and T_s if T_{cw} = 25 °C, Cp = 4.2 kJ/kg °C, and Cp_v = 1.884 kJ/kg °C. Also, determine the specific power consumption of the compressor and the flow rates of the brine and feed seawater.
5. For the same conditions in the previous problem determine T_b, T_d, T_o, T_f and T_s if T_{cw} drops to 15 °C. Also, determine the specific power consumption and the flow rates of the brine and feed seawater.
6. If fouling conditions arise in the system described in problem 2, where the overall heat transfer coefficient in the evaporator is drop to 1.8 kW/m^2 °C. If all other conditions are kept the same, determine T_b, T_d, T_o, T_f, and T_s at the new fouling conditions. Also, calculate the specific power consumption and the flow rates of brine and feed streams.

3.3 *Single Effect Absorption Vapor Compression*

The absorption vapor compression (ABVC) single or multiple effect desalination processes are not found on full commercial or industrial scale. However, the literature includes a large number of studies on development, innovation, and performance evaluation of ABVC systems for refrigeration and air conditioning processes, Kuehn et al. (1998). On the other hand, evaluation of the combined systems of these heat pumps and various thermal desalination processes is limited to a small number of studies in the literature. Weinberg et al. (1980) evaluated the performance of a coupled system of multiple effect evaporation, vacuum freezing, and lithium bromide absorption heat pump. The system is thought to enhance the performance ratio of the multiple effect evaporation to high values of 18-20 and operating temperatures between 0 to 60 °C. The low temperature operation minimizes corrosion and scaling problems. Alefeld and Ziegler (1985) proposed a fully integrated desalination system combined with LiBr-H_2O absorption heat pump. The system includes three stages, which process seawater and generates fresh water. Aly (1988) and Fathalah and Aly (1991) analyzed a solar powered LiBr-H_2O heat pump, which generates high grade steam to operate MEE desalination system. More emphasis, in their analysis, was given to the performance of the solar power unit and air conditioning in the evaporator unit. Yanniotis and Pilavachi (1996) modeled the performance of sodium hydroxide heat pumps in MEE systems. Model results are validated against experimental measurements and were found to have reasonable agreement. Al-Juwayhel et al. (1997) studied the performance of single effect evaporation desalination systems combined with various types of heat pumps. As discussed before, results for the ABVC gave thermal performance ratios close to three times higher than the single effect thermal vapor compression system. On the other hand, El-Dessouky and Ettouney (1997) showed 50% increase in the thermal performance ratio for the MEE-ABVC and MEE-ADVC systems over the MEE-TVC with values close to 20.

3.3.1 *Process Description*

Elements of the ABVC system are shown in Fig. 20. In this system, the evaporator constitutes horizontal falling film tubes, brine spray nozzles, demister, and the brine pool. The down condenser has a similar shell and tube configuration, where condensation takes place on the shell side. The absorber is also a shell and tube falling film configuration. Absorption of water vapor by the LiBr-H_2O solution occurs on the shell side of the absorber, while heating of the feed seawater and vapor formation takes place on the tube side of the absorber. The generator has a similar layout to the evaporator, where dilute LiBr-H_2O solution forms a falling film on the outside surface of the tubes and the motive

steam is condensed inside the tubes. The heat exchange unit between the concentrated and diluted LiBr-H_2O solution is used to exchange heat from the concentrated to the dilute solution. This improves the overall process efficiency. The process is described in the following points:

- The intake seawater stream flows through the down condenser, where it condenses part of the vapor formed in the evaporator. The remaining part of the vapor is fed to the shell side of the absorber in the heat pump.
- The intake seawater temperature increases from (T_{cw}) to (T_f) as it absorbs the latent heat of condensation of the condensing vapor. Part of the feed seawater is rejected back to the sea (M_{cw}) which is known as the cooling seawater. The remaining portion of the intake seawater is the feed seawater stream (M_f), which is chemically treated and deaerated before being fed to the tube side of the absorber.
- The concentrated LiBr-H_2O solution absorbs the vapor stream entering the absorber. The absorption process is exothermic and releases sufficient amount of heat that sustains increase of the feed seawater temperature to the saturation temperature. Also, vapor is formed from the feed seawater within the absorber. This vapor forms part of the heating steam in the evaporator.
- The temperature of the absorbed vapor and the concentration of the outlet dilute LiBr-H_2O solution define the equilibrium conditions in the absorber. It should be noted that boiling point elevation for the LiBr-H_2O, or the temperature difference between the dilute LiBr-H_2O solution and the absorbed vapor, varies over a range of 10-50 °C as the mass fraction of LiBr-H_2O in the dilute solution is increased from 0.25-0.45.
- The dilute LiBr-H_2O solution enters the generator, where it is sprayed on the outside surface of the tubes. The solution absorbs the latent heat of motive steam that condenses on the tube side of the generator. The heating process increases the temperature of the LiBr-H_2O solution to saturation and results in evaporating the same amount of water absorbed by the solution in the absorber. The concentration of the concentrated LiBr-H_2O solution and the temperature of the formed vapor define the equilibrium conditions in the generator.
- The combined vapor formed in the generator and absorber derives the evaporation process in the evaporator. The brine stream leaving the absorber is sprayed on the outside surface of the evaporator tubes, where it absorbs the latent heat of condensation from the condensing steam on the tube side of the evaporator.
- The concentrated brine leaving the evaporator is rejected back to the sea and the formed vapor is routed to the down condenser. The sum of the condensate of the heating steam and the condensate in the down condenser forms the distillate product stream.
- Demisters in various units prevent droplet entrainment of brine and LiBr.

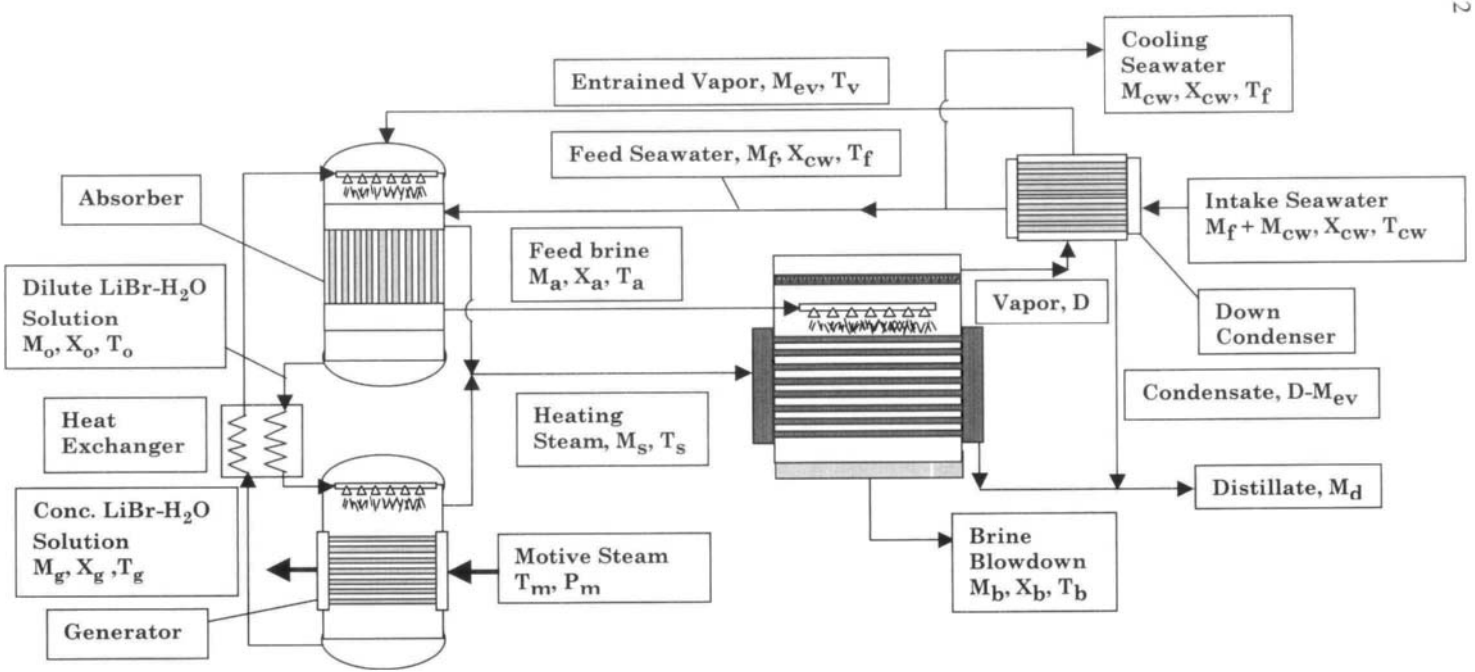

Fig. 20. Single effect absorption vapor compression desalination process (ABVC)

3.3.2 Process Modeling

The steady-state model includes a set of material and energy balances, heat transfer equations, and thermodynamic relations. Assumptions used in the model include:

- The vapor formed in the evaporator, absorber and generator is salt free. This assumes that the entrainment of brine droplets by the vapor stream is negligible and has no effect on salinity of the distillate product.
- Energy losses from the effects to the surroundings are negligible. This is because of operation at relatively low temperatures, between 100-40 °C, and the effects are well insulated.
- The physical properties of various streams are calculated at the average temperature of influent and effluent streams.

The overall material and salt balances are given by

$$M_f = M_d + M_b \tag{48}$$

$$M_b = M_f (X_f / X_b) \tag{49}$$

where M is the mass flow rate, X is the salt concentration, and the subscript b, d, and f denotes the brine, the distillate, and the feed seawater. In Eq. (49) the brine blow down salinity (X_b) is set at 90% of the saturation salinity of the $CaSO_4$ solution

$$X_b=0.9(457628.5-11304.11T_b+107.5781T_b^2-0.360747T_b^3) \tag{50}$$

This equation is obtained by curve fitting of the salinity/temperature relation for the solubility of $CaSO_4$, El-Dessouky et al. (2000b).

In the evaporator, the saturated falling brine film absorbs the latent heat of the condensing steam. This evaporates a controlled mass of vapor, D at T_v, where

$$M_s \lambda_s = D \lambda_v \tag{51}$$

where λ is the latent heat. The subscripts s and v denote the heating steam and the vapor formed, respectively. In the evaporator, absorber, and generator the boiling temperature are higher than the corresponding vapor saturation temperature by the boiling point elevation, (BPE(T_b,X_b)), and the temperature rise caused by the hydrostatic pressure head, ΔT_y. This is

$$T_b = T_v + BPE(T_b,X_b) + \Delta T_y \tag{52}$$

The term, ΔT_y, is negligible in horizontal falling films, because of the very small thickness of the boiling film.

The condensation temperature in the down condenser, T_c, is lower than the evaporation temperature, T_v, by the boiling point elevation, $(BPE(T_b,X_b))$, and the saturation temperature depressions associated with pressure losses in the demister, (ΔP_p), transmission lines between the effects, (ΔP_t), and vapor condensation inside the tubes, (ΔP_c). The resulting condensation temperature is

$$T_c = T_b - (BPE(T_b,X_b) + \Delta T_p + \Delta T_t + \Delta T_c) \tag{53}$$

The pressure drop during condensation, ΔP_c, is defined as the algebraic sum of the decrease caused by friction (ΔP_r) and the increase caused by gravity (ΔP_g) and vapor deceleration (ΔP_a). This relation is given by

$$\Delta P_c = (\Delta P_r - \Delta P_g - \Delta P_a) \tag{54}$$

Correlations for the pressure drop components ΔP_p, ΔP_t, ΔP_r, ΔP_g, and ΔP_a are given in the study by El-Dessouky et al. (1998).

In the down condenser, the temperature of the intake seawater, $M_{cw}+M_f$, is increased from T_{cw} to T_f. Condensing part of the vapors formed in the evaporator provides the required heating energy. This energy balance is given by

$$(D - M_{ev})\lambda_c = (M_{cw} + M_f)\, C_p (T_f - T_{cw}) \tag{55}$$

where the subscripts c, cw, and ev denote the condensing vapors, the intake seawater, and the entrained vapor in the absorber.

The following relation gives the flow rate of the heating steam

$$M_s = M_{ev} + M_{ab} \tag{56}$$

where M_{ev} is the amount of entrained vapor in the absorber, subsequently released in the generator as a part of the heating steam. M_{ab} is remaining part of heating steam generated in the absorber. Inspection of Fig. 20 shows that the total distillate flow rate is given by

$$M_d = D + M_{ab} \tag{57}$$

The energy balance around the absorber is given by

$$M_g H_g + M_{ev} H''_{ev} + M_f H_f = (M_g + M_{ev}) H_o + M_{ab} H''_s + M_a H_a \tag{58}$$

where M_g is the flow rate of the concentrated LiBr-H_2O solution entering the absorber, M_a is the brine mass flow leaving the absorber. The water vapor saturation enthalpies H''_{ev} and H''_s are obtained at the condensation temperature in the down condenser (T_c) and the heating steam temperature in the evaporator (T_s), respectively. In Eq. (57) H_g and H_o are the enthalpies of the concentrated and diluted LiBr-H_2O solution evaluated at (C_g,T_g) and (C_o,T_o). It should be noted that T_g and T_o are obtained from the equilibrium relation in Appendix A at the water vapor saturation temperatures of T_s and T_c, respectively. The enthalpies of the feed seawater and the feed brine H_f and H_a are calculated at (T_f, X_{cw}) and (T_a, X_a), respectively. The heating steam temperature is related to the feed brine temperature by the boiling point elevation, or,

$$T_s = T_a - BPE(X_a,T_a) \tag{59}$$

The energy equation for the generator balances the amount of input energy in the motive steam and the dilute LiBr-H_2O solution against the amount of output energy in the concentrated LiBr-H_2O solution and the heating steam. This relation is given by

$$(M_g + M_{ev}) H_o + M_m H''_m = M_g H_g + M_{ev} H''_s \tag{60}$$

where M_m and H''_m are the mass flow rate and enthalpy of motive steam.

The material and salt balance around the absorber for the feed seawater and the feed brine are given by

$$M_f = M_a + (M_s - M_{ev}) \tag{61}$$

$$X_f M_f = M_a X_a \tag{62}$$

Similarly, the following relations give the total mass and salt balance for the concentrated and diluted LiBr-H_2O solutions

$$M_o = M_g + M_{ev} \tag{63}$$

$$M_o C_o = M_g C_g \tag{64}$$

The design equations for the heat transfer area are developed for the evaporators, the preheaters, and the down condenser. For the evaporators, the heat transfer area, A_e, is

$$A_e = \frac{M_s \lambda_s}{U_e (T_s - T_b)} \tag{65}$$

where U is the overall heat transfer coefficient, and the subscript e refers to the evaporator.

The heat transfer area of the down condenser is given by

$$A_c = \frac{(D - M_{ev})\,\lambda_c}{U_c A_c (LMTD)_c} \tag{66}$$

$$(LMTD)_c = \frac{T_f - T_{cw}}{\ln \dfrac{T_c - T_{cw}}{T_c - T_f}} \tag{67}$$

The overall heat transfer coefficient in the evaporator and condenser are:

$$U_e = 1.9394 + 1.40562 \times 10^{-3} T_b - 2.0752 \times 10^{-4} (T_b)^2 + 2.3186 \times 10^{-6} (T_b)^3 \tag{68}$$

$$U_c = 1.6175 + 0.1537 \times 10^{-3} T_v + 0.1825 \times 10^{-3} (T_v)^2 - 8.026 \times 10^{-8} (T_v)^3 \tag{69}$$

where U_e and U_c are the overall heat transfer coefficient in the evaporator and down condenser in $kW/m^2\ ^oC$, T_b is the brine boiling temperature, and T_v is the vapor condensation temperature in the condenser. All temperatures in the above correlations are in ^oC. The standard deviations for the above correlations are 2.03% and 1.76%. These correlations are tested and proved to be reliable through comparison against other correlations in the literature and available experimental and design data.

The system performance is defined in terms of the following parameters:

- Performance ratio, which is defined as the amount of the distillate product per unit mass of the motive steam

$$PR = M_d / M_m \tag{70}$$

- Specific flow rate of cooling water, which is defined as the amount of the cooling water per unit mass of distillate product

$$sM_{cw} = M_{cw}/M_d \quad (71)$$

- Specific heat transfer area, which is defined as the ratio of the total heat transfer area of the evaporator and condenser to the total flow rate of distillate product

$$sA = (A_e+A_c)/M_d \quad (72)$$

- Conversion ratio, which is defined as the amount of distillate product per unit mass of feed seawater

$$CR = M_d/M_f \quad (73)$$

Solution Method

The solution procedure is shown in Fig. 21. Solution of the model equations requires definition of the following system variables:

- The distillate flow rate, M_d, is 1 kg/s.
- The intake seawater temperature, T_{cw}, is 25°C.
- The heating steam temperature, T_s, is higher than the brine boiling temperature T_b by 2-10 °C.
- The feed seawater temperature, T_f, is lower than the vapor condensation temperature T_c by 5 °C.
- The feed brine temperature, T_a, is lower than the temperature of the dilute LiBr-H_2O solution T_b by 5 °C.
- The motive steam temperature, T_m, is higher than the temperature of the concentrated LiBr-H_2O solution T_g by 5 °C.
- The range for the heating steam temperature, T_s, is 50-100 °C.
- The feed seawater salinity, X_f, is 36000 ppm.

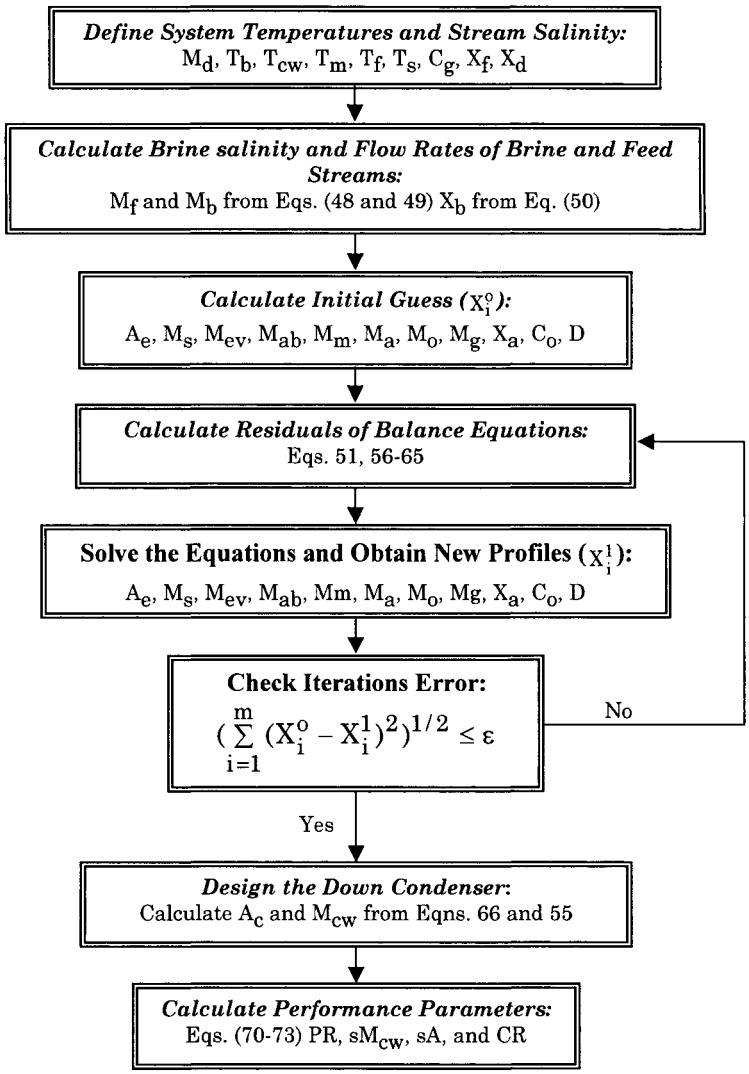

Fig. 21. Solution algorithm of the absorption heat pump and the single effect evaporation desalination system.

As is shown in Fig. 21 solution sequence proceeds as follows:
- The system capacity, stream temperatures, and stream salinity are defined as specified above.
- Eqs. 48-50 are solved to determine the feed and brine flow rates and the salinity of the brine blowdown.
- An initial guess is assumed for the following:
  - Evaporator area.
  - The flow rates of the heating steam, motive steam, entrained vapor, vapor formed in the absorber, dilute LiBr-H_2O, and the concentrated LiBr-H_2O.
  - Concentrations of the dilute LiBr-H_2O solution and brine leaving the absorber.
- The above variables are calculated by solution of Eqs. 51, 56-65. Solution proceeds iteratively using Newton's method. Iterations continue until the tolerance criterion is achieved with a value of $1x10^{-4}$ for ε.
- The flow rate of the cooling seawater and the heat transfer area of the condenser are calculated from Eqs. 55 and 66, respectively.
- The performance parameters are calculated from Eqs. 70-73.

Example 1:

Design a single effect evaporation desalination unit combined with absorption vapor compression. The system operates at the following conditions:
- The system capacity is 1 kg/s.
- Compressed vapor temperature is 80 °C.
- The brine boiling temperature is 77 °C.
- The mass fraction of LiBr in the concentrated solution is 0.7.
- The intake seawater temperature is 25 °C.
- The intake seawater salinity is 36000 ppm.
- The temperature of the seawater stream leaving the condenser is lower than the temperature of the condensing vapor by 5 °C.
- The motive steam temperature is higher than the boiling temperature of the concentrated LiBr solution by 5 °C.
- The temperature of the seawater stream leaving the absorber is lower than the boiling temperature of the dilute LiBr solution by 5 °C.
- The temperature approach for the hot and cold ends in the LiBr heat exchanger is 3 °C.
- Seawater velocity inside the condenser tubes is 1.5 m/s.
- Salinity of product fresh water is 0 ppm.
- Outer diameter of the condenser and evaporator tubes is 0.015 m.
- Wall thickness of the condenser and evaporator tubes is 0.005 m.
- Thermal conductivity of the condenser and evaporator tubes is 0.042 kW/m °C.
- Total fouling resistance inside/outside the condenser and evaporator tubes is 0.001 kW.

- Velocity of steam condensate inside the evaporator tubes is 1.5 m/s.
- Velocity of falling film on the outside surface of the evaporator tubes is 1.5 m/s.
- Thickness of falling film on the outside surface of the evaporator tubes is 0.001 m.

Solution:

The model solution starts with evaluation of some the system parameters, which includes X_b, $BPE(X_b,T_b)$, T_v, T_f, M_f, and M_b. The rejected brine salinity is calculated from the saturation correlation, where

$$X_b = 0.9(457628.5-(11304.11)T_b+ (107.5781)T_b^2-(0.36074702)T_b^3)$$

$$X_b = 54314.7 \text{ ppm}$$

The boiling point elevation in the evaporator is obtained from the correlation in Appendix B

$$BPE(X_b,T_b) = 1.36 \text{ °C}$$

Therefore, the vapor temperature in the evaporator is obtained from

$$T_v = T_b - BPE(T_b,X_b) = 77 - 1.36 = 75.64 \text{ °C}$$

This gives a feed seawater temperature of

$$T_f = T_v - 5 = 75.64 - 5 = 70.64 \text{ °C}$$

The flow rates of the feed seawater and rejected brine are obtained from the following equations

$$M_f = (M_d)(X_b)/(X_b-X_f) = (1)(54314.7)/(54314.7-36000) = 2.97 \text{ kg/s}$$

$$M_b = M_f - M_d = 2.97 - 1. = 1.97 \text{ kg/s}$$

The second part of the model solution involves iterative and simultaneous solution of the mass and energy balances and the heat transfer equations to determine the following system variables:

- Flow rate of compressed vapor (M_s) = 0.666 kg/s
- Heat transfer area of the evaporator (A_e) = 257.8 m^2
- Flow rate of entrained vapor (M_{ev}) = 0.342 kg/s

- Flow rate of vapor formed in the absorber (M_{ab}) = 0.324 kg/s
- Flow rate of motive steam (M_m) = 0.37 kg/s
- Flow rate of concentrated LiBr-H_2O solution = 0.34 kg/s
- Flow rate of seawater leaving absorber (M_a) = 2.64 kg/s
- Salinity of seawater leaving absorber (X_a) = 40413.1 ppm
- Mass fraction of LiBr in dilute solution (X_o) = 0.349
- Boiling vapor flow rate from evaporator (D) = 0.663 kg/s
- Flashing vapor flow rate from evaporator (D_f) = 0.0132 kg/s

Other system parameters obtained after the final iteration include the following:

- Performance ratio (PR) = $\frac{1}{M_m} = \frac{1}{0.37} = 2.7$
- Boiling temperature of concentrated LiBr-H_2O (T_g) = 158.7 °C
- Boiling temperature of diluted LiBr-H_2O (T_a) = 85.9 °C
- Temperature of compressed vapor (T_s) = 80.04 °C
- Temperature of seawater leaving absorber (T_a) = 80.93 °C
- Motive steam temperature (T_m) = 163.7 °C
- Pressure of motive steam (P_m) = 677.4 kPa

Enthalpy data at the above conditions include the following:

- Enthalpy of compressed vapor = 2636.27 kJ/kg
- Enthalpy of concentrated LiBr-H_2O = 4851.4 kJ/kg
- Enthalpy of diluted LiBr-H_2O = 1387.6 kJ/kg
- Enthalpy of seawater leaving condenser = 283.7 kJ/kg
- Enthalpy of seawater leaving absorber = 323.8 kJ/kg
- Enthalpy of motive steam = 2077.03 kJ/kg

Analysis of the condenser unit gives the following results:

- Flow rate of cooling seawater (M_{cw}) = 1.28 kg/s
- Condenser heat transfer coefficient (U_c) = 3.48 kJ/m^2 °C
- Condenser heat transfer area (A_c) = 11.3 m^2

3.3.3 System Performance

System performance is evaluated as a function of the heating steam temperature, the temperature difference of the heating steam and the boiling brine, and the mass fraction of LiBr-H_2O in the concentrated solution. Effects of the heating steam temperature and the mass fraction of the LiBr-H_2O in the concentrated solution are shown in Figs. 22-24 for the variations in the

performance ratio, the specific heat transfer area, and the specific flow rate of cooling water. The three figures show insensitive and independent behavior of the system parameters on the mass fraction of LiBr-H_2O in the concentrated solution. The following causes this behavior:

- Various system temperatures, which includes the heating steam, the boiling temperature, the feed seawater, and the feed brine are independent of the LiBr-H_2O mass fraction in the concentrated solution. These temperatures affect the system variables, which are used to calculate the system performance parameters.
- Increase in the LiBr-H_2O mass fraction in the concentrated solution affects only the flow rate of the concentrated solution. At higher concentrations, the solution enthalpy increases and results in reduction of the concentrated solution flow rate. This is necessary to balance the system energy in the absorber and generator.

The main effect of increasing the LiBr-H_2O mass fraction in the concentrated solution is the need for higher pressure motive steam. The is illustrated in the following data are, which are obtained for a heating steam temperature of 100 °C:

- C_g = 0.75, Tg = 201.87 °C, T_m = 206.87, P_m = 1789 kPa (17.89 bar), PR = 2.4, sA = 220.9, sM_{cw} = 0, CR = 0.092.
- C_g = 0.45, T_g = 122.93 °C, T_m = 127.93, P_m = 253 kPa (2.53 bar), PR = 2.3, sA = 212.9, sM_{cw} = 0, CR = 0.092.

Selection between the two points depends on the following factors:

- Availability of high pressure steam, i.e., 17 bar versus 3 bar.
- Increase in the system second law efficiency upon operation at low steam pressures, Hamed et al. (1996), Darwish and El-Dessouky (1996).
- Use of smaller tube diameter for higher pressure steam, El-Dessouky et al. (2000a).
- Elimination of the control loops required for reduction of the steam pressure to lower values of 3 bar, Alatiqi et al. (1999).

As is shown in Figs. 22-24 effects of the heating steam temperature on the system performance are more pronounced than the mass fraction of the LiBr-H_2O in the concentrated solution. This behavior is dramatic concerning the specific heat transfer area and the specific flow rate of cooling water. As is shown in Fig. 23, the specific heat transfer area has values above 400 $m^2/(kg/s)$ at heating steam temperatures close to 50 °C. On the other hand, the specific heat transfer area decreases to values between 200-250 $m^2/(kg/s)$, which are considered the industrial practice, as the temperature is increased to values between 80-100 °C. This behavior is primarily caused by increase in the overall heat transfer coefficient at higher temperatures. This enhances the heat transfer rate and results in reduction of the required heat transfer area. A lesser factor is the reduction in the latent heat of evaporation or condensation at higher temperatures, which results in reduction in the thermal load of the evaporator

and the down condenser. It should be stressed that the temperature difference driving force between heating steam and boiling brine has no effect because it is kept constant in the calculations.

At higher heating steam temperatures, the specific flow rate of cooling water is zero, Fig. 24. This is because of the limitations imposed on the salinity of the brine blow down stream, Fig. 25, where at higher temperatures the difference in the salinity of the feed seawater and the brine blow down is less than 1000-2000 ppm. As a result of the constant production capacity, the feed flow rate of seawater increases to higher values and reduces the flow rate of the cooling seawater. The opposite behavior occurs at lower temperature, where higher conversion ratios are achieved. This reduces the feed flow rate and results in the increase in the cooling seawater flow rate.

Variations in the system performance as a function of the heating steam temperature and the temperature difference between the heating steam and the boiling brine are shown in Figs. 26-28. As is shown the two parameters have strong effect on the specific heat transfer area and the specific flow rate of cooling water. As is shown in Fig. 27, the increase in the temperature reduces the specific heat transfer area. At larger temperature differences, the driving force for heat transfer increases and results in reduction in the heat transfer area. Simultaneously, this effect increases the amount of distillate product, which increases conversion ratio. As discussed before, increase in the conversion ratio is associated with simultaneous decrease in the feed seawater flow rate and increase in the flow rate of cooling seawater, Fig. 28.

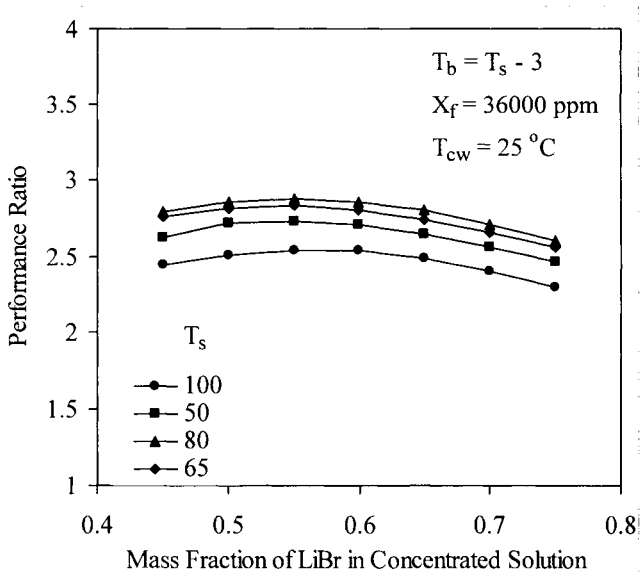

Fig. 22. Variation in the performance ratio as a function of the mass fraction of LiBr in concentrated solution and the heating steam temperature

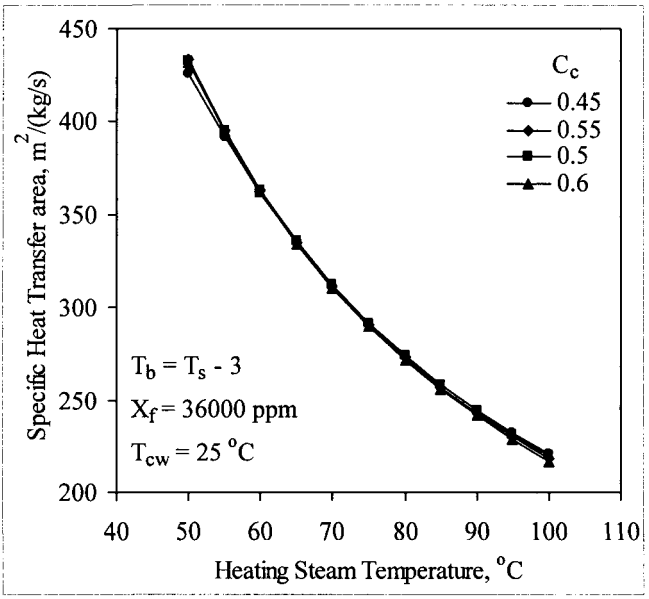

Fig. 23. Variation in the specific heat transfer as a function of the mass fraction of LiBr in concentrated solution and the heating steam temperature

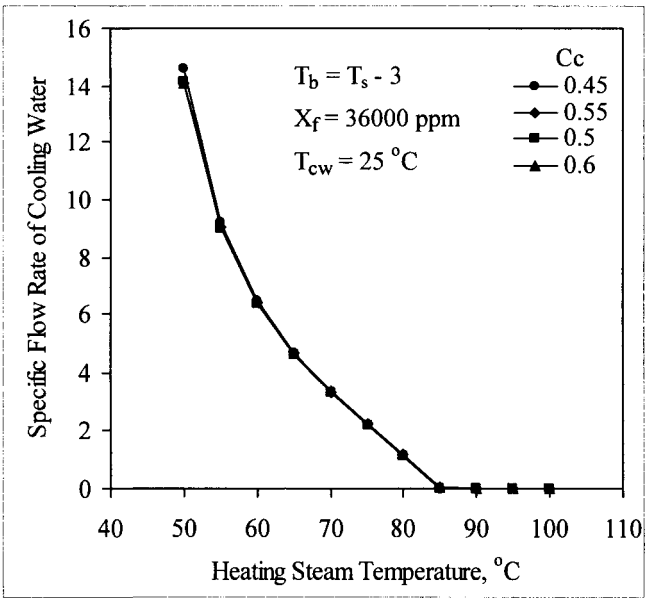

Fig. 24. Variation in the specific flow rate of cooling as a function of the mass fraction of LiBr in concentrated solution and the heating steam temperature

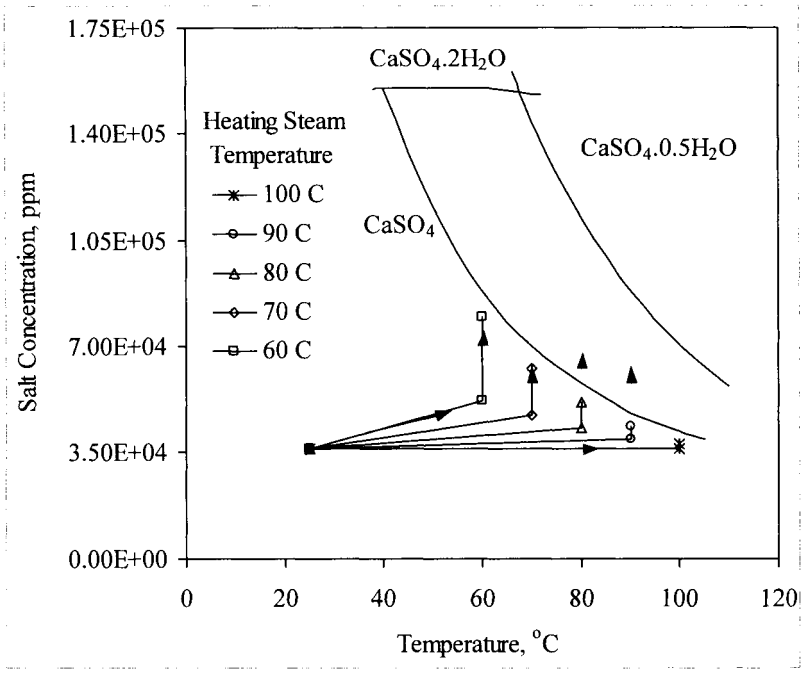

Fig. 25. Calcium sulfate solubility and top brine temperature for ABVC system.

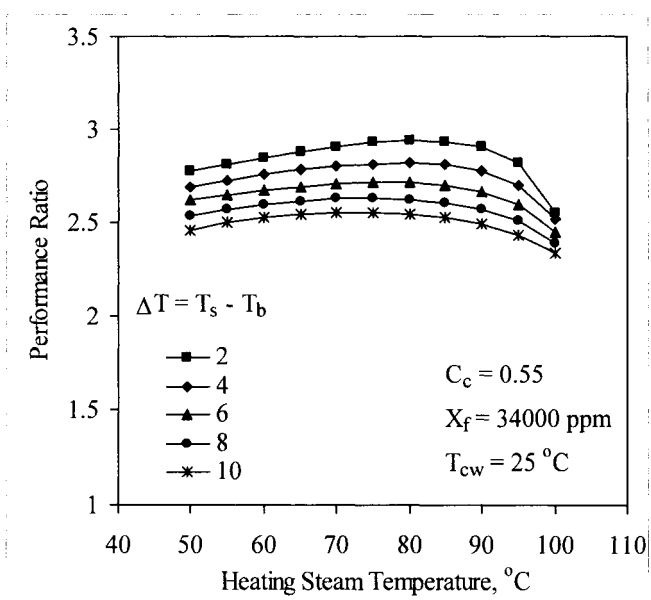

Fig. 26. Variation in the performance ratio as a function of the temperature difference of heating steam and top brine temperature and the heating steam temperature

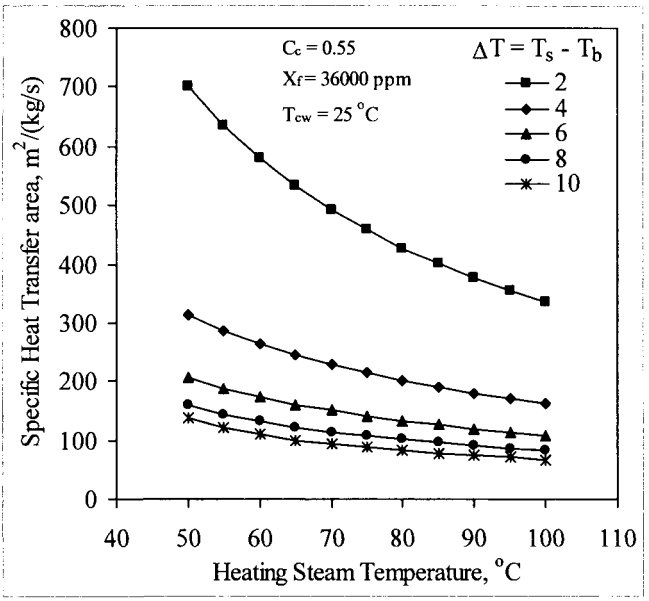

Figure 27: Variation in the specific heat transfer area as a function of the temperature difference of heating steam and top brine temperature and the heating steam temperature

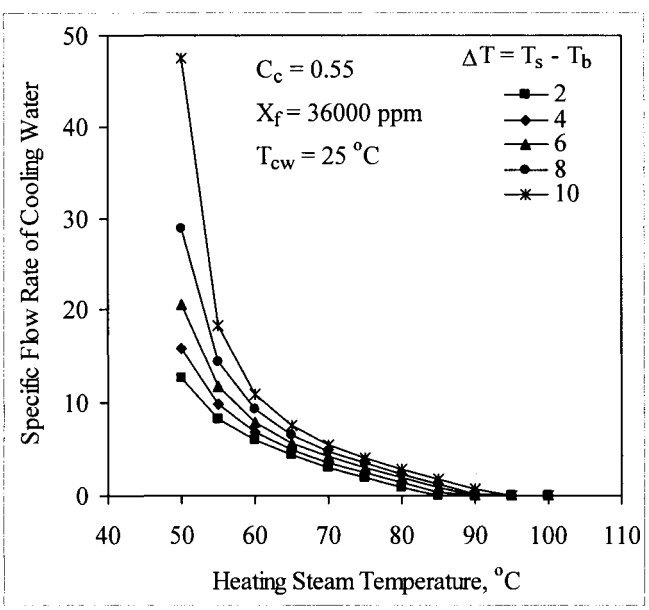

Fig. 28. Variation in the cooling water specific flow rate as a function of the temperature difference of heating steam and top brine temperature and the heating steam temperature

3.3.4 Summary

The absorption heat pump combined with the single effect evaporation desalination process is analyzed as a function of the design and operating parameters. The following conclusions are made in light of results and analysis:

- The thermal performance ratio varies over a range of 2.4-2.8 and is close to 50-70% higher than that of the single effect thermal vapor compression, El-Dessouky and Ettouney (1999).
- Effects of the LiBr mass fraction in the concentrated solution are minimal on the system performance. However, choice of this parameter is dependent on steam availability.
- The specific heat transfer area decreases with the increase in the heating steam temperature and the temperature difference of the heating steam and boiling brine.
- The specific flow rate of cooling water decreases at higher heating steam temperatures and lower temperature difference between the heating steam and boiling brine.

In summary, selection of the optimum design and operating conditions should take into considerations attractive features for system operation at higher temperatures. At these conditions, drastic reduction occurs in the specific flow rate of cooling water and the specific heat transfer area. Both factors result in considerable savings in the capital and production cost.

References

Alatiqi, I., Ettouney, H.M., and El-Dessouky, H.T., Process control in water desalination industry: An overview, Desalination, **126**(1999)33-40.

Alefeld, G., Ziegler, F., Advanced heat pump and air-conditioning cycles for the working pair H_2O/LiBr: Industrial applications, ASHRAE Tech. Data Bull., June 1985, pp 11-24.

Al-Juwayhel, F., El-Dessouky, H.T., and Ettouney, H.M., Analysis of single-effect evaporator desalination systems driven by vapor compression heat pumps, Desalination, **114**(1997)253-275.

Aly, S.E., vapour compression distillation using waste heat absorption systems, Desalination, **68**(1988)57-68.

Darwish M.A., and El-Dessouky, H., The heat recovery thermal vapour-compression desalting system: A Comparison with other thermal desalination Processes, Applied Thermal Engineering, **18**(1996)523-537.

El-Dessouky, H.T., and Ettouney, H.M., Simulation of Combined Multiple Effect Evaporation-Vapor Compression Desalination Processes, 1st IDA Int. Desalination Conference in Egypt, Cairo, Egypt, September, 1997.

El-Dessouky, H.T., Alatiqi, I., Bingulac, S., and Ettouney, H.M., Steady-state analysis of the multiple effect evaporation desalination process, Chem. Eng. Tech., **21**(1998)15-29.

El-Dessouky, H.T., and Ettouney, H.M., Single effect thermal vapor compression desalination process: Thermal analysis, Heat Transfer Eng., **20**(1999)52-68.

El-Dessouky, H.T., Ettouney, H.M., Al-Fulaij, H., and Mandani, F., Multistage flash desalination combined with thermal vapor compression, Chem. Eng. Proc., in print, 2000a.

El-Dessouky, H.T., Ettouney, H.M., and Al-Juwayhel, F., Parallel feed multiple effect evaporation with thermal vapor compression, Trans. I. Chem. E., in print, 2000b.

Fathalah, K., and Aly, S.E., Theoretical study of a solar powered absorption/MED combined system, Energy Convers., **31**(1991)529-544.

Hamed, O.A., Zamamiri, A.M., Aly, S., and Lior, N., Thermal performance and exergy analysis of thermal vapor compression desalination system, Energy Convers. Mgmt, **37**(1996)379-387.

Kuehn, T.H., Ramsey, J.W., Threlkeld, J.L., Thermal environmental engineering, 3rd ed., Prentice Hall, New York, 1998.

Weinberg, J., Ophir, A., and Fisher, U., Coupling of multi-effect distillation with vacuum freezing to reduce energy cost in sea water desalination, Proceedings of the 7th Int. Symposium on Fresh Water from the Sea, 1980, Vol. I, 283-292.

Yanniotis, S., and Pilavachi, P.A., Mathematical modeling and experimental validation of an absorption-driven multiple –effect evaporator, Chem. Eng. Technol., **19**(1996)448-455.

3.4 Single Effect Adsorption Vapor Compression

The adsorption-desorption heat pump is environmentally friendly. The pump uses benign fluids, which does not contribute in the destruction of the ozone layer. Their role in the greenhouse effect is negligible because they can be driven by renewable or waste energy sources and also due to their high thermal efficiency. Moreover, the process is simple, does not include moving parts, has a long life, and is vibration free. For these reasons, in recent years, the adsorption-desorption heat pump has attracted increasing attention in the concern of replace the traditional compressor-based systems, which utilize ozone harmful fluids. Applications of the adsorption-desorption heat pumps are found in air conditioning and in ice making.

3.4.1 Process Description

The ADVC system is shown diagrammatically in Fig. 29. The system includes the evaporator/condenser unit, two adsorption beds, feed preheaters, and a heat exchanger for the thermal fluid circulating between the adsorption and desorption beds. It is interesting to note that the evaporator and condenser form a single unit in this configuration, which replaces the individual condenser and evaporator in conventional adsorption heat pumps. Also, the feed preheaters are plate type and are used to exchange heat between the feed seawater and the condensed vapor and the rejected brine. The adsorber plays the role of the bottom condenser in the TVC system. That is, this adsorber absorbs or rejects the excess heat added to the system in the second adsorber.

The closed cycle of the heat pump is composed of the following steps:

1. Initially, bed I is assumed to be cold and saturated with water. The mass of the bed is the mass of the adsorbent M_z plus the associated water M_d. The temperature of the bed is T_a. The second bed is dry and hot at T_c. The temperature of the cold bed T_a must be less than the temperature of the water adsorbed in the bed. This temperature is fixed by the equilibrium relationship for the zeolite-water pair. On the other hand, the temperature of the hot bed T_c is equal to the temperature of heating steam flowing to the first effect. The first step commences, when the circulating fluid starts to transfer heat between the two beds. Thus, heating the first bed and cooling the second bed occurs simultaneously. During this phase, no heat is exchanged between the adsorbers and any external heat source or sink. The heat flowing into the first adsorber, Q_{2-1}, is represented by the path abe_1 on the Clapeyron diagram (Fig. 30), while, the heat transferred from the second bed, Q_{2-1}, is described by the route cde_2 on the same diagram. The process is terminated when the

first bed is heated to T_{e_1} and second bed is cooled to T_{e_2}. For the heat transfer to take place T_{e_2} should be higher than T_{e_1}.

2. The second step starts when the first bed is connected to the external source of heating steam (boiler), where its temperature is increased from T_{e_1} to T_c. At the same time, a stream of cooling-water is used to reduce the second bed temperature from T_{e_2} to T_a.
3. During the heating process and once the pressure inside the first bed becomes higher than the condenser pressure, the bed is opened to the tube side of the evaporator where the generated steam condenses.
4. At the same time, when the pressure in the second bed becomes less than the evaporator pressure, the bed is opened to the shell side of the evaporator where the vapor formed in the evaporator flows to the bed where it is adsorbed.

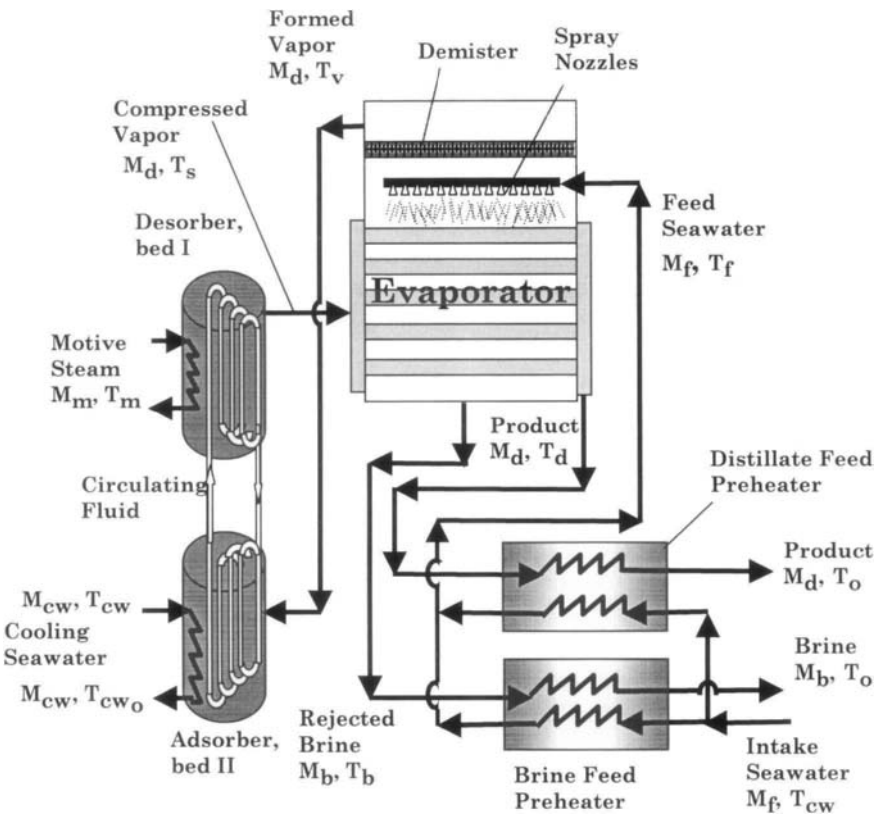

Fig. 29. Single effect-evaporator driven by adsorption heat pump

The previously described four steps represent the first half of the heat pump cycle. The second half of the cycle originates by circulating the heat transfer fluid in the reverse direction. During this second half of the cycle, bed I is cooled and adsorbs vapor from the evaporator. Simultaneously, bed II is heated and generates the heating steam, which condenses inside the evaporator tubes.

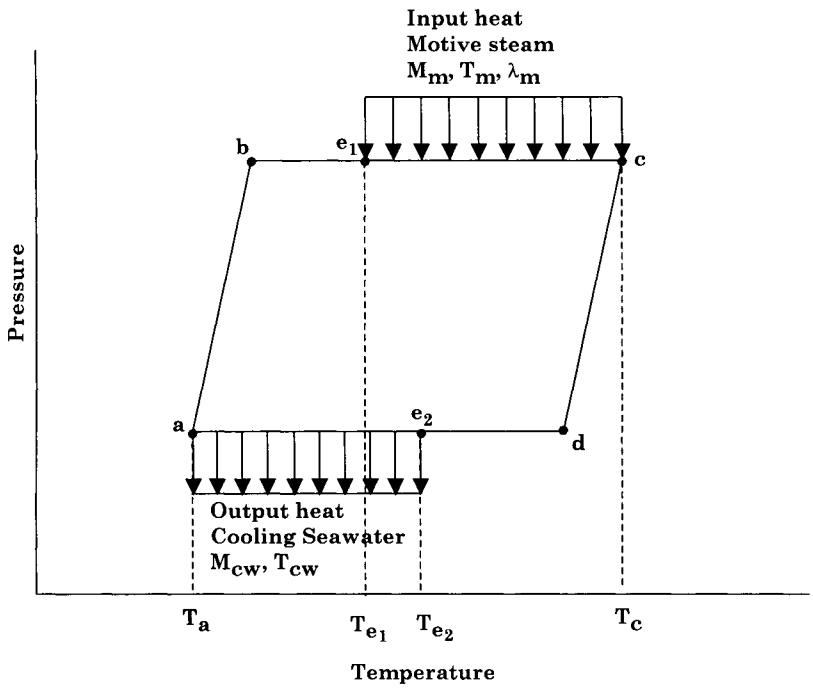

Fig. 30. Clapeyron diagram for the adsorption/desorption vapor compression cycle

3.4.2 Process Modeling

The mathematical model for the single effect adsorption vapor compression desalination system includes balance equations for the evaporator, feed preheaters, adsorption bed, and desorption bed. The model assumptions used in development include the following:

- Steady state conditions. This implies use of a minimum of two adsorption/desorption units. Therefore, as one of the two units go through the process of circulating the thermal fluid between the two beds the other unit is

used for simultaneous absorption of vapor from the evaporator and generation of heating steam.
- The adsorber pressure is uniform. Therefore, the vapor pressure and the adsorbent temperature are related by the adsorption equilibrium equation.
- The bed contents are in thermal equilibrium. Therefore, the adsorbent and the adsorbate have the same temperature.
- No heat losses to the surroundings.
- Model parameters, such as the fluid density, heat transfer coefficients, and velocity are assumed constant.
- The mass of vapor adsorbed in the second bed is equal to the amount of steam generated in the first bed,
- Constant and equal rates for adsorption and desorption, and
- Constant rate of heat exchange between the two beds.

The model equations include the following:
- Overall material and salt balances

$$M_f = M_d + M_b \tag{74}$$

$$M_b = M_f (X_f / X_b) \tag{75}$$

- Preheaters energy balance

$$M_f C_p (T_f - T_{cw}) = M_d (H(T_d) - H(T_o)) + M_b C_p (T_b - T_o) \tag{76}$$

- Evaporator energy balance

$$M_f C_p (T_b - T_f) + M_d \lambda_v = M_d \lambda_d + M_d C_{p_v} (T_s - T_d) \tag{77}$$

- Boiling point elevation

$$T_b = T_v + BPE(T_b, X_b) + \Delta T_y \tag{78}$$

- Evaporator heat transfer area

$$A_e = \frac{M_d \lambda_d + M_d C_{p_v} (T_s - T_d)}{U_e (T_d - T_b)} \tag{79}$$

- Feed/distillate preheater heat transfer area

$$A_d = \frac{M_d (H(T_d) - H(T_o))}{U_d (LMTD)_d} = \frac{\alpha M_f C_p (T_f - T_{cw})}{U_d (LMTD)_d} \tag{80}$$

$$(LMTD)_d = \frac{(T_d - T_f) - (T_o - T_{cw})}{\ln \frac{T_d - T_f}{T_o - T_{cw}}} \quad (81)$$

- Feed/brine preheaters heat transfer area

$$A_b = \frac{M_b C_p (T_b - T_o)}{U_b (LMTD)_b} = \frac{(1-\alpha) M_f C_p (T_f - T_{cw})}{U_b (LMTD)_b} \quad (82)$$

$$(LMTD)_b = \frac{(T_b - T_f) - (T_o - T_{cw})}{\ln \frac{T_b - T_f}{T_o - T_{cw}}} \quad (83)$$

- Correlations for the overall heat transfer coefficient in the evaporator

$$U_e = 1.9394 + 1.40562 \times 10^{-3} T_b - 2.0752 \times 10^{-4} (T_b)^2 + 2.3186 \times 10^{-6} (T_b)^3 \quad (84)$$

where U_e is the overall heat transfer coefficient in the evaporator in kW/m^2 ^{o}C and T_b is the brine boiling temperature in ^{o}C.

- Energy balance during cooling of the second bed from T_{e_2} to T_a

$$M_{cw} C_p (T_{cw_o} - T_{cw_i}) = M_z C_{p_z} (T_{e_2} - T_a) \quad (85)$$

- Heat transferred from the second to the first bed

$$Q_{21} = M_d \lambda_v + M_z C_{p_z} (T_c - T_{e_2}) + M_d (H(T_v) - H(T_a)) \quad (86)$$

- Energy required to heat the first bed

$$Q_{21} + M_m \lambda_m = M_d \lambda_s + M_z C_{p_z} (T_c - T_a) + M_d (H(T_c) - H(T_a)) \quad (87)$$

- Combined energy balance (Eqs. 86 and 87)

$$M_m \lambda_m = M_d (\lambda_d - \lambda_v) + M_z C_{p_z} (T_{e_2} - T_a) + M_d (H(T_c) - H(T_v)) \quad (88)$$

- Combined energy balance (Eqs. 86 and 88)

$$M_m \lambda_m = M_d (\lambda_d - \lambda_v) + M_{cw} C_p (T_{cw_o} - T_{cw_i}) + M_d C_p (T_c - T_v) \quad (89)$$

- Efficiency of the circulating fluid heat exchanger

$$\eta = M_z C_{p_z} (T_{e_2} - T_a)/(M_{cw} C_p (T_{e_2} - T_{cw_i})) \quad (90)$$

- Energy balance of the circulating fluid heat exchanger

$$M_z C_{p_z} (T_{e_2} - T_a) = M_{cw} C_p (T_{cw_o} - T_{cw_i}) \quad (91)$$

- Combined energy balance and heat exchanger efficiency for circulating fluid (Eqs. (90) and (91))

$$T_{e_2} = (T_{cw_o} - T_{cw_i} (1 - \eta))/\eta \quad (92)$$

- Constraint on the temperature of inlet/outlet cooling water

$$T_{cw_i} = T_{cw} \quad (93)$$

$$T_{cw_o} = T_{e_2} - \Delta T \quad (94)$$

- Equilibrium relations for adsorber and desorber

$$\ln(P) = a + b/T \quad (95)$$

where

$$a = 20.49 - 60.4\,\alpha + 787\,\alpha^2 - 2.14\text{x}10^3\alpha^3$$

$$b = -8013 + 33.83\text{x}10^3\alpha - 3\text{x}10^5\alpha^2 + 7.9\text{x}10^5\alpha^3$$

- Water balance in adsorber between points a and c

$$M_z = M_m/(\alpha_g - \alpha_a) \quad (96)$$

In the above equations P and T are the equilibrium pressure and temperature of the adsorber and desorber. In the above relation T is in K and P is in mbar. For the absorber P is equal to vapor pressure in the evaporator and for the desorber P is equal to the heating steam vapor pressure. Also, T equals to T_a for the absorber and equals to T_c for the desorber. The constant α is in kg of water per kg of zeolite, Karagiorgas and Meunier (1987).

Other system constraints include the following:

- ΔT varies between 3 and 5 °C, Van Benthem, et al., 1995,
- η varies between 0.85 and 0.9,
- α_a varies between 0.06 and 0.15 kg H_2O/kg zeolite,
- T_c is higher than T_s by 3 to 10 °C, and
- T_m is higher than T_c by 3 to 10 °C.
- T_f is lower than T_b by 2 to 5 °C.
- T_d is higher than T_b by 2 to 5 °C.

Solution Method

The solution procedure is shown in Fig. 31 and it includes the following steps:

- The system capacity, brine temperature, intake seawater temperature, the water content in the adsorber at point (a), the heat exchanger efficiency, and the temperature difference in the heat exchanger, the equilibrium water content at point (a), and salinity of intake seawater and rejected brine are specified.
- The system constraints are defined, which includes the saturation temperature of the condensate and the feed seawater temperature.
- Eqs. 74-75 are solved to determine the feed and brine flow rates.
- The boiling point elevation and the vapor temperature in the evaporator are calculated from the correlation given in Appendix B and Eq. 78.
- An initial guess is assumed for T_s and T_o. This is followed by iterative solution of Eqs. 76 and 77. Newton's method is used with an iteration error of $1x10^{-4}$.
- The evaporator and preheaters heat transfer areas are determined from Eqs. 79, 80, and 82.
- The constraints on the desorber temperature at point g and the motive steam temperature are used to determine both temperatures.
- The absorber temperature, T_a, is evaluated from Eq. 95.
- The temperatures of inlet and outlet cooling seawater, T_{cw_i} and T_{cw_o}, and the desorber temperature at point (e_2), T_{e_2}, are obtained from Eqs. 92-94.
- The desorber water content, α_g, is obtained from Eq. 95.
- The solid mass in the adsorber is determined from Eq. 96.
- The motive steam and the cooling seawater flow rates are obtained from Eqs. 88 and 89.

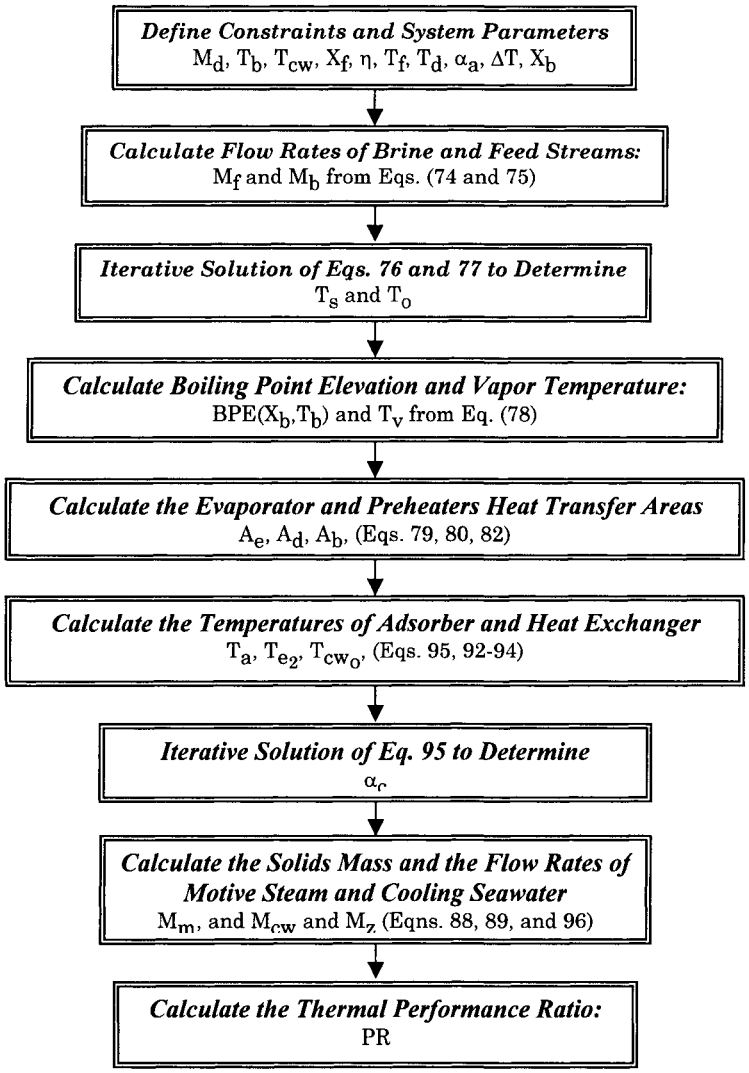

Fig. 31. Solution algorithm of the adsorption heat pump and the single effect evaporation desalination system.

Example 1:

A single effect adsorption vapor compression system is to be designed at the following conditions:

- Brine reject concentration (X_b) = 70000 ppm
- Intake seawater salinity (X_f) = 42000 ppm
- Intake seawater temperature (T_{cw}) = 25 °C
- System capacity (M_d) = 1 kg/s
- Boiling temperature (T_b) = 65 °C
- Specific heat of the vapor at constant pressure, Cp_v = 1.884 kJ/kg °C.
- Specific heat of zeolite, Cp_z = 0.9 kJ/kg K.
- Efficiency of heat exchanger in adsorber (η) = 0.9.
- Water content in adsorber (α_a) = 0.14 kg H_2O/kg solids
- Temperature difference of heat exchanger in adsorber (ΔT) = 5 °C

Determine the evaporator heat transfer area, thermal performance ratio, and flow rate of cooling water in the adsorber.

Solution:

The design procedure requires specification of the following parameters:

- Feed seawater temperature (T_f) = $T_b - 2$ = 63 °C
- Condensing vapor temperature (T_d) = $T_b + 2$ = 67 °C
- Desorber temperature (T_c) = (T_s + 5) °C
- Motive steam temperature (T_m) = (T_c + 5) °C

The vapor temperature in the evaporator is calculated by determining the boiling point elevation. The values of B and C are evaluated from

$$B = \left(6.71 + 6.34x10^{-2}(T_b) + 9.74x10^{-5}(T_b)^2\right)10^{-3}$$
$$= \left(6.71 + 6.34x10^{-2}(65) + 9.74x10^{-5}(65)^2\right)10^{-3} = 0.0112425$$

$$C = \left(22.238 + 9.59x10^{-3}(T_b) + 9.42x10^{-5}(T_b)^2\right)10^{-8}$$
$$= \left(22.238 + 9.59x10^{-3}(65) + 9.42x10^{-5}(65)^2\right)10^{-8}$$
$$= 2.3259345x10^{-7}$$

Substituting the values of B and C in the BPE equation gives

$$BPE = X_b\,(B + (X_b)(C))10^{-3}$$
$$= 70000\left(0.0112425 + (70000)\left(2.3259345x10^{-7}\right)\right)10^{-3} = 1.927\ ^{\circ}C$$

Therefore the vapor temperature (T_v) = 65 – 1.927 = 63.073 °C and the latent heat of the formed vapor (λ_v) = 2350.8 kJ/kg.

Solution of the overall material and salt balance for the feed seawater, distillate and rejected brine (Eqs. 74 and 75) gives:

- Flow rate of feed seawater (M_f) = 2.5 kg/s
- Flow rate of the rejected brine (M_b) = 1.5 kg/s

Iterative solution then proceeds for Eq. 76 to determine T_o, which gives a value of 27.9. The iteration sequence is shown in the following table:

Iteration	T_o	Error
Initial Guess	27	–
1	27.00932312	0.0009323
2	27.90120506	0.89188
3	27.90138435	0.00017929

Similarly Eq. 77 is solved iteratively to determine the compressed vapor temperature. The iteration sequence is shown in the following table:

Iteration	T_s	Error
Initial Guess	77	-
1	77.02658844	0.0265
2	83.06096649	6.034
3	83.06159973	0.000633

The compressed vapor temperature (T_s) is then used to calculate the

- Adsorber temperature (T_c) = T_s + 5 = 83.06 + 5 = 88.06 °C
- Motive steam temperature (T_m) = T_c + 5 = 88.06 + 5 = 93.06 °C
- Latent heat of motive steam (λ_m) = 2275.43 kJ/kg.

The heat transfer area of the evaporator is obtained by calculating the following:

$$\lambda_d = 2501.897149 - 2.407064037\ T_d + 1.192217\times10^{-3}\ T_d^2 - 1.5863\times10^{-5}\ T_d^3$$
$$= 2501.897149 - 2.407064037\ (67) + 1.192217\times10^{-3}\ (67)^2 - 1.5863\times10^{-5}\ (67)^3$$
$$= 2341.2 \text{ kJ/kg}$$

$$U_e = 1.9695+1.2057\times10^{-2}T_b-8.5989\times10^{-5}(T_b)^2+2.5651\times10^{-7}(T_b)^3$$
$$= 1.9695+1.2057\times10^{-2}(65)-8.5989\times10^{-5}(65)^2+2.5651\times10^{-7}(65)^3$$
$$= 2.4603 \text{ kJ/s m}^2\ ^\circ\text{C}$$

$$A_e = \frac{M_d(\lambda_d + Cp_v(T_s - T_d))}{U_e(T_d - T_b)}$$
$$= \frac{(1)(2341.2 + 1.84(83.06 - 67))}{4.2\,(67 - 65)}$$
$$= 282.3\ m^2$$

The adsorber pressure and temperature at point (a) are then calculated

$P_a = P(T_v) = 22.95$ kPa

$$a = 20.49 - 60.4\,\alpha_a + 787\,(\alpha_a)^2 - 2.14x10^3\,(\alpha_a)^3$$
$$= 20.49 - 60.4\,(0.14) + 787\,(0.14)^2 - 2.14x10^3\,(0.14)^3$$
$$= 21.587$$

$$b = -8013 + 33.83x10^3\,(0.14) - 3x10^5\,(\alpha_a)^2 - 7.9x10^5\,(\alpha_a)^3$$
$$= -8013 + 33.83x10^3\,(0.14) - 3x10^5\,(0.14)^2 - 7.9x10^5\,(0.14)^3$$
$$= -6989.04$$

$$T_a = b/(\log(P_a/100) - a)$$
$$= -6989.04/(\log(22.95/100) - 21.587) - 273$$
$$= 30.09\ ^oC$$

$$T_{cw_o} = (-(T_{cw_i}\,(1-\eta))/\eta - \Delta T)/(1 - 1/\eta)$$
$$= (-(25\,(1-0.9))/0.9 - 5)/(1 - 1/0.9)$$
$$= 70\ ^oC$$

$$T_{e_2} = (T_{cw_o} - T_{cw_i}(1-\eta))/\eta$$
$$= (70 - 25(1-0.9))/0.9$$
$$= 75.097\ ^oC$$

Iterative solution then proceeds for Eq. 95 to determine α_g, which gives a value of 0.0124. The iteration sequence is shown in the following table

Iteration	α_g	Error
Initial Guess	9.99999978E-03	–
1	1.00034522E-02	3.45242E-06
2	1.23926941E-02	0.002389242
3	1.24159195E-02	2.32254E-05
4	1.24160266E-02	1.071E-07

The solid mass is obtained from Eq. 96

$M_z = M_d/(\alpha_a - \alpha_g)$
$= 1/(0.14\text{-}0.0124) = 7.84$ kg dry zeolite

The motive steam flow rate is then calculated from Eqs. 88

$$M_m = (M_d (\lambda_d - \lambda_v) + M_z C_{p_z} (T_{e_2} - T_a) + M_d (H(T_c) - H(T_v)))/\lambda_m$$
$$= ((2341.2\text{–}2350.8) + 7.84\ (0.9)(75.097 - 30.09)$$
$$+(1)(368.73 - 264))/2275.43$$
$$= 0.181 \text{ kg/s}$$

The cooling water flow (M_{cw}) is obtained from Eq. 89

$$M_m\lambda_m = M_d(\lambda_d - \lambda_v) + M_{cw}C_p(T_{cw_o} - T_{cw_i}) + M_d (H(T_c) - H(T_v))$$

which gives $M_{cw} = 1.666$ kg/s. Finally the system thermal performance ratio is obtained, where

$PR = M_d/M_m = 1/0.181 = 5.52$

3.4.3 System Performance

The system performance is evaluated as a function of the following parameters:

- The brine boiling temperature, T_b.
- The temperature difference between the condensing vapor temperature and boiling brine, T_d-T_b.
- The water content in the cold adsorber bed, α_a.

The results are shown in Figs. 32-37 and it includes variations in the thermal performance ratio, the specific heat transfer area, and the specific flow rate of cooling water. These results are obtained at the following system parameters:

- Brine reject concentration (X_b) = 70000 ppm
- Intake seawater salinity (X_f) = 42000 ppm
- Intake seawater temperature (T_{cw}) = 25 °C
- System capacity (M_d) = 1 kg/s
- Boiling temperature (T_b) = 65 °C
- Specific heat of the vapor at constant pressure, $Cp_v = 1.884$ kJ/kg °C.
- Specific heat of zeolite, $Cp_z = 0.9$ kJ/kg K.

- Efficiency of heat exchanger in adsorber (η) = 0.9.
- Water content in adsorber (α_a) = 0.14 kg H_2O/kg solids
- Temperature difference of heat exchanger in adsorber (ΔT) = 5 °C
- Feed seawater temperature (T_f) = (T_b – 2) °C
- Desorber temperature (T_c) = (T_s + 5) °C
- Motive steam temperature (T_m) = (T_c + 5) °C

Variations in the thermal performance ratio are shown in Fig. 32 as a function of the brine boiling temperature, T_b, and the temperature difference between the condensing vapor and the boiling brine, T_d-T_b. As is shown the thermal performance ratio increases at higher boiling temperatures and larger difference in the temperature of the condensing vapor and boiling brine. As is shown a thermal performance ratio close to 10 can be reached as the brine boiling temperature increases to 110 °C. However, it should be noted that achieving such higher thermal performance is subject to reducing the water content in the adsorber at point (g) to values between zero and 0.01 kg H_2O/kg zeolite. On the other hand, the thermal performance ratio varies around a value of 4-5 for brine boiling temperatures between 40-60 °C. The superior performance of the ADVC is certainly pronounced in comparison with other single effect systems.

Irrespective of the high thermal performance ratio, the ADVC system has similar design features to other single effect vapor compression systems. As is shown in Fig. 33 the evaporator heat transfer area decreases drastically upon the increase in the temperature difference of the condensing vapor and the boiling brine. This is because of the increase in the temperature driving force between the condensing vapor and the boiling brine. A similar effect takes place in the cooling seawater heat exchanger, Fig. 34, where increase in the system temperature increases the driving force between the bed and the cooling seawater stream. This in turn reduces the flow rate of the cooling seawater stream.

System performance as a function of the water content in the adsorber at point (a) and the brine boiling temperature are shown in Figs. 35-37. As is shown in Fig. 35 the thermal performance ratio varies between 2 and 7. As discussed before, the high performance ratio of 13 can only be achieved if the water content of the adsorber at point (g) is reduced to values below 0.01 kg H_2O/kg zeolite. As is shown in Fig. 36, the evaporator heat transfer area has no dependence on the water content in the adsorber bed at point (a) and it only depends on the brine boiling temperature. As for the specific flow rat of cooling water it depends on both parameters, where it decreases with the increase of the brine boiling temperature. Effect of the water content in the adsorber varies, where at low boiling temperatures its increase reduces the specific flow rate of cooling water. The opposite effect is obtained at higher boiling temperatures.

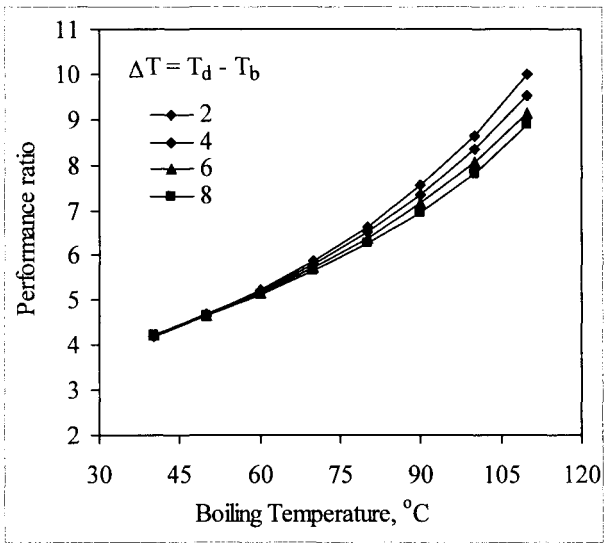

Fig. 32. Effect of boiling temperature and the temperature difference of condensed vapor and boiling brine on the thermal performance ratio of the ADVC system.

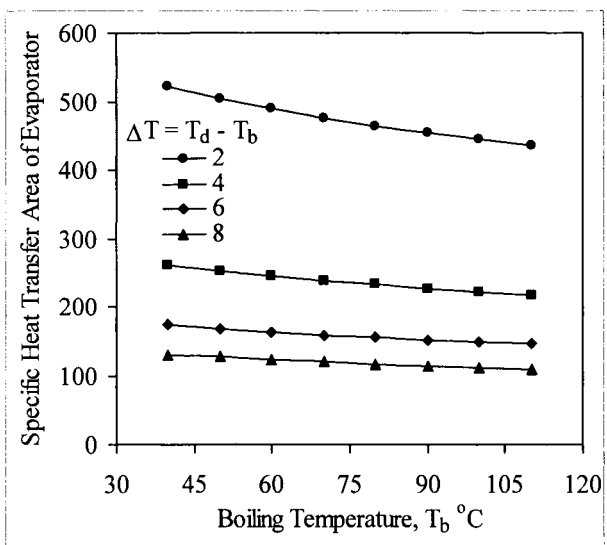

Fig. 33. Effect of boiling temperature and the temperature difference of condensed vapor and boiling brine on the evaporator specific heat transfer area for the ADVC system.

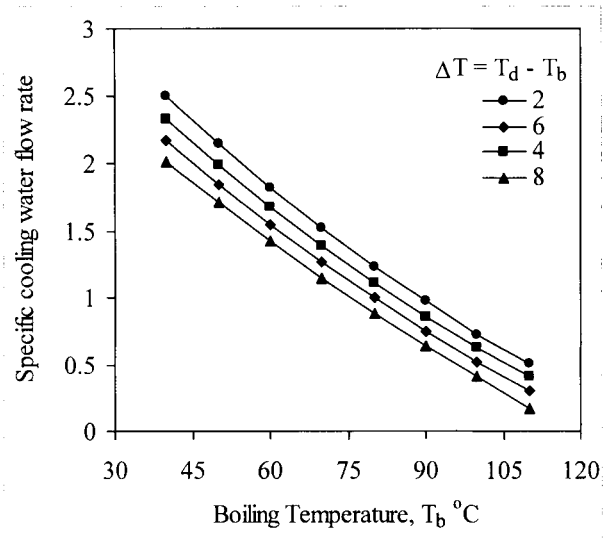

Fig. 34. Effect of boiling temperature and the temperature difference of condensed vapor and boiling brine on the specific flow rate of cooling water for the ADVC system.

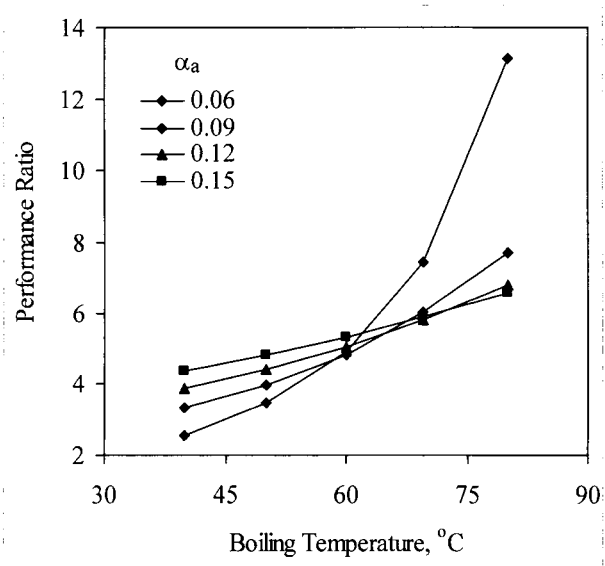

Fig. 35. Effect of boiling temperature and the water content in adsorber at point (a) on the thermal performance ratio of the ADVC system.

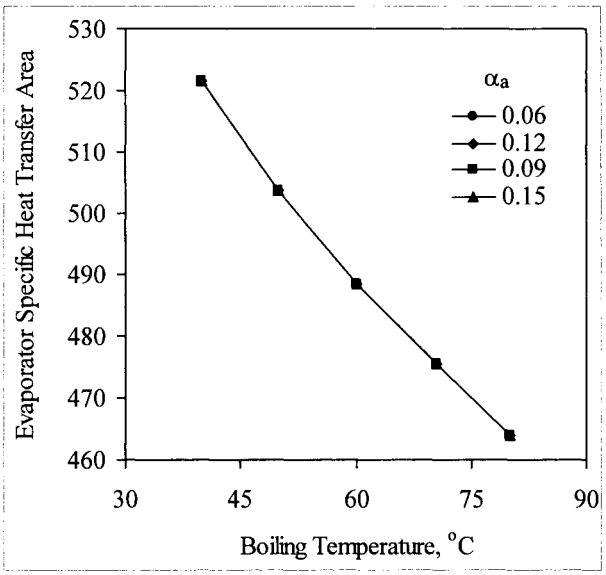

Fig. 36. Effect of boiling temperature and the water content in adsorber at point (a) on the evaporator specific heat transfer area for the ADVC system.

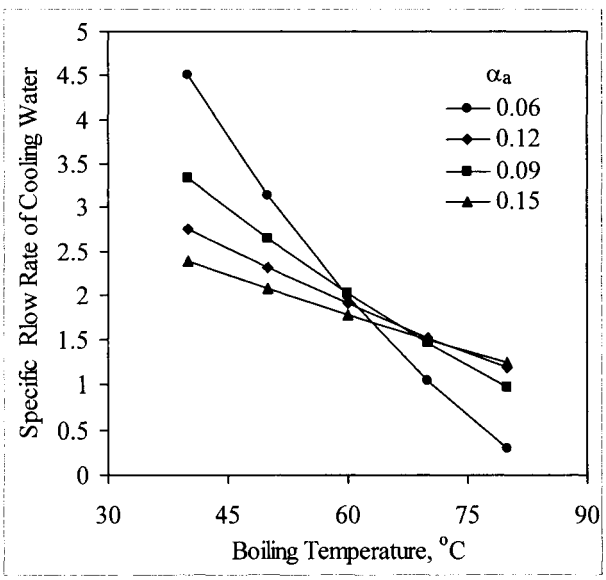

Fig. 37. Effect of boiling temperature and the water content in adsorber at point (a) on the specific flow rate of cooling water for the ADVC system.

3.4.4 Summary

The ADVC system is one of the most efficient single effect vapor compression desalination system. The system includes conventional unit processes found in other single effect configuration, i.e., evaporator and feed preheaters. In addition, its heat pump is rather simple and it includes two zeolite beds for adsorption and desorption. Operation of these beds is controlled by the design pressure and temperature for vapor adsorption and generation of the compressed vapor. A steady state mathematical model is presented to design and evaluate the system performance. The model is used to present step-by-step design calculations for the ADVC system. In addition, overall system performance is presented as a function main design and operating parameters. Results are presented in terms of variations in the thermal performance ratio, specific heat transfer area for the evaporator, and the specific flow rate of the cooling water. The system performance ratio is the highest among all other single effect vapor compression configurations. Also, the specific heat transfer area for the evaporator and the specific flow rate of the cooling water are similar to systems.

References

Karagiorgas, M., and Meunier, F., The dynamics of solid-adsorption heat pump connected with outside heat sources of finite capcity, Heat Recovery Systems & CHP, 7(1987)285-299.

Van Benthem, G.H.W., Cacciola, G., and Restuccia, G., Regenerative adsorption heat pumps: Optimization of the design, Heat Recovery Systems & CHP, 15(1995)531-544.

Problems

1. An ADVC system is to be designed to produce 2500 m^3/d of fresh water. The boiling temperature is 75 °C and the temperature of the saturated condensate is higher by 8 °C. The feed temperature is less than the brine boiling temperature by 3 °C and the water content in the adsorber at point (a) is 0.12 kg H_2O/kg zeolite. The salinity of the feed seawater is 39000 ppm and the rejected brine salinity is 70000 ppm. For preliminary design considerations assume the following:
   - All thermodynamic losses (including BPE) are negligible.
   - Constant specific heat for all liquid stream (4.2 kJ/kg °C).
   - Constant latent heat for all vapor streams (2500 kJ/kg).

- Constant specific heat for the vapor streams (1.884 kJ/kg °C).
- Constant overall heat transfer coefficients of 3.2, 7.5, and 8.2 kW/m^2 °C for the evaporator, distillate preheater, and brine preheater, respectively.

Calculate the following: M_b, M_f, T_s, T_o, A_b, A_d, A_e, PR, M_z, and M_{cw}. Assume a heat exchanger efficiency of 0.85.

2. Repeat the previous problem by considering the simultaneous effects of the following parameters:
   - Dependence of the specific heat on temperature and composition.
   - Effect of the boiling point rise.
   - Effect of demister losses.
   - Dependence of the latent on temperature.
   - Dependence of overall heat transfer coefficient on temperature.

   Compare results with the example solved in the Section 3.3.3.
3. An ADVC system is used to desalinate seawater at 37 °C with 42000 ppm salinity. The maximum allowable brine temperature is 90 °C. The heat transfer coefficient for the evaporator and the two preheaters is constant and equals to 6 kW/m^2 °C. The specific heat transfer area is 250 m^2 per (kg/s) of fresh water and the heat transfer area of the distillate preheater is 200 m^2. The flow rates of the hot and cold stream in the preheaters are equal. The temperatures of the distillate and rejected brine flowing from the preheaters are 45 °C and 40 °C, respectively. Calculate the thermal performance ratio.
4. An ADVC system has the following design data:

   M_d = 1 kg/s.

   A_d = 15 m^2.

   A_b = 25 m^2.

   A_e = 400 m^2.

   U_e = 2.4 kW/m^2 °C.

   U_d = 6.7 kW/m^2 °C.

   U_b = 6.3 kW/m^2 °C.

   X_f = 42000 ppm.

   X_b = 70000 ppm.

   Determine T_b, T_d, T_o, T_f, and T_s if T_{cw} = 28 °C, Cp = 4.2 kJ/kg °C, and Cp_v = 1.884 kJ/kg °C. Also, determine the thermal performance ratio and the flow rates of the brine and feed seawater.